QUANTUM MECHANICAL COMPUTATION OF BILLIARD SYSTEMS WITH ARBITRARY SHAPES

İNCİ ERHAN

DECEMBER 2003

QUANTUM MECHANICAL COMPUTATION OF BILLIARD SYSTEMS WITH
ARBITRARY SHAPES

A THESIS SUBMITTED TO
THE GRADUATE SCHOOL OF NATURAL AND APPLIED SCIENCES
OF
THE MIDDLE EAST TECHNICAL UNIVERSITY

BY

İNCİ ERHAN

IN PARTIAL FULFILLMENT OF THE REQUIREMENTS FOR THE DEGREE OF
DOCTOR OF PHILOSOPHY
IN
THE DEPARTMENT OF MATHEMATICS

DECEMBER 2003

Approval of the Graduate School of Natural and Applied Sciences

_____

Prof. Dr. Canan ÖZGEN

Director

I certify that this thesis satisfies all the requirements as a thesis for the degree of Doctor of Philosophy.

_____

Prof. Dr. Şafak ALPAY

Head of Department

This is to certify that we have read this thesis and that in our opinion it is fully adequate, in scope and quality, as a thesis for the degree of Doctor of Philosophy.

_____

Prof. Dr. Hasan TAŞELİ

Supervisor

Examining Committee Members

Prof. Dr. Hasan TAŞELİ   _____

Prof. Dr. Münevver TEZER   _____

Prof. Dr. Marat AKHMET   _____

Assoc. Prof. Dr. Hakan TARMAN   _____

Assoc. Prof. Dr. N. Abdülbaki BAYKARA   _____

ABSTRACT

QUANTUM MECHANICAL COMPUTATION OF BILLIARD SYSTEMS WITH ARBITRARY SHAPES

İnci Erhan

Ph.D., Department of Mathematics

Supervisor: Prof. Dr. Hasan TAŞELİ

December 2003, 88 pages

An expansion method for the stationary Schrödinger equation of a particle moving freely in an arbitrary axisymmetric three dimensional region defined by an analytic function is introduced. The region is transformed into the unit ball by means of coordinate substitution. As a result the Schrödinger equation is considerably changed. The wavefunction is expanded into a series of spherical harmonics, thus, reducing the transformed partial differential equation to an infinite system of coupled ordinary differential equations. A Fourier-Bessel expansion of the solution vector in terms of Bessel functions with real orders is employed, resulting in a generalized matrix eigenvalue problem.

The method is applied to two particular examples. The first example is a prolate spheroidal billiard which is also treated by using an alternative method. The numerical results obtained by both methods are compared. The second example is a billiard family depending on a parameter. Numerical results concerning the second example include the statistical analysis of the eigenvalues.

Keywords: Billiard Systems, Schrödinger Equation, Eigenfunction Expansion, Eigenvalue Problem, Spherical Harmonics

ÖZ

KEYFİ ŞEKİLLİ BİLARDO SİSTEMLERİNİN KUANTUM MEKANİKSEL HESAPLAMALARI

İnci Erhan

Doktora, Matematik Bölümü

Tez Yöneticisi: Prof. Dr. Hasan TAŞELİ

Aralık 2003, 88 sayfa

Analitik bir fonksiyon ile tanımlanan ve dönel simetrisi olan keyfi bir üç boyutlu bölgede, serbest hareket eden bir parçacığın Schrödinger denklemi için açılım yöntemi verilmektedir. Bir koordinat dönüşümü vasıtası ile bölge birim küreye dönüştürül- mektedir. Bunun sonucunda, Schrödinger denklemi de önemli ölçüde değişikliğe uğramaktadır. Dalga fonksiyonu küresel harmonikler cinsinden seriye açılmaktadır ve böylece, değişmiş olan kısmi diferansiyel denklemi sonsuz boyutlu bir diferan- siyel denklem sistemine indirgemektedir. Çözüm vektörü için reel mertebeli Bessel fonksiyonları cinsinden Fourier-Bessel açılımları kullanilmaktadır ve denklem sistemi genelleştirilmiş bir matris özdeğer problemine dönüştürülmektedir.

Yöntem iki özel örneğe uygulanmaktadır. Birinci örnek "prolate spheroid" şek- lindeki bilardo sistemidir ve aynı anda alternatif bir yöntemle daha incelenmektedir. Her iki yöntemle elde edilen sayısal sonuçlar karşılaştırılmaktadır. İkinci örnek bir parametreye bağlı bir bilardo ailesidir. Bu örneğe ait sayısal sonuçlar özdeğerlerin istatistiksel analizini de içermektedir.

Anahtar Kelimeler: Bilardo Sistemleri, Schrödinger Denklemi, Özfonksiyon Açı lımı, Özdeğer Problemi, Küresel Harmonikler

To my lovely Selin,

ACKNOWLEDGMENTS

TABLE OF CONTENTS

LIST OF TABLES

LIST OF FIGURES

CHAPTER 1

INTRODUCTION

Investigation of quantum mechanical systems whose classical counterparts are chaotic systems has received considerable interest in the last few decades. In classical mechanics, chaos is characterized by exponential instability with respect to the initial conditions. The reason why such an exponentially unstable system is called chaotic is that the motion is unpredictable. However, it took a long time trying to answer the question how chaos in a classical system shows itself in the corresponding quantum mechanical system. Unfortunately, this question still remains unanswered in the sense of a rigorous theoretical analysis. On the other hand, numerical investigations have given some very encouraging results.

In 1973 Percival [37] conjectured that the energy spectrum of a quantum system whose classical analog is irregular (i.e., chaotic) is more sensitive to slowly changing or fixed perturbations than those of a quantum system with regular (i.e., non chaotic) classical counterpart. Pomphrey [38] showed that the idea worked well with the so called Henon-Heiles potential.

Later, in order to shed more light on the relationship between classically chaotic systems and their quantum analogs, scientists started to study the "billiard" systems. The billiard problems, that is, problems of free motion in a closed finite domain are amongst the oldest problems in quantum mechanics, which have recently started regaining remarkable interest [21, 42]. This is primarily due to the fact that these simple systems, with only few exceptions, exhibit chaotic properties. In fact, depending on the shape of the billiard, the motion of the particle inside can show a rich variety of behaviors going from most regular to most chaotic.

1.1 Billiard systems in classical and quantum mechanics

The name of the billiard system comes from the billiard game familiar to almost everyone. As is well known, this game is played on a special rectangular table. If a player strikes a ball with a cue stick it follows straight line trajectories between hits at the edges of the table. If he strikes a second ball nearly but not exactly, it will follow a trajectory close to that of the first ball. This is not the case if the billiard table is in the shape of a stadium, i.e., if the two short edges of the rectangle are replaced by semicircles. In fact, in a stadium shaped billiard, even a small error in the initial struck will lead to a completely different trajectory. These two examples illustrate two completely different types of motion, regular in the first case and irregular in the second one.

Classically, a billiard system is the free motion of a point particle in a closed region with elastic reflection when the particle bounces at the boundary. Such a system is conservative since the particle does not lose energy. Therefore, the quantum mechanical billiard problem can be modelled by the stationary Schrödinger equation

$$-\Delta\Psi = E\Psi \qquad \text{in} \quad D \subset \mathbb{R}^d, \tag{1.1}$$

where D is a closed domain and the accompanying boundary condition is of Dirichlet type,

$$\Psi = 0 \qquad \text{on} \quad \partial D. \tag{1.2}$$

Due to their simplicity, two dimensional billiards have been thoroughly studied from both classical and quantum mechanical points of view. In 1984 Bohigas, Giannoni and Schmit [12] computed the quantum energy spectrum of the classically chaotic Sinai billiard which is in the shape of a square with a reflecting circular obstacle in the middle, and conjectured that the statistical properties of the energy eigenvalues of quantum systems with chaotic classical counterparts will be quite different than those with regular classical analogs. Since then, a number of results reinforcing this conjecture have been reported. Before discussing the details of the statistical analysis of the energy levels we will give a brief summary of the studies related to billiard systems.

Energy level statistics of the rectangular billiards have been given by Berry and Tabor [10]. Spectral properties of the aforementioned stadium billiard , also called Bunimovich stadium after the Russian scientist Bunimovich, have also been studied [13, 14]. Classical mechanics of an alternative stadium, the so called elliptical stadium in which the semicircles in the stadium are replaced by semi-ellipses, has been investigated recently [32]. Robnik has designed a family of plane billiards defined by the conformal map of the unit disc in a complex plane w as follows,

$$\mathcal{B} = \{w \mid w = z + \lambda z^2, \mid z \mid \leq 1\}, \quad 0 \leq \lambda \leq \frac{1}{2} \qquad (1.3)$$

Depending on values of λ, the shape of the billiard $\mathcal{B}$ varies from a circle to a cardioid. Robnik studied this billiard family from both classical [43] and quantum point of view [44, 41]. In another work by Bäcker and Steiner [4] the statistical analysis of the energy spectra of the quantum cardioid billiard has been presented. Perhaps one of the most popular billiard systems is the Sinai billiard. This system is known to be classically chaotic and a detailed study of the corresponding quantum mechanical system can be found in [12, 8]. Sieber and Steiner considered the motion in a hyperbola billiard defined as follows,

$$\mathcal{B} = \{(x,y) \mid x \geq 0, y \geq 0, y \leq \frac{1}{x}\}. \qquad (1.4)$$

They report that the hyperbola billiard is classically chaotic [45] and analyzed the statistical properties of the energy spectra of the quantum hyperbola [46]. Another one-parameter family of billiard systems has been studied recently both as classical and quantum mechanical system. The boundary of this family has been defined by the curve

$$y(x) = \pm(1 - \mid x \mid^\delta), \quad x \in [-1,1], \quad 1 \leq \delta \leq \infty, \qquad (1.5)$$

where the parameter δ determines the shape of the billiard. For δ=2 the shape of the billiard is lemon-like, hence the billiard family has been called generalized parabolic lemon shaped billiard [30]. Some results about quantum polygon billiard problem [27] and rhombus billiard [17] has also been obtained. A survey on two dimensional billiards can be found in [62]. Much less has been done on three-dimensional billiard systems. There are only few results concerning the generalized three dimensional stadium [36], three-dimensional Sinai billiard [39, 40] and conical billiard [28, 29].

3

The Schrödinger equation (1.1) is not exactly solvable unless the boundary of the billiard is constant in some coordinate system. However, in order to perform a reliable statistical analysis one needs to compute hundreds of energy levels. Therefore the use of efficient numerical methods gains a lot of significance. One of the most practical methods is the boundary element method [24, 6]. This method uses integral equation representation and discretization of the boundary which results in a homogeneous algebraic linear system. The zeros of the determinant give the eigenvalues. This method has been widely used but has recently been shown to have problems if the billiard is non-convex [26]. Another method is the point matching (collocation) method, which uses an expansion of the wave function in suitable basis functions and then forces this expansion to be zero on the discretized boundary [19, 20]. This method has also a drawback as it can not be relied upon for accurate spectra. The conformal mapping method is an elegant and efficient method which solves the billiard problem by finding a suitable conformal mapping to transform the billiard to the unit disc [41]. Unfortunately, the method can be applied only to two dimensional billiards for which a conformal map can be found. The recently proposed constraint operator method solves the billiard problem by using an enlarged billiard on which the Schrödinger equation is exactly solvable and then "cuts away" the unwanted part of that billiard to obtain the original one [33]. It is interesting from both mathematical and physical points of view because it can represent the Hamiltonian of a chaotic billiard by the eigenfunctions of a regular one. The method reduces the Schrödinger equation to a matrix eigenvalue problem. A similar method, using an expansion in eigenfunctions of square billiard has been proposed recently [25]. The scaling method for computation of highly exited states of billiards [57] and the Korringa-Kohn-Rostoker method [8] are also worth mentioning here. In some recent studies two-dimensional quantum billiards have been studied experimentally by means of microwave cavities [22, 47] and highly excited energy levels have been obtained in this manner.

1.2 Statistical Properties of the Energy Spectra of Quantum Systems and Random Matrix Theory

The pioneering work of Berry and Tabor [10] and the work of Bohigas, Giannoni and Schmit [12] led to an enormous interest in the Random Matrix Theory (RMT) developed by Wigner, Dyson, Mehta and others in 1950-1960. The most detailed and complete monograph about RMT is the second enlarged edition of "Random Matrices" written by Mehta [34].

The quantum mechanical system is represented by its Hamiltonian operator which in turn can be represented by a Hermitian matrix. For billiard systems this matrix is real symmetric and is invariant under orthogonal transformations. More precisely, let $\mathbf{H}$ be the real symmetric matrix representation of the Hamiltonian operator in any arbitrary basis. Then the matrix $\mathbf{H}'$ defined by

$$\mathbf{H}' = \mathbf{OHO^T} \tag{1.6}$$

is also real and symmetric, where $\mathbf{O}$ is an orthogonal matrix. If the system is regular and the basis is suitably chosen, then the matrix $\mathbf{H}$ is diagonal. In this case the eigenvalues of the system are not correlated. Denote the ordered eigenvalues by $E_1 \leq E_2 \leq E_3 \leq \ldots \leq E_N \leq \ldots$, and the spacings between them by $s_i = E_{i+1} - E_i$, $i = 1, 2, 3, \ldots$, then it can be shown that the probability distribution function for these spacings, the so-called Nearest Neighbor Spacing Distribution(NNSD) has the form

$$p(s) = e^{-s}. \tag{1.7}$$

This is the well known Poisson distribution function. Hence, the NNSD of regular systems is expected to be Poissonian. If the quantum system is not regular, then the matrix $\mathbf{H}$ belongs to the Gaussian Orthogonal Ensemble(GOE) in RMT. Two other ensembles: Gaussian Unitary(GUE) and Gaussian Symplectic(GSE) have to be mentioned here, but none of them will be used in this work, so we will not discuss them. The NNSD for the eigenvalues of matrices from the GOE can be obtained from the joint probability density function by long integration and has the following

form

$$p(s) = \frac{\pi}{2} s e^{-\frac{\pi}{4} s^2}. \tag{1.8}$$

Most classical billiards are neither completely regular nor completely chaotic. In such systems, called generic, both types of motion co-exist. The NNSD of the energy levels of generic systems is neither Poissonian nor like that of the GOE. Several theoretical models have been developed for this class of systems. The first model was introduced by Brody [50],

$$p(s) = (\nu + 1) a_\nu s^\nu \exp(-a_\nu s^{\nu+1}) \tag{1.9}$$

where

$$a_\nu = \left[\Gamma \left(\frac{\nu + 2}{\nu + 1} \right) \right]^{\nu+1}. \tag{1.10}$$

For $\nu = 0$, the Brody distribution reduces to Poissonian and for $\nu = 1$ the NNSD of the GOE is obtained. Another approach is that of Izrailev [23], who proposed the following distribution,

$$p(s) = A s^\nu \exp \left[-\frac{\pi^2}{16} \nu s^2 - \left(C - \frac{\nu}{2} \right) \frac{\pi}{2} s \right] \tag{1.11}$$

where the constants A and C can be obtained using normalization conditions. The distribution becomes Poissonian for $\nu = 0$, and it coincides with the NNSD of the GOE for $\nu = 1$. The derivation of the above distributions and some other theoretical models interpolating between the Poisson and GOE cases can be found in a recent monograph by Stöckmann [48].

Other frequently used statistics are the Dyson-Mehta or spectral rigidity statistics Δ_3 and the number variance Σ^2. Definition and derivation of these statistics can be found in [34] and [48], but will not be discussed here.

One of the two examples considered in this study is the integrable prolate spheroidal billiard, the other is a generic billiard depending on a parameter. As it will be shown in chapter 4, the NNSD of the numerically calculated spectra for the prolate spheroid agrees with Poisson distribution (1.7), while for the second generic billiard the NNSD is similar to Brody's model (1.9). Unfortunately, due to computational difficulties in evaluating the matrix elements of the Hamiltonian of the system, the statistical analysis has been performed using a relatively small number of spacings, however the resulting distribution properties have shown good agreement with the predictions of Random Matrix Theory.

1.3 Mathematical Model of a Quantum Billiard System Defined by a Shape Function

In this study we propose a numerical method for solving a quite general class of axisymmetric three dimensional billiard systems obtained by rotating a closed finite region in the yz-plane about the z-axis. To be specific, let us consider the region

$$\mathcal{B} = \{(r, \theta) \mid 0 \leq r \leq f(\theta),\ 0 \leq \theta \leq \pi\} \tag{1.12}$$

where r is the magnitude of the position vector $\vec{r}$ of a point with coordinates (r, θ). Note that θ stands for the angle between the positive z-axis and $\vec{r}$ (see Figure 1.1). The function $f(\theta)$ can be identified as the shape function since it determines the shape of the billiard and is assumed to be an arbitrary analytic function of θ. The idea is not original, in fact, the billiards in (1.3) and (1.5) were also constructed by means of shape functions. Nevertheless, they contain a single parameter and therefore, can generate only a limited class of billiards. The function $f(\theta)$, proposed in this work, however, is very general depending on infinitely many parameters. Similar shape function has been previously used by Taşeli and Demiralp [51] and Taşeli and Eid [52] to determine the Stokes flow past an arbitrary body. To our knowledge, studies concerning billiard systems with such a general shape do not appear in the literature. Thus, we design our three-dimensional axisymmetric billiard, say $\mathcal{D}$, by rotating the region (1.12) about the z-axis (see Figure 1.2), that is,

$$\mathcal{D} = \{(r, \theta, \phi) \mid 0 \leq r \leq f(\theta),\ 0 \leq \theta \leq \pi,\ 0 \leq \phi \leq 2\pi\}, \qquad \mathcal{D} \subset \mathbb{R}^3 \tag{1.13}$$

where $(r,\ \theta,\ \phi)$ are the spherical coordinates.

The Schrödinger equation for a particle moving freely inside the region $\mathcal{D}$ can be written as

$$-\left\{\frac{\partial^2}{\partial r^2} + \frac{2}{r}\frac{\partial}{\partial r} + \frac{1}{r^2}\frac{\partial^2}{\partial \theta^2} + \frac{\cot\theta}{r^2}\frac{\partial}{\partial \theta} + \frac{1}{r^2\sin^2\theta}\frac{\partial^2}{\partial \phi^2}\right\}\Psi(r,\theta,\phi) = E\Psi(r,\theta,\phi) \tag{1.14}$$

where the wavefunction Ψ vanishes on the boundary,

$$\Psi = 0 \ \text{ on } \ \partial\mathcal{D}. \tag{1.15}$$

In addition, the wavefunction is assumed to satisfy the square integrability condition

$$\int\int_{\mathcal{D}}\int \mid \Psi \mid^2 dV < \infty \tag{1.16}$$

7
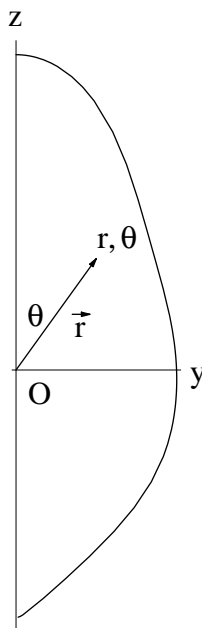
Figure 1.1: Two-Dimensional Region Generating an Axisymmetric Billiard

arising from the fact that Ψ must belong to the Hilbert space of square integrable functions on $\mathcal{D} \subset \mathbb{R}^3$.

The mathematical problem so defined is an eigenvalue problem. It is of great importance not only in the study of quantum chaos, but also in many other areas like acoustics, where the function Ψ represents a sound wave, in nuclear physics, electromagnetics and also in connection with diffusion problems. Clearly, the Laplacian is a self-adjoint operator on the Hilbert space of square integrable functions over $\mathcal{D} \subset \mathbb{R}^3$. An eigenvalue problem associated with the Laplacian has an infinite set of discrete real eigenvalues corresponding to an orthogonal set of eigenfunctions. Moreover, the Dirichlet type boundary conditions imply the positiveness of the eigenvalues as stated in the following theorem, the proof of which can be found in [49], or any textbook on the partial differential equations.

Theorem 1.1. *The eigenvalues of the Laplace operator on a closed bounded domain are real and discrete and the corresponding eigenfunctions are orthogonal. If, in addition, the boundary conditions are of Dirichlet type, the eigenvalues are all positive.*

Unfortunately, the numerical implementation of the problem within a reasonable degree of accuracy still remains a very difficult task. Despite the plentiful literature
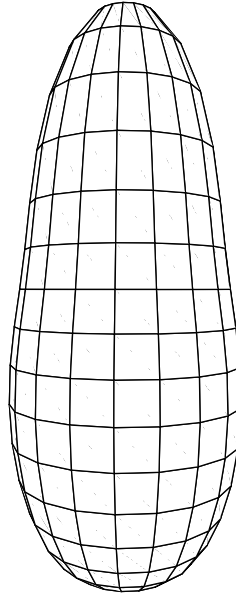
Figure 1.2: Three-Dimensional Axisymmetric Billiard.

about its numerical treatment in two dimensions, results on the three-dimensional case are only few. This is mainly due to the fact that solving three-dimensional problems by means of the aforementioned methods is much more difficult than solving two-dimensional ones. Moreover, some of the methods are applicable only in two dimensions.

Therefore, the main objective of this study is to develop a method to deal numerically with the problem (1.14)-(1.16). However, it will be made clear in the forthcoming chapters that this thesis seems to be interesting from two different aspects. In other words, it has applications in both mathematics and physics. First, it provides a numerical method for a quite general class of eigenvalue problems. Second, the general form of the shape function $f(\theta)$ makes it possible to design a wide variety of three-dimensional billiards and investigate them not only as quantum but also as classical systems.

CHAPTER 2

DEVELOPMENT OF A METHOD FOR SOLVING THREE-DIMENSIONAL BILLIARDS

2.1 The Shape Function and the New Coordinates

In this section we introduce a coordinate transformation which transforms the region under consideration into the unit ball.

Consider again the billiard

$$\mathcal{D} = \{(r, \theta, \phi) \mid 0 \leq r \leq f(\theta),\ 0 \leq \theta \leq \pi,\ 0 \leq \phi \leq 2\pi\} \tag{2.1}$$

where (r, θ, ϕ) are the usual spherical coordinates related to the rectangular coordinates by $x = r \sin \theta \cos \phi$, $y = r \sin \theta \sin \phi$ and $z = r \cos \theta$. The analyticity of $f(\theta)$ suggests proposing a shape function of the form

$$f(\theta) = 1 + \sum_{k=1}^{\infty} \alpha_k \cos^k \theta, \qquad \alpha_k \in \mathbb{R} \tag{2.2}$$

where α_k's are regarded as the shape parameters. Note that, $1 \leq f(\theta) < \infty$ must hold for all $\theta \in [0, \pi]$ in order to have a bounded geometrical region. By means of the flexible parameters α_k introduced in (2.2), it is possible to deal with various billiards including prolate and oblate spheroids, the three-dimensional version of the cardioid billiard mentioned in Section 1.1 and many others. Furthermore, even very

simple choices of $f(\theta)$ like finite sums containing only few terms can generate plenty of shapes. Note also that the particular case, in which $\alpha_k = 0$ for all $k \in \mathbb{Z}^+$, corresponds to the exactly solvable spherical billiard.

We introduce the new coordinates

$$
\begin{aligned}
\xi &= \frac{r}{f(\theta)}, & \xi &\in [0, 1] \\
\eta &= \cos \theta, & \eta &\in [-1, 1]
\end{aligned}
\tag{2.3}
$$

where the third coordinate ϕ remains unchanged. The region $\mathcal{D}$ is now transformed into

$$
\mathcal{D} = \{(\xi, \eta, \phi) \mid 0 \le \xi \le 1, \ -1 \le \eta \le 1, \ 0 \le \phi \le 2\pi\},
\tag{2.4}
$$

which is a unit ball. Partial derivative operators involved in the Schrödinger equation take very complicated forms such that

$$
\frac{\partial}{\partial r} = \frac{1}{F(\eta)} \frac{\partial}{\partial \xi}, \qquad \frac{\partial^2}{\partial r^2} = \frac{1}{[F(\eta)]^2} \frac{\partial^2}{\partial \xi^2}, \qquad \frac{\partial}{\partial \theta} = \sqrt{1 - \eta^2} \left[\frac{F'(\eta)}{F(\eta)} \xi \frac{\partial}{\partial \xi} - \frac{\partial}{\partial \eta} \right]
$$

and

$$
\begin{aligned}
\frac{\partial^2}{\partial \theta^2} &= (1 - \eta^2) \frac{[F'(\eta)]^2}{[F(\eta)]^2} \xi^2 \frac{\partial^2}{\partial \xi^2} - 2(1 - \eta^2) \frac{F'(\eta)}{F(\eta)} \xi \frac{\partial^2}{\partial \xi \partial \eta} \\[2mm]
&\quad - \frac{(1 - \eta^2) F''(\eta) F(\eta) - \eta F'(\eta) F(\eta) - 2(1 - \eta^2) [F'(\eta)]^2}{[F(\eta)]^2} \xi \frac{\partial}{\partial \xi} \\[2mm]
&\quad + (1 - \eta^2) \frac{\partial^2}{\partial \eta^2} - \eta \frac{\partial}{\partial \eta}
\end{aligned}
\tag{2.5}
$$

where the function $F(\eta)$,

$$
F(\eta) = 1 + \sum_{k=1}^{\infty} \alpha_k \eta^k.
\tag{2.6}
$$

is the shape function written in terms of the new variable η. Obviously, the coordinate system (ξ, η, ϕ) is quite an unusual one, which is not orthogonal. This fact, unfortunately, has some very unpleasant consequences as will be seen later. Nevertheless, in almost all studies summarized in Section 1.1 concerning quantum billiard problems even in two dimensions, serious difficulties of one kind or other have been encountered.

Let us recall our mathematical problem consisting of the Schrödinger equation and the additional conditions in (1.14)-(1.16). We employ the substitutions in (2.3)

11

and partial derivatives in (2.5) to transform the Schrödinger equation to a new partial differential equation. Thus, we get

$$
- \left\{ \left[\frac{1}{F^2} + (1-\eta^2)\frac{(F')^2}{F^4} \right] \frac{\partial^2}{\partial \xi^2} - 2(1-\eta^2)\frac{F'}{F^3}\frac{1}{\xi}\frac{\partial^2}{\partial \xi \partial \eta} \right.
$$

$$
+ \left[\frac{2}{F^2} + \frac{2(1-\eta^2)\,(F')^2 - (1-\eta^2)F''F + 2\eta F'F}{F^4} \right] \frac{1}{\xi}\frac{\partial}{\partial \xi}
$$

$$
\left. + \frac{1}{F^2\xi^2}\left[(1-\eta^2)\frac{\partial^2}{\partial \eta^2} - 2\eta\frac{\partial}{\partial \eta} - \frac{1}{1-\eta^2}\frac{\partial^2}{\partial \phi^2} \right] \right\} \Psi(\xi,\eta,\phi) = E\Psi(\xi,\eta,\phi)
$$

which becomes

$$
- \left\{ \left[F^2 + (1-\eta^2)\,(F')^2 \right] \frac{\partial^2}{\partial \xi^2} - 2(1-\eta^2)F'F\frac{1}{\xi}\frac{\partial^2}{\partial \xi \partial \eta} \right.
$$

$$
+ \left[2F^2 + 2(1-\eta^2)\,(F')^2 - (1-\eta^2)F''F + 2\eta F'F \right]\frac{1}{\xi}\frac{\partial}{\partial \xi}
$$

$$
\left. + \frac{F^2}{\xi^2}\left[(1-\eta^2)\frac{\partial^2}{\partial \eta^2} - 2\eta\frac{\partial}{\partial \eta} - \frac{1}{1-\eta^2}\frac{\partial^2}{\partial \phi^2} \right] \right\} \Psi(\xi,\eta,\phi) = EF^4\Psi(\xi,\eta,\phi)
$$

$$(2.7)$$

upon multiplication of both sides by F^4, where we have dropped the η-dependance of the shape function $F(\eta)$ for simplicity. The resulting partial differential equation cannot be treated by the method of separation of variables. In fact, it is completely different from the original one, since the shape function has been inserted into it. As a result, shape effects are now characterized mainly by the partial differential equation. However, this new equation will be solved in the standardized region (2.4), i.e., in the unit ball. It seems that an expansion method for the wavefunction will be more appropriate.

The Jacobian determinant of the transformation (2.3) is

$$
\frac{\partial(\xi,\eta,\phi)}{\partial(r,\theta,\phi)} = \begin{vmatrix} \frac{1}{f(\theta)} & -r\frac{f'(\theta)}{f^2(\theta)} & 0 \\ 0 & -\sin\theta & 0 \\ 0 & 0 & 1 \end{vmatrix} = -\frac{\sin\theta}{f(\theta)}
$$

leading to a square integrability condition of the form

$$
\int_0^{2\pi}\int_{-1}^{1}\int_0^1 |\Psi(\xi,\eta,\phi)|^2\,\xi^2\,[F(\eta)]^3\,\mathrm{d}\xi\mathrm{d}\eta\mathrm{d}\phi < \infty. \tag{2.8}
$$

over the new region. As is shown, this square integrability condition contains the unspecified shape function as a weight. More precisely, (2.8) implies that the wavefunction must belong to the Hilbert space of square integrable functions over $\mathcal{D}$ under the weight $\xi^2 \left[F(\eta)\right]^3$. Thus, to find a suitable expansion basis becomes a very difficult task. However, from the definition of $F(\eta)$, it follows that $1 \leq F(\eta)$ for all $\eta \in [-1, 1]$, and therefore,

$$\int_0^{2\pi} \int_{-1}^1 \int_0^1 |\Psi(\xi, \eta, \phi)|^2\, \xi^2 \mathrm{d}\xi \mathrm{d}\eta \mathrm{d}\phi \leq \int_0^{2\pi} \int_{-1}^1 \int_0^1 |\Psi(\xi, \eta, \phi)|^2\, \xi^2 \left[F(\eta)\right]^3 \mathrm{d}\xi \mathrm{d}\eta \mathrm{d}\phi \tag{2.9}$$

implying the boundedness of the integral

$$\int_0^{2\pi} \int_{-1}^1 |\Psi(\xi, \eta, \phi)|^2\, \mathrm{d}\eta \mathrm{d}\phi < \infty, \tag{2.10}$$

for every fixed $\xi \in (0, 1]$. In what follows, (2.10) suggests that $\Psi(\xi, \eta, \phi)$ can also be regarded as a square integrable function over the region $[-1, 1] \times [0, 2\pi]$ with the unit weight for a fixed ξ. In fact, this region represents a sphere of radius ξ defined by

$$\mathcal{D}_\xi = \{(\xi, \eta, \phi) | \xi = c, -1 \leq \eta \leq 1, 0 \leq \phi \leq 2\pi\} \tag{2.11}$$

where ξ is assumed to be constant.

Let us now consider the differential operator

$$\mathcal{T} = (1 - \eta^2)\frac{\partial^2}{\partial \eta^2} - 2\eta \frac{\partial}{\partial \eta} - \frac{1}{1 - \eta^2}\frac{\partial^2}{\partial \phi^2} \tag{2.12}$$

appearing on the last term of the left hand side of (2.7). The eigenvalue problem related to this operator, i.e.,

$$\mathcal{T} y = \lambda y \tag{2.13}$$

generates the orthogonal sequence of the spherical harmonics defined as [15]

$$Y_m^n(\eta, \phi) = P_m^{|n|}(\eta)\mathrm{e}^{in\phi} \tag{2.14}$$

corresponding to the eigenvalues $\lambda = -m(m + 1)$, where the indices range over $-m \leq n \leq m$, $0 \leq m \leq \infty$. Here the functions $P_m^{|n|}(\eta)$ are the associated Legendre functions of the first kind. As a matter of fact, (2.13) has also solutions of the form $Q_m^{|n|}(\eta)\mathrm{e}^{in\phi}$, where the $Q_m^{|n|}(\eta)$ denote the associated Legendre functions of the second

13

kind. However, these functions are not bounded at $\eta = \pm 1$, and, therefore, they are not suitable as an expansion basis for our problem.

We now give the following theorems which complete the analysis related to the choice of an expansion basis.

Theorem 2.1. *The system of spherical harmonics $\{Y_m^n\}$, where $m = 0, 1, \ldots \infty$, $-m \leq n \leq m$ is complete.*

Theorem 2.2. *Every function, square integrable over a sphere can be expanded in terms of spherical harmonics.*

The proofs of Theorems 2.1 and 2.2 can be found in [15] or [56].

2.2 An Eigenfunction Expansion for the Transformed Equation

In this section, we propose an expansion in spherical harmonics for the wavefunction $\Psi(\xi, \eta, \phi)$ and insert this expansion into the transformed equation. The discussion of the previous section demonstrates the advantage of using such an expansion, for, it is clear that this expansion will replace the differential operator in (2.12) by its eigenvalues. Thus, we assume

$$\Psi(\xi, \eta, \phi) = \sum_{m=0}^{\infty} \sum_{n=-m}^{m} \chi_m^n(\xi) P_m^{|n|}(\eta) e^{in\phi}$$

where the $\chi_m^n(\xi)$ denote the Fourier coefficient functions. It is more appropriate for our analysis to rewrite this expansion as

$$\Psi(\xi, \eta, \phi) = \sum_{m=0}^{\infty} \left\{ \Phi_m^0(\xi) P_m^0(\eta) + \sum_{n=1}^{m} [\Phi_m^n(\xi) \cos n\phi + \psi_m^n(\xi) \sin n\phi] P_m^n(\eta) \right\} \quad (2.15)$$

where now the expansion coefficients are the Φ_m^n and ψ_m^n. Theorems 2.1 and 2.2 together with the condition (2.10) imply that this expansion converges in the mean to the function $\Psi(\xi, \eta, \phi)$ for every fixed $\xi \in (0, 1]$, provided that the $\Phi_m^n(\xi)$ and

$\psi_m^n(\xi)$ are the Fourier coefficients defined by

$$\Phi_m^0(\xi) = \frac{1}{4\pi} \frac{2}{(2m+1)} \int_0^{2\pi} \int_{-1}^1 \Psi(\xi, \eta, \phi) P_m^0(\eta) \mathrm{d}\eta \mathrm{d}\phi$$

$$\Phi_m^n(\xi) = \frac{1}{2\pi} \frac{2}{(2m+1)} \frac{(m+n)!}{(m-n)!} \int_0^{2\pi} \int_{-1}^1 \Psi(\xi, \eta, \phi) P_m^n(\eta) \cos n\phi \mathrm{d}\eta \mathrm{d}\phi \quad (2.16)$$

and

$$\psi_m^n(\xi) = \frac{1}{2\pi} \frac{2}{(2m+1)} \frac{(m+n)!}{(m-n)!} \int_0^{2\pi} \int_{-1}^1 \Psi(\xi, \eta, \phi) P_m^n(\eta) \sin n\phi \mathrm{d}\eta \mathrm{d}\phi$$

respectively, for $n = 1, 2, \ldots, m$ and $m = 0, 1, 2, \ldots, \infty$.

Before proceeding, let us have a closer look at the shape function $F(\eta)$. From a computational point of view, the power series representation of $F(\eta)$ should be truncated. Therefore, we use the truncated shape function, say $G(\eta)$,

$$G(\eta) = 1 + \sum_{k=1}^K \alpha_k \eta^k. \quad (2.17)$$

instead of the original shape function unless $F(\eta)$ is already defined by a finite sum. Note that,

$$F(\eta) = \lim_{K \to \infty} G(\eta).$$

In what follows, we will replace the function $F(\eta)$ in the equation (2.7) by $G(\eta)$.

Remark 1. In order to have a "numerically" convergent algorithm it is important that the power series describing $F(\eta)$ converges very rapidly, i.e., the coefficients α_k form a rapidly decreasing sequence, Otherwise, one must take a large truncation order K which will cause long computing time, large memory and may even lead to a divergent algorithm. $\diamond$

We shall make the following definitions for the sake of brevity

$$\begin{aligned}
\mathcal{G}_0(\eta) &:= [G(\eta)]^2 \\
\mathcal{G}_1(\eta) &:= [G(\eta)]^2 + (1 - \eta^2) [G'(\eta)]^2 \\
\mathcal{G}_2(\eta) &:= 2\eta G'(\eta) G(\eta) \\
\mathcal{G}_3(\eta) &:= (1 - \eta^2) G''(\eta) G(\eta).
\end{aligned} \quad (2.18)$$

It follows easily from the definition of $G(\eta)$ that all the functions $\mathcal{G}_i(\eta)$ where $i = 0, 1, 2, 3$, are polynomials of degree $2K$ in η. We employ (2.18) and (2.12) to rewrite

15

equation (2.7) as

$$
\begin{aligned}
- & \left\{ \mathcal{G}_1(\eta)\frac{\partial^2}{\partial\xi^2} + [2\mathcal{G}_1(\eta) + \mathcal{G}_2(\eta) - \mathcal{G}_3(\eta)]\frac{1}{\xi}\frac{\partial}{\partial\xi} - \frac{(1-\eta^2)}{\xi\eta}\mathcal{G}_2(\eta)\frac{\partial^2}{\partial\xi\partial\eta} \right. \\
+ & \left. \frac{\mathcal{G}_0(\eta)}{\xi^2}\mathcal{T} \right\}\Psi(\xi,\eta,\phi) = E\left[\mathcal{G}_0(\eta)\right]^2\Psi(\xi,\eta,\phi).
\end{aligned}
\tag{2.19}
$$

Substituting the expansion (2.15) in equation (2.19) and using (2.13) we obtain

$$
\begin{aligned}
& -\sum_{m=0}^{\infty}\sum_{n=0}^{m}\left\{\mathcal{G}_1(\eta)P_m^n(\eta)\frac{\mathrm{d}^2}{\mathrm{d}\xi^2}\Phi_m^n(\xi) + [2\mathcal{G}_1(\eta) + \mathcal{G}_2(\eta) - \mathcal{G}_3(\eta)]\frac{1}{\xi}\frac{\mathrm{d}}{\mathrm{d}\xi}\Phi_m^n(\xi)\right. \\[2mm]
& \left. -\frac{\mathcal{G}_2(\eta)}{\eta}(1-\eta^2)\frac{\mathrm{d}}{\mathrm{d}\eta}P_m^n(\eta)\frac{1}{\xi}\frac{\mathrm{d}}{\mathrm{d}\xi}\Phi_m^n(\xi) - m(m+1)\,\mathcal{G}_0(\eta)P_m^n(\eta)\frac{1}{\xi^2}\Phi_m^n(\xi)\right\}\cos n\phi \\[2mm]
& -\sum_{m=0}^{\infty}\sum_{n=1}^{m}\left\{\mathcal{G}_1(\eta)P_m^n(\eta)\frac{\mathrm{d}^2}{\mathrm{d}\xi^2}\psi_m^n(\xi) + [2\mathcal{G}_1(\eta) + \mathcal{G}_2(\eta) - \mathcal{G}_3(\eta)]\frac{1}{\xi}\frac{\mathrm{d}}{\mathrm{d}\xi}\psi_m^n(\xi)\right. \\[2mm]
& \left. -\frac{\mathcal{G}_2(\eta)}{\eta}(1-\eta^2)\frac{\mathrm{d}}{\mathrm{d}\eta}P_m^n(\eta)\frac{1}{\xi}\frac{\mathrm{d}}{\mathrm{d}\xi}\psi_m^n(\xi) - m(m+1)\,\mathcal{G}_0(\eta)P_m^n(\eta)\frac{1}{\xi^2}\psi_m^n(\xi)\right\}\sin n\phi \\[2mm]
& = E\sum_{m=0}^{\infty}\left\{[\mathcal{G}_0(\eta)]^2\sum_{n=0}^{m}P_m^n(\eta)\Phi_m^n(\xi)\cos n\phi + \sum_{n=1}^{m}P_m^n(\eta)\psi_m^n(\xi)\sin n\phi\right\}.
\end{aligned}
\tag{2.20}
$$

The range of the index n of the inner sums involved in this equation depends on the index m of the outer sums, otherwise one could easily get rid of one summation using the orthogonality of the trigonometric functions over $[0,2\pi]$. On the other hand, notice that, one can reorder the two double sums as $\sum_{n=0}^{\infty}\sum_{m=n}^{\infty}$ and $\sum_{n=1}^{\infty}\sum_{m=n}^{\infty}$ respectively, bearing in mind the relation between the indices n and m. Then we multiply (2.20) by $\cos n\phi$ for $n = 0, 1, \ldots$ and by $\sin n\phi$ for $n = 1, 2, \ldots$ and integrate with respect to ϕ over $[0,2\pi]$. This yields

$$
\begin{aligned}
& -\sum_{m=n}^{\infty}\left\{\mathcal{G}_1(\eta)P_m^n(\eta)\frac{\mathrm{d}^2}{\mathrm{d}\xi^2}\Phi_m^n(\xi) + [2\mathcal{G}_1(\eta) + \mathcal{G}_2(\eta) - \mathcal{G}_3(\eta)]P_m^n(\eta)\frac{1}{\xi}\frac{\mathrm{d}}{\mathrm{d}\xi}\Phi_m^n(\xi)\right. \\[2mm]
& \left. -\frac{\mathcal{G}_2(\eta)}{\eta}(1-\eta^2)\frac{\mathrm{d}}{\mathrm{d}\eta}P_m^n(\eta)\frac{1}{\xi}\frac{\mathrm{d}}{\mathrm{d}\xi}\Phi_m^n(\xi) - m(m+1)\,\mathcal{G}_0(\eta)P_m^n(\eta)\frac{1}{\xi^2}\Phi_m^n(\xi)\right\} \\[2mm]
& = E\sum_{m=n}^{\infty}[\mathcal{G}_0(\eta)]^2\,P_m^n(\eta)\Phi_m^n(\xi)
\end{aligned}
\tag{2.21}
$$

16

for $n = 0, 1, 2, \ldots$ and

$$-\sum_{m=n}^{\infty} \left\{ \mathcal{G}_1(\eta) P_m^n(\eta) \frac{\mathrm{d}^2}{\mathrm{d}\xi^2} \psi_m^n(\xi) + [2\mathcal{G}_1(\eta) + \mathcal{G}_2(\eta) - \mathcal{G}_3(\eta)] P_m^n(\eta) \frac{1}{\xi} \frac{\mathrm{d}}{\mathrm{d}\xi} \psi_m^n(\xi) \right.$$

$$\left. - \frac{\mathcal{G}_2(\eta)}{\eta}(1 - \eta^2) \frac{\mathrm{d}}{\mathrm{d}\eta} P_m^n(\eta) \frac{1}{\xi} \frac{\mathrm{d}}{\mathrm{d}\xi} \psi_m^n(\xi) - m(m+1) \, \mathcal{G}_0(\eta) P_m^n(\eta) \frac{1}{\xi^2} \psi_m^n(\xi) \right\} \qquad (2.22)$$

$$= E \sum_{m=n}^{\infty} [\mathcal{G}_0(\eta)]^2 \, P_m^n(\eta) \psi_m^n(\xi)$$

for $n = 1, 2, \ldots$ in the virtue of the orthogonality of the trigonometric functions.

The two equation sets (2.21) and (2.22) for the Fourier coefficient functions Φ_m^n and ψ_m^n are independent of each other. This is a result of the axial symmetry of the region which allows a separation of the expansion (2.15) into two parts containing even and odd eigenfunctions in ϕ. Moreover (2.21) and (2.22) are identical for each $n \in \mathbb{Z}^+$, i.e., $\Phi_m^n(\xi) = \psi_m^n(\xi)$ for $n \in \mathbb{Z}^+$. Hereafter, we consider only the equations for $\Phi_m^n(\xi)$. By means of the differential-difference relation [1]

$$(1 - \eta^2) \frac{\partial}{\partial \eta} P_m^n(\eta) = (m+1)\eta P_m^n(\eta) - (m - n + 1) P_{m+1}^n(\eta)$$

it is possible to get rid of the derivative of $P_m^n(\eta)$ and obtain

$$-\sum_{m=n}^{\infty} \left\{ \mathcal{G}_1(\eta) P_m^n(\eta) \frac{\mathrm{d}^2}{\mathrm{d}\xi^2} \Phi_m^n(\xi) + [\mathcal{G}_1(\eta) - m\mathcal{G}_2(\eta) - \mathcal{G}_3(\eta)] P_m^n(\eta) \frac{1}{\xi} \frac{\mathrm{d}}{\mathrm{d}\xi} \Phi_m^n(\xi) \right.$$

$$\left. + \frac{\mathcal{G}_2(\eta)}{\eta}(m - n + 1) P_{m+1}^n(\eta) \frac{1}{\xi} \frac{\mathrm{d}}{\mathrm{d}\xi} \Phi_m^n(\xi) - m(m+1)\mathcal{G}_0(\eta) P_m^n(\eta) \frac{1}{\xi^2} \Phi_m^n(\xi) \right\}$$

$$= E \sum_{m=n}^{\infty} [\mathcal{G}_0(\eta)]^2 \, P_m^n(\eta) \Phi_m^n(\xi)$$

$$(2.23)$$

for every $n = 0, 1, 2, \ldots$. In our further analysis we will treat equation (2.23) for a fixed n keeping in mind that $n = 0, 1, \ldots$.

2.3 Reduction to a System of Ordinary Differential Equations

An eigenfunction expansion of the type (2.15) makes it possible to reduce a partial differential equation to a system of ordinary differential equations [54, 16]. The technical details of such a reduction, which leads to an infinite system of coupled ordinary differential equations for the functions $\Phi_m^n(\xi)$ will be introduced in this section.

Let us consider the η-dependent expressions in equation (2.23). The polynomials $\mathcal{G}_i(\eta)$ involved in these expressions can be written as

$$\mathcal{G}_i(\eta) = \sum_{k=0}^{2K} g_{i,k}\eta^k \tag{2.24}$$

for $i = 0, 1, 2, 3$. Rewriting the truncated shape function $G(\eta)$ in the form $G(\eta) = \sum_{k=0}^{K} \alpha_k \eta^k$, where $\alpha_0 = 1$ and using the definitions of $\mathcal{G}_i(\eta)$ given in (2.18), we compute the coefficients $g_{i,k}$ as

$$
\begin{aligned}
g_{0,k} &= \sum_{t=0}^{k} \alpha_t \alpha_{k-t} & k = 0, 1, \ldots, 2K \\
g_{1,k} &= \sum_{t=0}^{k} \alpha_t \alpha_{k-t} + (t+1)(k-t+1)\alpha_{t+1}\alpha_{k-t+1} & k = 0, 1 \\
g_{1,k} &= \sum_{t=0}^{k} \alpha_t \alpha_{k-t} + (t+1)(k-t+1)\alpha_{t+1}\alpha_{k-t+1} & \\
&\quad - \sum_{t=0}^{k-2} (t+1)(k-t-1)\alpha_{t+1}\alpha_{k-t-1} & k = 2, 3, \ldots, 2K-2 \\
g_{1,k} &= \sum_{t=0}^{k} \alpha_t \alpha_{k-t} - \sum_{t=0}^{k-2} (t+1)(k-t-1)\alpha_{t+1}\alpha_{k-t-1} & k = 2K-1, 2K \\
g_{2,0} &= 0 & \\
g_{2,k} &= 2\sum_{t=0}^{k} (k-t+1)\alpha_t \alpha_{k-t+1} & k = 1, 2, \ldots, 2K
\end{aligned}
$$

$$
\begin{aligned}
g_{3,k} &= \sum_{t=0}^{k}(k-t+1)(k-t+2)\alpha_t\alpha_{k-t+2} & k=0,1 \\
g_{3,k} &= \sum_{t=0}^{k}(k-t+1)(k-t+2)\alpha_t\alpha_{k-t+2} & \\
&\quad -\sum_{t=0}^{k-2}(k-t-1)(k-t)\alpha_t\alpha_{k-t} & k=2,3,\ldots,2K-2 \\
g_{3,k} &= -\sum_{t=0}^{k-2}(k-t-1)(k-t)\alpha_t\alpha_{k-t} & k=2K-1,2K
\end{aligned}
\tag{2.25}
$$

where clearly $\alpha_0 = 1$ and $\alpha_r = 0$ for all $r = K+1, K+2, \ldots, 2K$. The right-hand-side of (2.23) contains $[\mathcal{G}_0(\eta)]^2$, which can be explicitly written as

$$
[\mathcal{G}_0(\eta)]^2 = \sum_{k=0}^{4K} g_{4,k}\eta^k, \qquad g_{4,k} = \sum_{t=0}^{k} g_{0,t}g_{0,k-t}, \qquad k=0,1,\ldots,4K.
\tag{2.26}
$$

Now, using (2.24) and (2.26), we rewrite equation (2.23) in the form

$$
\begin{aligned}
-\sum_{m=n}^{\infty}&\left\{\left[\sum_{k=0}^{2K} g_{1,k}\eta^k P_m^n(\eta)\right]\frac{\mathrm{d}^2}{\mathrm{d}\xi^2}\Phi_m^n(\xi)\right. \\
&+\left[\sum_{k=0}^{2K}(2g_{1,k}-mg_{2,k}-g_{3,k})\eta^k P_m^n(\eta) + (m-n+1)\sum_{k=0}^{2K-1} g_{2,k+1}\eta^k P_{m+1}^n(\eta)\right]\frac{1}{\xi}\frac{\mathrm{d}}{\mathrm{d}\xi}\Phi_m^n(\xi) \\
&\left.-m(m+1)\left[\sum_{k=0}^{2K} g_{0,k}\eta^k P_m^n(\eta)\right]\frac{1}{\xi^2}\Phi_m^n(\xi)\right\} = E\sum_{m=n}^{\infty}\left\{\left[\sum_{k=0}^{4K} g_{4,k}\eta^k P_m^n(\eta)\right]\Phi_m^n(\xi)\right\}
\end{aligned}
\tag{2.27}
$$

The product $\eta^k P_m^n(\eta)$ can be expanded into a series of $P_l^n(\eta)$,

$$
\eta^k P_m^n(\eta) = \sum_{l=n}^{\infty}\gamma_{l,m,k}^{(n)}P_l^n(\eta),
\tag{2.28}
$$

where

$$
\gamma_{m,l,k}^{(n)} = \int_{-1}^{1}\eta^k P_m^n(\eta)P_l^n(\eta)\mathrm{d}\eta.
\tag{2.29}
$$

Evaluation of the coefficients $\gamma_{l,m,k}^{(n)}$ is much easier than it looks, thanks to the recurrence relation of the associated Legendre functions [7],

$$
\eta P_m^n(\eta) = \frac{m-n+1}{2m+1}P_{m+1}^n + \frac{m+n}{2m+1}P_{m-1}^n.
\tag{2.30}
$$

Clearly, the computation of $\gamma_{l,m,0}^{(n)}$ is sufficient to obtain all the other coefficients $\gamma_{l,m,k}^{(n)}$ up to any desired degree k. The orthogonality relation of the associated Legendre

19

functions on the other hand, determines $\gamma_{l,m,0}^{(n)}$ as

$$\gamma_{l,m,0}^{(n)} = \int_{-1}^{1} P_m^n(\eta) P_l^n(\eta) \mathrm{d}\eta = \frac{2}{(2m+1)} \frac{(m+n)!}{(m-n)!} \delta_{l,m} \qquad (2.31)$$

where $\delta_{l,m}$ stands for Kronecker's delta. We employ (2.28) and define the matrices $\mathbf{A}^n := \left[a_{l,m}^n \right]$, $\mathbf{B}^n := \left[b_{l,m}^n \right]$, $\mathbf{C}^n := \left[c_{l,m}^n \right]$ and $\mathbf{D}^n := \left[d_{l,m}^n \right]$ with entries

$$
\begin{aligned}
a_{l,m}^n &= \sum_{k=0}^{2K} g_{1,k} \gamma_{l,m,k}^{(n)} \\
b_{l,m}^n &= \sum_{k=0}^{2K} \left(2g_{1,k} - m g_{2,k} - g_{3,k} \right) \gamma_{l,m,k}^{(n)} + (m-n+1) \sum_{k=0}^{2K-1} g_{2,k+1} \gamma_{l,m+1,k}^{(n)} \\
c_{l,m}^n &= m(m+1) \sum_{k=0}^{2K} g_{0,k} \gamma_{l,m,k}^{(n)} \\
d_{l,m}^n &= \sum_{k=0}^{4K} g_{4,k} \gamma_{l,m,k}^{(n)}
\end{aligned}
\qquad (2.32)
$$

where n is fixed. Notice that in the definition of the matrices, the superscript "n" is used merely as a notation and cannot mean the power. Thus, equation (2.27) turns out to be

$$\sum_{l=n}^{\infty} \left\{ \sum_{m=n}^{\infty} \left[a_{l,m}^n \frac{\mathrm{d}^2}{\mathrm{d}\xi^2} \Phi_m^n(\xi) + b_{l,m}^n \frac{1}{\xi} \frac{\mathrm{d}}{\mathrm{d}\xi} \Phi_m^n(\xi) - c_{l,m}^n \frac{1}{\xi^2} \Phi_m^n(\xi) + E d_{l,m}^n \Phi_m^n(\xi) \right] \right\} P_l^n(\eta) = 0.$$

Since the set $\left\{ P_n^n(\eta), P_{n+1}^n(\eta), P_{n+2}^n(\eta), \ldots \right\}$ is linearly independent for a fixed n, we must have

$$\sum_{m=n}^{\infty} \left[a_{l,m}^n \frac{\mathrm{d}^2}{\mathrm{d}\xi^2} \Phi_m^n(\xi) + b_{l,m}^n \frac{1}{\xi} \frac{\mathrm{d}}{\mathrm{d}\xi} \Phi_m^n(\xi) - c_{l,m}^n \frac{1}{\xi^2} \Phi_m^n(\xi) + E d_{l,m}^n \Phi_m^n(\xi) \right] = 0, \qquad (2.33)$$

for each $l = n, n+1, \ldots$, and fixed n. That is, we obtain an infinite system of coupled ordinary differential equations for the determination of the coefficient functions $\Phi_n^n(\xi)$, $\Phi_{n+1}^n(\xi)$, ... In matrix-vector form the system is written as

$$\left\{ \mathbf{A}^n \frac{\mathrm{d}^2}{\mathrm{d}\xi^2} + \mathbf{B}^n \frac{1}{\xi} \frac{\mathrm{d}}{\mathrm{d}\xi} - \mathbf{C}^n \frac{1}{\xi^2} \right\} \mathbf{\Phi}^n = -E \mathbf{D}^n \mathbf{\Phi}^n \qquad (2.34)$$

where $\mathbf{\Phi}^n$ stands for the vector

$$\mathbf{\Phi}^n = \left[\Phi_n^n(\xi), \Phi_{n+1}^n(\xi), \Phi_{n+2}^n(\xi), \ldots \right]^T. \qquad (2.35)$$

20

This vector differential equation cannot have an exact analytical solution unless the matrices $\mathbf{A}^n$, $\mathbf{B}^n$, $\mathbf{C}^n$ and $\mathbf{D}^n$ are diagonal. Then the ordinary differential equations (ODEs) will be uncoupled, i.e., they will be independent of each other. Unfortunately, this happens only in the special case of the spherical billiard which will be discussed in detail later.

For a complete reformulation of the problem, we need to redefine the boundary and square integrability conditions in accordance with the vector differential equation just obtained.

2.4   Transformation of the Boundary and Square Integrability Conditions

In the previous section, we have discussed how the transformation (2.3) changes the form of the equation (1.14). In addition, we have asserted an expansion for the wavefunction into the complete set of spherical harmonics which has reduced the partial differential equation under consideration to a system of coupled ordinary differential equations. What remains to be investigated is how the transformation changes the boundary and square integrability conditions. Let us first deal with the boundary condition (1.15). Upon substitution of the expansion (2.15) it becomes

$$\sum_{m=0}^{\infty} \left\{ \Phi_m^0(1) P_m^0(\eta) + \sum_{n=1}^{m} P_m^n(\eta) \left[\Phi_m^n(1) \cos n\phi + \psi_m^n(1) \sin n\phi \right] \right\} = 0 \qquad (2.36)$$

where $\eta \in [-1, 1]$ and $\phi \in [0, 2\pi]$. This immediately gives

$$\Phi_m^n(1) = 0, \qquad \psi_m^n(1) = 0 \qquad (2.37)$$

for all $n = 0, 1, \ldots, m$ and $m = 0, 1, \ldots$ since the spherical harmonics are linearly independent. Recall that, for purposes of determination of an expansion basis, we have used the fact that the wavefunction satisfies a square integrability condition of the form (2.9). Now substitute (2.15) in (2.9) and deduce that

$$\int_0^{2\pi} \int_{-1}^{1} \int_0^1 \left| \sum_{m=0}^{\infty} \sum_{n=0}^{m} P_m^n(\eta) \Phi_m^n(\xi) \cos n\phi + \sum_{m=0}^{\infty} \sum_{n=1}^{m} P_m^n(\eta) \psi_m^n(\xi) \sin n\phi \right|^2 \xi^2 \mathrm{d}\xi \mathrm{d}\eta \mathrm{d}\phi < \infty$$

which is equivalent to

$$
\int_0^{2\pi} \int_{-1}^1 \int_0^1 \sum_{m=0}^\infty \sum_{l=0}^\infty \left\{ \sum_{n=0}^m \sum_{t=0}^m \Phi_m^n(\xi) \Phi_l^t(\xi) P_m^n(\eta) P_l^t(\eta) \cos n\phi \cos t\phi \right.
$$
$$
+ \sum_{n=0}^m \sum_{t=1}^m \Phi_m^n(\xi) \psi_l^t(\xi) P_m^n(\eta) P_l^t(\eta) \cos n\phi \sin t\phi
$$
$$
+ \left. \sum_{n=1}^m \sum_{t=1}^m \psi_m^n(\xi) \psi_l^t(\xi) P_m^n(\eta) P_l^t(\eta) \sin n\phi \sin t\phi \right\} \xi^2 \mathrm{d}\xi \mathrm{d}\eta \mathrm{d}\phi < \infty.
$$

Interchanging formally the summation and integration with respect to ϕ and using the orthogonality of trigonometric functions we obtain

$$
\int_{-1}^1 \int_0^1 \sum_{m=0}^\infty \sum_{l=0}^\infty \left\{ \sum_{n=0}^m \Phi_m^n(\xi) \Phi_l^n(\xi) P_m^n(\eta) P_l^n(\eta) \right.
$$
$$
+ \left. \sum_{n=1}^m \psi_m^n(\xi) \psi_l^n(\xi) P_m^n(\eta) P_l^n(\eta) \right\} \xi^2 \mathrm{d}\xi \mathrm{d}\eta < \infty.
$$

Similarly, the orthogonality of the associated Legendre functions implies that

$$
\int_0^1 \sum_{m=0}^\infty \left\{ \sum_{n=0}^m (\Phi_m^n(\xi))^2 + \sum_{n=1}^m (\psi_m^n(\xi))^2 \right\} \xi^2 \mathrm{d}\xi < \infty. \tag{2.38}
$$

A necessary condition for (2.38) is

$$
\int_0^1 \sum_{m=0}^\infty \sum_{n=0}^m (\Phi_m^n(\xi))^2 \xi^2 \mathrm{d}\xi < \infty \tag{2.39}
$$

from which

$$
\int_0^1 \xi^2 |\Phi_m^n(\xi)|^2 \mathrm{d}\xi < \infty \tag{2.40}
$$

is easily concluded for $n = 0, 1, \ldots m$ and $m = 0, 1, 2, \ldots$.

2.5 The Special Case of Spherical Billiard and the Truncated System of ODEs

In this section we discuss a special case in which the axisymmetric billiard under consideration reduces into a ball of unit radius. This billiard is usually called "spherical

billiard". In this case, the shape function is simply $F(\eta) = G(\eta) = 1$. Therefore, the entries of the coefficient matrices are defined by

$$a^n_{l,m} = \gamma^{(n)}_{l,m,0}, \qquad b^n_{l,m} = 2\gamma^{(n)}_{l,m,0}, \qquad c^n_{l,m} = m(m+1)\gamma^{(n)}_{l,m,0}, \qquad d^n_{l,m} = \gamma^{(n)}_{l,m,0}$$

which immediately tells us that they should satisfy the relations

$$\mathbf{B}^n = 2\mathbf{A}^n, \qquad \mathbf{C}^n = \mathbf{M}^n \mathbf{A}^n, \qquad \mathbf{D}^n = \mathbf{A}^n$$

where

$$\mathbf{M}^n = \mathrm{diag}\left\{ n(n+1), \ (n+1)(n+2), \ (n+2)(n+3), \ \ldots \right\}.$$

The definition of $\gamma^{(n)}_{l,m,0}$ on the other hand, implies that the matrix $\mathbf{A}^n$ is diagonal, that is,

$$\mathbf{A}^n = \mathrm{diag}\left\{ \gamma^{(n)}_{n,n,0}, \gamma^{(n)}_{n+1,n,0}, \gamma^{(n)}_{n+2,n,0}, \cdots \right\}.$$

Note that, this matrix is nonsingular, since none of its diagonal entries is zero. Hence, the vector differential equation for the spherical billiard upon multiplication of both sides by the inverse of $\mathbf{A}^n$ becomes

$$\left\{ \mathbf{I}\frac{\mathrm{d}^2}{\mathrm{d}\xi^2} + 2\mathbf{I}\frac{1}{\xi}\frac{\mathrm{d}}{\mathrm{d}\xi} - \mathbf{M}^n\frac{1}{\xi^2} \right\} \mathbf{\Phi}^n = -E\mathbf{\Phi}^n \tag{2.41}$$

where $\mathbf{I}$ denotes the identity matrix. Thus, we have a system of uncoupled ODEs for every fixed n. The functions $\Phi^n_m(\xi)$ satisfy the boundary conditions

$$\Phi^n_m(1) = 0 \qquad \text{for} \qquad m = n, n+1, n+2, \ldots \tag{2.42}$$

and the square integrability conditions

$$\int_0^1 |\Phi^n_m(\xi)|^2\, \xi^2 \mathrm{d}\xi \qquad \text{for} \qquad m = n, n+1, n+2, \ldots. \tag{2.43}$$

Observe that, the system in (2.41) can be completely characterized by the single differential equation

$$\left\{ \frac{\mathrm{d}^2}{\mathrm{d}\xi^2} + 2\frac{1}{\xi}\frac{\mathrm{d}}{\mathrm{d}\xi} - m(m+1)\frac{1}{\xi^2} \right\} \Phi^n_m(\xi) = -E\Phi^n_m(\xi) \tag{2.44}$$

where m takes the values $n, n+1, n+2, \ldots$. The general solution of this equation is known to be

$$\Phi^n_m(\xi) = c_1 j_m(\sqrt{E}\xi) + c_2 j_{-m}(\sqrt{E}\xi)$$

where $j_\nu(x)$ denote the so-called spherical Bessel function defined by [1]

$$j_\nu(x) = \sqrt{\frac{2}{\pi x}} J_{\nu+\frac{1}{2}}(x)$$

in which $J_\mu(x)$ is the usual Bessel function of the first kind of order μ. The square integrability condition does not hold for the second solution $j_{-m}(\sqrt{E}\xi)$, which is rejected. Therefore, we must take

$$\Phi_m^n(\xi) = j_m(\sqrt{E}\xi).$$

On the other hand, the boundary condition implies that,

$$\Phi_m^n(1) = j_m(\sqrt{E}) = 0,$$

determining the eigenvalues,

$$E_{m,p} = \lambda_{m,p}^2 \qquad \text{for} \qquad m = n, n+1, \dots \quad \text{and} \quad p = 1, 2, \dots$$

where $\lambda_{m,p}$ stands for the p-th positive zero of j_m, or equivalently of $J_{m+\frac{1}{2}}$.

The spherical billiard is the only exactly solvable billiard amongst the axisymmetric billiards defined by the general shape function $F(\eta)$. Therefore, we seek for approximate solutions of the system (2.34) in finite-dimensional subspaces. More specifically, we assume that the index m varies from 0 to some $M < \infty$. Then we have

$$\sum_{m=n}^{M} \left[a_{l,m}^n \frac{\mathrm{d}^2}{\mathrm{d}\xi^2} \Phi_m^n(\xi) + b_{l,m}^n \frac{1}{\xi} \frac{\mathrm{d}}{\mathrm{d}\xi} \Phi_m^n(\xi) - c_{l,m}^n \frac{1}{\xi^2} \Phi_m^n(\xi) + E d_{l,m}^n \Phi_m^n(\xi) \right] = 0, \quad (2.45)$$

for $l = n, n+1, \dots, M$, where n is fixed. In this case the range of the index n is also $[0, M]$. An important point to bear in mind is that the dimension of the truncated system (2.45) is not the same for each n. In fact, it decreases as n varies from 0 to M and we have $M+1$ equations for $n = 0$, M equations for $n = 1$ and finally one equation for $n = M$. It is also convenient to apply shifting transformations of the form

$$\begin{aligned} i &= l - n + 1, & i &= 1, 2, \dots, M+1-n \\ j &= m - n + 1, & j &= 1, 2, \dots, M+1-n, \end{aligned} \qquad (2.46)$$

for the entries of the coefficient matrices and the vector $\mathbf{\Phi}^n$, which give the usual indexing of these entries. Letting $N = M + 1 - n$ we obtain the system

$$\sum_{j=1}^{N} \left[\widehat{a}_{i,j}^n \frac{\mathrm{d}^2}{\mathrm{d}\xi^2} \widehat{\Phi}_j^n(\xi) + \widehat{b}_{i,j}^n \frac{1}{\xi} \frac{\mathrm{d}}{\mathrm{d}\xi} \widehat{\Phi}_j^n(\xi) - \widehat{c}_{i,j}^n \frac{1}{\xi^2} \widehat{\Phi}_j^n(\xi) + E \widehat{d}_{i,j}^n \widehat{\Phi}_j^n(\xi) \right] = 0 \qquad (2.47)$$

24

where $i = 1, 2, \ldots, N$ and

$$
\begin{aligned}
\widehat{a}_{i,j}^n &:= a_{l,m}^n \\
\widehat{b}_{i,j}^n &:= b_{l,m}^n \\
\widehat{c}_{i,j}^n &:= c_{l,m}^n \\
\widehat{d}_{i,j}^n &:= d_{l,m}^n \\
\widehat{\Phi}_j^n &:= \Phi_m^n.
\end{aligned}
\tag{2.48}
$$

Explicitly, we have the following truncated system of ODEs

$$
\begin{bmatrix}
\mathcal{L}_{1,1}^n & \mathcal{L}_{1,2}^n & \cdots & \mathcal{L}_{1,N}^n \\
\mathcal{L}_{2,1}^n & \mathcal{L}_{2,2}^n & \cdots & \mathcal{L}_{2,N}^n \\
\vdots & \vdots & \ddots & \vdots \\
\mathcal{L}_{N,1}^n & \mathcal{L}_{N,2}^n & \cdots & \mathcal{L}_{N,N}^n
\end{bmatrix}
\begin{bmatrix}
\widehat{\Phi}_1^n \\
\widehat{\Phi}_2^n \\
\vdots \\
\widehat{\Phi}_N^n
\end{bmatrix}
= -E
\begin{bmatrix}
\widehat{d}_{1,1}^n & \widehat{d}_{1,2}^n & \cdots & \widehat{d}_{1,N}^n \\
\widehat{d}_{2,1}^n & \widehat{d}_{2,2}^n & \cdots & \widehat{d}_{2,N}^n \\
\vdots & \vdots & \ddots & \vdots \\
\widehat{d}_{N,1}^n & \widehat{d}_{N,2}^n & \cdots & \widehat{d}_{N,N}^n
\end{bmatrix}
\begin{bmatrix}
\widehat{\Phi}_1^n \\
\widehat{\Phi}_2^n \\
\vdots \\
\widehat{\Phi}_N^n
\end{bmatrix}
\tag{2.49}
$$

where $\mathcal{L}_{i,j}^n$ is a differential operator of the form

$$
\mathcal{L}_{i,j}^n = \widehat{a}_{i,j}^n \frac{\mathrm{d}^2}{\mathrm{d}\xi^2} + \widehat{b}_{i,j}^n \frac{1}{\xi} \frac{\mathrm{d}}{\mathrm{d}\xi} - \widehat{c}_{i,j}^n \frac{1}{\xi^2}
\tag{2.50}
$$

for $i, j = 1, 2, \ldots, N$ and fixed n. The functions Φ_i^n satisfy the boundary conditions

$$
\Phi_i^n(1) = 0 \qquad i = 1, 2, \ldots, N
\tag{2.51}
$$

and the square integrability conditions

$$
\int_0^1 |\Phi_i^n(\xi)|^2 \, \xi^2 \mathrm{d}\xi \qquad i = 1, 2, \ldots, N.
\tag{2.52}
$$

Remark 2. It is evident from (2.30) that,

$$
\gamma_{l,m,k}^{(n)} = \frac{m - n + 1}{2m + 1} \gamma_{l,m+1,k-1}^{(n)} + \frac{m + n}{2m + 1} \gamma_{l,m-1,k-1}^{(n)}.
\tag{2.53}
$$

The largest degree k of the $\gamma_{l,m,k}^{(n)}$ required for evaluation of the matrices (2.32) is $4K$. Hence, for each $k = 0, 1, \ldots 4K$ the following arrays must be computed,

$$
\begin{bmatrix}
\gamma_{-1,-1,k}^{(n)} & \gamma_{-1,0,k}^{(n)} & \gamma_{-1,1,k}^{(n)} & \gamma_{-1,2,k}^{(n)} & \cdots & \gamma_{-1,M+4K-k,k}^{(n)} \\
\gamma_{0,-1,k}^{(n)} & \gamma_{0,0,k}^{(n)} & \gamma_{0,1,k}^{(n)} & \gamma_{0,2,k}^{(n)} & \cdots & \gamma_{0,M+4K-k,k}^{(n)} \\
\gamma_{1,-1,k}^{(n)} & \gamma_{1,0,k}^{(n)} & \gamma_{1,1,k}^{(n)} & \gamma_{1,2,k}^{(n)} & \cdots & \gamma_{1,M+4K-k,k}^{(n)} \\
\gamma_{2,-1,k}^{(n)} & \gamma_{2,0,k}^{(n)} & \gamma_{2,1,k}^{(n)} & \gamma_{2,2,k}^{(n)} & \cdots & \gamma_{2,M+4K-k,k}^{(n)} \\
\vdots & \vdots & \vdots & \vdots & \ddots & \vdots \\
\gamma_{M+4K-k,-1,k}^{(n)} & \gamma_{M+4K-k,0,k}^{(n)} & \gamma_{M+4K-k,1,k}^{(n)} & \gamma_{M+4K-k,2,k}^{(n)} & \cdots & \gamma_{M+4K-k,M+4K-k,k}^{(n)}
\end{bmatrix}
$$

where M is the dimension of the finite-dimensional subspace on which the problem will be solved. $\diamondsuit$

2.6 Investigation of the Coefficient Matrices

Further development of the method will be performed after a detailed investigation of the coefficient matrices. Their entries have been defined in (2.32) in terms of the coefficients $g_{i,k}$ and the elements of the three-dimensional array $\gamma_{l,m,k}^{(n)}$. This form is well suited for rapid computer calculation. However, to study the properties of these matrices, we use their interpretations in terms of the truncated shape function itself,

$$a_{l,m}^n = \int_{-1}^1 \left\{ [G(\eta)]^2 + (1 - \eta^2) [G'(\eta)]^2 \right\} P_l^n(\eta) P_m^n(\eta) \mathrm{d}\eta \qquad (2.54)$$

$$\begin{aligned} b_{l,m}^n = {} & \int_{-1}^1 \left\{ 2 [G(\eta)]^2 + 2(1 - \eta^2) [G'(\eta)]^2 + 2\eta G'(\eta) G(\eta) \right. \\ & \left. - (1 - \eta^2) G''(\eta) G(\eta) \right\} P_l^n(\eta) P_m^n(\eta) \mathrm{d}\eta \\ & - 2 \int_{-1}^1 (1 - \eta^2) G'(\eta) G(\eta) P_l^n(\eta) \frac{\mathrm{d}}{\mathrm{d}\eta} P_m^n(\eta) \mathrm{d}\eta \end{aligned} \qquad (2.55)$$

$$c_{l,m}^n = m(m+1) \int_{-1}^1 [G(\eta)]^2 P_l^n(\eta) P_m^n(\eta) \mathrm{d}\eta \qquad (2.56)$$

and

$$d_{l,m}^n = \int_{-1}^1 [G(\eta)]^4 P_l^n(\eta) P_m^n(\eta) \mathrm{d}\eta \qquad (2.57)$$

where $l, m = n, n+1, \ldots$ and n is fixed. Some important properties of the coefficient matrices will be stated and proved now.

Proposition 2.1. *The matrices* $\mathbf{A}^n, \mathbf{D}^n$ *and the matrix* $\mathbf{C}_1^n := \left[(c_1)_{l,m}^n \right]$ *defined by*

$$(c_1)_{l,m}^n = \int_{-1}^1 [G(\eta)]^2 P_l^n(\eta) P_m^n(\eta) \, d\eta, \qquad (2.58)$$

are symmetric positive definite.

Proof. The symmetry follows easily from the definitions (2.54), (2.57) and (2.58). Consider the quadratic forms Q_A, Q_D and Q_C related to the matrices $\mathbf{A}^n$, $\mathbf{D}^n$ and $\mathbf{C}_1^n$ respectively,

$$\begin{aligned} Q_A &= \mathbf{x}^T \mathbf{A}^n \mathbf{x} \qquad &(2.59) \\ Q_D &= \mathbf{x}^T \mathbf{D}^n \mathbf{x} \qquad &(2.60) \\ Q_C &= \mathbf{x}^T \mathbf{C}_1^n \mathbf{x} \qquad &(2.61) \end{aligned}$$

26

where $\mathbf{x}$ is a nonzero vector. The definitions (2.54), (2.57) and (2.58) imply

$$Q_A = \sum_{l=n}^{\infty}\sum_{m=n}^{\infty} x_l x_m \int_{-1}^{1} \left[\{G(\eta)\}^2 + (1-\eta^2)[G'(\eta)]^2 \right] P_l^n(\eta) P_m^n(\eta) \mathrm{d}\eta,$$

$$Q_D = \sum_{l=n}^{\infty}\sum_{m=n}^{\infty} x_l x_m \int_{-1}^{1} [G(\eta)]^4 \, P_l^n(\eta) P_m^n(\eta) \mathrm{d}\eta \tag{2.62}$$

$$Q_C = \sum_{l=n}^{\infty}\sum_{m=n}^{\infty} x_l x_m \int_{-1}^{1} [G(\eta)]^2 \, P_l^n(\eta) P_m^n(\eta) \mathrm{d}\eta$$

Define the function $h(\eta)$ as

$$h(\eta) = \sum_{m=n}^{\infty} x_m P_m^n(\eta) \tag{2.63}$$

and use it to rewrite (2.62) in the form

$$\begin{aligned}
Q_A &= \int_{-1}^{1} [h(\eta)]^2 \left\{ [G(\eta)]^2 + (1-\eta^2)[G'(\eta)]^2 \right\} \mathrm{d}\eta, \\
Q_D &= \int_{-1}^{1} [h(\eta)]^2 [G(\eta)]^4 \, \mathrm{d}\eta \\
Q_C &= \int_{-1}^{1} [h(\eta)]^2 [G(\eta)]^2 \, \mathrm{d}\eta.
\end{aligned} \tag{2.64}$$

Clearly, all the integrals in (2.64) are positive, for, the integrand functions are non-negative and not identically zero. Hence, the matrices $\mathbf{A}^n$ and $\mathbf{D}^n$ and $\mathbf{C}_1^n$ are positive definite. $\qquad\square$

Proposition 2.2. *The matrix $\mathbf{B}^n$ can be written as $\mathbf{B}^n = 2\mathbf{A}^n + \mathbf{B}_P^n + \mathbf{B}_S^n$, where $\mathbf{B}_P^n$ is symmetric positive semidefinite matrix and $\mathbf{B}_S^n$ is a skew-symmetric matrix.*

Proof. Observe that

$$-\frac{\mathrm{d}}{\mathrm{d}\eta} \left\{ (1-\eta^2)G'(\eta)G(\eta) \right\}$$

$$= 2\eta G'(\eta)G(\eta) - (1-\eta^2)G''(\eta)G(\eta) - (1-\eta^2)[G'(\eta)]^2.$$

Now, add and subtract the term $\int_{-1}^{1} (1-\eta^2)[G'(\eta)]^2 \, P_l^n(\eta) P_m^n(\eta) \mathrm{d}\eta$ to the right hand

side of (2.55)

$$b_{l,m}^n = \int_{-1}^{1} \left\{ 2\left[G(\eta)\right]^2 + 2(1-\eta^2)\left[G'(\eta)\right]^2 \right\} P_l^n(\eta) P_m^n(\eta) \mathrm{d}\eta$$

$$+ \int_{-1}^{1} (1-\eta^2)\left[G'(\eta)\right]^2 P_l^n(\eta) P_m^n(\eta) \mathrm{d}\eta$$

(2.65)

$$- \int_{-1}^{1} \frac{\mathrm{d}}{\mathrm{d}\eta}\left[(1-\eta^2)G'(\eta)G(\eta)\right] P_m^n(\eta) P_l^n(\eta) \mathrm{d}\eta$$

$$- 2\int_{-1}^{1} (1-\eta^2)G'(\eta)G(\eta) P_l^n(\eta) \frac{\mathrm{d}}{\mathrm{d}\eta} P_m^n(\eta) \mathrm{d}\eta$$

The first integral in (2.65) is exactly $2a_{l,m}^n$. Denote the second integral by $(b_P)_{l,m}^n$ and the sum of the last two by $(b_S)_{l,m}^n$, where $(b_P)_{l,m}^n$ and $(b_S)_{l,m}^n$ are regarded as the entries of the matrices $\mathbf{B}_P^n$ and $\mathbf{B}_S^n$ respectively. Positive semidefiniteness of $\mathbf{B}_P^n$ can be easily proven using the method of the proof of Proposition 2.1. The quadratic form $\mathbf{x}^T\mathbf{B}_P^n\mathbf{x} \geq 0$ and the equality holds only in the case $G(\eta)$=constant, which corresponds to the exactly solvable case of a spherical billiard, where we actually have $\mathbf{B}^n = 2\mathbf{A}^n$. Consider now

$$(b_S)_{l,m}^n = - \int_{-1}^{1} \frac{\mathrm{d}}{\mathrm{d}\eta}\left[(1-\eta^2)G'(\eta)G(\eta)\right] P_m^n(\eta) P_l^n(\eta)$$

(2.66)

$$- 2\int_{-1}^{1} (1-\eta^2)G'(\eta)G(\eta) P_l^n(\eta) \frac{\mathrm{d}}{\mathrm{d}\eta} P_m^n(\eta) \mathrm{d}\eta.$$

With

$$U = P_l^n(\eta) P_m^n(\eta) \qquad\qquad \mathrm{d}U = \left\{\left[P_l^n(\eta)\right]' P_m^n(\eta) + \left[P_m^n(\eta)\right]' P_l^n(\eta)\right\} \mathrm{d}\eta$$
$$\mathrm{d}V = \frac{\mathrm{d}}{\mathrm{d}\eta}\left[(1-\eta^2)G'(\eta)G(\eta)\right] \mathrm{d}\eta \quad V = \left[(1-\eta^2)G'(\eta)G(\eta)\right]$$

(2.67)

we apply integration by parts to evaluate the first integral

$$(b_S)_{l,m}^n = - (1-\eta^2)G'(\eta)G(\eta) P_l^n(\eta) P_m^n(\eta)\Big|_{-1}^{1}$$

$$+ \int_{-1}^{1} (1-\eta^2)G'(\eta)G(\eta) \left\{\left[P_l^n(\eta)\right]' P_m^n(\eta) + \left[P_m^n(\eta)\right]' P_l^n(\eta)\right\} \mathrm{d}\eta \quad\text{(2.68)}$$

$$- 2\int_{-1}^{1} (1-\eta^2)G'(\eta)G(\eta) \left[P_m^n(\eta)\right]' P_l^n(\eta) \mathrm{d}\eta.$$

From the last equation the entries of $\mathbf{B}_S^n$ are found to be

$$(b_S)_{l,m}^n = \int_{-1}^1 (1-\eta)^2 G'(\eta)G(\eta)\left\{[P_l^n(\eta)]' P_m^n(\eta) - [P_m^n(\eta)]' P_l^n(\eta)\right\}\mathrm{d}\eta \qquad (2.69)$$

so that the matrix is obviously skew-symmetric. Hence, the proof is complete. $\qquad\square$

Remark 3. Notice that Propositions 2.1 and 2.2 hold also for the shifted matrices $\widehat{\mathbf{A}}^n$, $\widehat{\mathbf{B}}^n$, $\widehat{\mathbf{C}}^n$ and $\widehat{\mathbf{D}}^n$. $\qquad\qquad\diamond$

2.7 Truncated Solution in One Dimensional Subspace

As a first approximation, we deal with the truncated solution of the problem in one-dimensional subspace. In other words, we assume M=0, or equivalently, N=1. Then the system in (2.47) reduces to a single differential equation of the form

$$a\frac{\mathrm{d}^2\widehat{\Phi}_1^0(\xi)}{\mathrm{d}\xi^2} + b\frac{1}{\xi}\frac{\mathrm{d}\widehat{\Phi}_1^0(\xi)}{\mathrm{d}\xi} - c\frac{1}{\xi^2}\widehat{\Phi}_1^0(\xi) + Ed\widehat{\Phi}_1^0(\xi) = 0 \qquad (2.70)$$

where the accompanying boundary condition reads as

$$\widehat{\Phi}_1^0(1) = 0, \qquad (2.71)$$

and the square integrability condition is

$$\int_0^1 \xi^2 \mid \widehat{\Phi}_1^0(\xi) \mid^2 \mathrm{d}\xi < \infty. \qquad (2.72)$$

Here we have set

$$a = \widehat{a}_{1,1}^0, \quad b = \widehat{b}_{1,1}^0 \quad c = \widehat{c}_{1,1}^0, \quad d = \widehat{d}_{1,1}^0. \qquad (2.73)$$

The coefficient a is, in fact, a leading principal submatrix of dimension 1 of the matrix $\widehat{\mathbf{A}}^0$. By Proposition 2.1, a must be positive. Similarly, by Proposition 2.2, $b = 2a + b_P + b_S$, where $b_P = (\widehat{b}_P)_{1,1}^0 \geq 0$ and $b_S = (\widehat{b}_S)_{1,1}^0 = 0$ implies $2 \leq \dfrac{b}{a} \leq 3$. On the other hand, by Proposition 2.1, $c \geq 0$ and $\dfrac{d}{a} > 0$. Upon dividing both sides by a we get,

$$\frac{\mathrm{d}^2\widehat{\Phi}_1^0(\xi)}{\mathrm{d}\xi^2} + \frac{b}{a}\frac{1}{\xi}\frac{\mathrm{d}\widehat{\Phi}_1^0(\xi)}{\mathrm{d}\xi} - \frac{c}{a}\frac{1}{\xi^2}\widehat{\Phi}_1^0(\xi) + E\frac{d}{a}\widehat{\Phi}_1^0(\xi) = 0. \qquad (2.74)$$

We propose a solution $\widehat{\Phi}_1^0(\xi)$ of the form

$$\widehat{\Phi}_1^0(\xi) = \xi^\mu Z(\xi) \tag{2.75}$$

where $\mu \in \mathbb{R}$. It can be easily shown that the function $Z(\xi)$ satisfies the differential equation

$$\frac{d^2 Z(\xi)}{d\xi^2} + \left[2\mu + \frac{b}{a} \right] \frac{1}{\xi} \frac{dZ(\xi)}{d\xi} + \left[\mu(\mu-1) + \mu\frac{b}{a} - \frac{c}{a} \right] \frac{1}{\xi^2} Z(\xi) + E\frac{d}{a} Z(\xi) = 0, \tag{2.76}$$

the boundary condition

$$Z(1) = 0, \tag{2.77}$$

and the square integrability condition

$$\int_0^1 \xi^{2+2\mu} \mid Z(\xi) \mid^2 d\xi < \infty. \tag{2.78}$$

Define now

$$\mu = \frac{1}{2}\left(1 - \frac{b}{a}\right) \qquad \nu = \sqrt{\mu^2 + \frac{c}{a}}$$

and note that $-1 \leq \mu \leq -\frac{1}{2}$ and also that $0 < \nu$. The linear transformation

$$x = \lambda\xi, \quad \text{where } \lambda = \sqrt{E\frac{d}{a}} > 0,$$

on the independent variable ξ yields the equation

$$\frac{d^2 Z(x)}{dx^2} + \frac{1}{x}\frac{dZ(x)}{dx} + \left(1 - \frac{\nu^2}{x^2}\right) Z(x) = 0, \tag{2.79}$$

the boundary condition

$$Z(\lambda) = 0 \tag{2.80}$$

and the square integrability condition

$$\int_0^\lambda x^{2+2\mu} \mid Z(x) \mid^2 dx < \infty. \tag{2.81}$$

The equation (2.79) can be recognized as the Bessel's differential equation, the general solution of which is given by

$$Z(x) = c_1 J_\nu(x) + c_2 J_{-\nu}(x). \tag{2.82}$$

Since the order ν is positive and moreover $\nu = \sqrt{\mu^2 + \frac{c}{a}} \geq |\mu|$, $J_\nu(x)$ satifies the condition (2.81), while the second solution $J_{-\nu}(x)$ does not, and, is thus rejected.

Finally, the boundary condition (2.80) requires $J_\nu\left(\sqrt{E\frac{d}{a}}\right) = 0$ and the eigenvalues E are obtained as

$$E_p = \frac{a}{d}\lambda_p^2, \qquad p = 1, 2, \ldots$$

where λ_p's are the positive roots of the equation $J_\nu(\lambda) = 0$.

2.8 Reduction of the System to a Matrix Eigenvalue Problem

The exact solution of the truncated system in one-dimensional subspace can be used as a hint while searching for solutions in finite-dimensional subspaces of dimension $N > 1$. In other words, it is expected that the coefficient functions $\Phi_m^n(\xi)$ in the eigenfunction expansion (2.15) will be represented in terms of Bessel functions, more precisely, in terms of Fourier-Bessel expansions. Unfortunately, the orders of the Bessel functions are closely related to the parameters α_k defining the shape function, which is one unpleasant consequence of using the non-orthogonal coordinates (2.3) and inserting the shape function into the Schrödinger equation.

Recall that the coefficient matrix $\widehat{\mathbf{A}}^n$ is positive definite by Proposition 2.1. Then according to the Cholesky decomposition theorem [58], $\widehat{\mathbf{A}}^n = \mathbf{L}\mathbf{L}^T$ where $\mathbf{L}$ is a lower triangular matrix with positive diagonal entries. Let

$$\mathbf{Z}^n(\xi) = \mathbf{L}^T\widehat{\boldsymbol{\Phi}}^n(\xi). \tag{2.83}$$

This immediately implies that $\mathbf{Z}^n(\xi)$ satisfies the vector differential equation

$$-\left\{\mathbf{L}\frac{\mathrm{d}^2}{\mathrm{d}\xi^2} + \widehat{\mathbf{B}}^n\mathbf{L}^{-T}\frac{1}{\xi}\frac{\mathrm{d}}{\mathrm{d}\xi} - \widehat{\mathbf{C}}^n\mathbf{L}^{-T}\frac{1}{\xi^2}\right\}\mathbf{Z}^n = E\widehat{\mathbf{D}}^n\mathbf{L}^{-T}\mathbf{Z}^n \tag{2.84}$$

the boundary condition

$$\mathbf{Z}^n(1) = [Z_1^n 1, Z_2^n(1), \ldots, Z_N^n(1)]^T = \mathbf{0} \tag{2.85}$$

and the square integrability condition

$$\int_0^1 |Z_i^n(\xi)|^2 \xi^2 \mathrm{d}\xi \qquad \text{for} \qquad i = 1, 2, \ldots, N. \tag{2.86}$$

Note that the existence of $\mathbf{L}^{-T}$ is guaranteed by the positive definiteness of $\widehat{\mathbf{A}}^n$. Multiplying both sides of (2.84) by $\mathbf{L}^{-1}$, we obtain

$$-\left\{\mathbf{I}\frac{\mathrm{d}^2}{\mathrm{d}\xi^2} + \mathbf{Q}^n\frac{1}{\xi}\frac{\mathrm{d}}{\mathrm{d}\xi} - \mathbf{R}^n\frac{1}{\xi^2}\right\}\mathbf{Z}^n = E\mathbf{T}^n\mathbf{Z}^n \qquad (2.87)$$

where the matrices $\mathbf{Q}^n := \left[q_{i,j}^n\right]$, $\mathbf{R}^n := \left[r_{i,j}^n\right]$ and $\mathbf{T}^n := \left[t_{i,j}^n\right]$ are defined by

$$\begin{aligned} \mathbf{Q}^n &= \mathbf{L}^{-1}\widehat{\mathbf{B}}^n\mathbf{L}^{-T} \\ \mathbf{R}^n &= \mathbf{L}^{-1}\widehat{\mathbf{C}}^n\mathbf{L}^{-T} \\ \mathbf{T}^n &= \mathbf{L}^{-1}\widehat{\mathbf{D}}^n\mathbf{L}^{-T} \end{aligned} \qquad (2.88)$$

and $\mathbf{I}$ denotes the identity matrix. In scalar form (2.87) becomes

$$-\sum_{j=1}^{N}\left\{\delta_{i,j}\frac{\mathrm{d}^2}{\mathrm{d}\xi^2} + q_{i,j}^n\frac{1}{\xi}\frac{\mathrm{d}}{\mathrm{d}\xi} - r_{i,j}^n\frac{1}{\xi^2}\right\}\mathbf{Z}_j^n = E\sum_{j=1}^{N}t_{i,j}^n\mathbf{Z}_j^n \qquad (2.89)$$

where $i = 1, 2, \ldots, N$ and n is fixed. The differential operators $\mathcal{H}_{i,j}^n$

$$\mathcal{H}_{i,j}^n = \delta_{i,j}\frac{\mathrm{d}^2}{\mathrm{d}\xi^2} + q_{i,j}^n\frac{1}{\xi}\frac{\mathrm{d}}{\mathrm{d}\xi} - r_{i,j}^n\frac{1}{\xi^2} \qquad (2.90)$$

for $i, j = 1, 2, \ldots, N$ and fixed n can be employed now to write (2.89) in matrix form as well

$$-\begin{bmatrix} \mathcal{H}_{1,1}^n & \cdots & \mathcal{H}_{1,N}^n \\ \mathcal{H}_{2,1}^n & \cdots & \mathcal{H}_{2,N}^n \\ \vdots & \ddots & \vdots \\ \mathcal{H}_{N,1}^n & \cdots & \mathcal{H}_{N,N}^n \end{bmatrix}\begin{bmatrix} Z_1^n \\ Z_2^n \\ \vdots \\ Z_N^n \end{bmatrix} = E\begin{bmatrix} t_{1,1}^n & \cdots & t_{1,N}^n \\ t_{2,1}^n & \cdots & t_{2,N}^n \\ \vdots & \ddots & \vdots \\ t_{N,1}^n & \cdots & t_{N,N}^n \end{bmatrix}\begin{bmatrix} Z_1^n \\ Z_2^n \\ \vdots \\ Z_N^n \end{bmatrix}. \qquad (2.91)$$

The following propositions are needed for further analysis.

Proposition 2.3. *The diagonal entries of the matrix $\mathbf{Q}^n$ satisfy $2 \leq q_{i,i}^n \leq 3$ for all $i = 1, 2, \ldots N$.*

Proof. By Proposition 2.2, the matrix $\mathbf{Q}^n$ is in the form $\mathbf{Q}^n = 2\mathbf{I} + \mathbf{Q}_P^n + \mathbf{Q}_S^n$, where $\mathbf{Q}_P^n = \mathbf{L}^{-1}\widehat{\mathbf{B}}_P^n\mathbf{L}^{-T}$ is a symmetric positive semidefinite matrix and $\mathbf{Q}_S^n = \mathbf{L}^{-1}\widehat{\mathbf{B}}_S^n\mathbf{L}^{-T}$ is a skew-symmetric matrix. Positive semidefiniteness of $\mathbf{Q}_P^n$ is easily seen from

$$\mathbf{x}^T\mathbf{L}^{-1}\widehat{\mathbf{B}}_P^n\mathbf{L}^{-T}\mathbf{x} = \mathbf{y}^T\widehat{\mathbf{B}}_P^n\mathbf{y} \geq 0$$

by taking $\mathbf{y} = \mathbf{L}^{-T}\mathbf{x}$, for every $\mathbf{x} \neq 0$. On the other hand,

$$\mathbf{Q}_S^{nT} = (\mathbf{L}^{-1}\widehat{\mathbf{B}}_S^n \mathbf{L}^{-T})^T = -\mathbf{L}^{-1}\widehat{\mathbf{B}}_S^n \mathbf{L}^{-T} = -\mathbf{Q}_S^n$$

shows that $\mathbf{Q}_S^n$ is skew-symmetric. Then $q_{i,i}^n$ satisfies

$$q_{i,i}^n = 2 + (q_P)_{i,i}^n \geq 2$$

where $(q_P)_{i,i}^n \geq 0$, since $\mathbf{Q}_P^n$ is positive semidefinite. Recall now the definition of $\widehat{\mathbf{C}}_1^n$ given in Proposition 2.1 and note that $\widehat{\mathbf{A}}^n = \widehat{\mathbf{B}}_P^n + \widehat{\mathbf{C}}_1^n$, consequently,

$$\mathbf{I} = \mathbf{Q}_P^n + \mathbf{L}^{-1}\widehat{\mathbf{C}}_1^n \mathbf{L}^{-T}.$$

Thus, $0 \leq (q_P)_{i,i}^n \leq 1$, since the matrix $\mathbf{L}^{-1}\widehat{\mathbf{C}}_1^n \mathbf{L}^{-T}$ is also positive definite. Hence,

$$2 \leq q_{i,i}^n \leq 3$$

easily follows for each $i = 1, 2, \ldots, N$. □

Proposition 2.4. *The diagonal entries of the matrix $\mathbf{R}^n$ are nonnegative.*

Proof. Since

$$\mathbf{R}^n = \mathbf{L}^{-1}\widehat{\mathbf{C}}^n \mathbf{L}^{-T}$$

then its diagonal entries are expressible as

$$r_{i,i}^n = (i + n - 1)(i + n)(r_1)_{i,i}^n$$

where $(r_1)_{i,i}^n$ are the entries of the matrix $\mathbf{R}_1^n = \mathbf{L}^{-1}\widehat{\mathbf{C}}_1^n{}^n \mathbf{L}^{-T}$. This matrix is positive definite, therefore, the diagonal entries of $\mathbf{R}^n$ are all positive except $r_{1,1}^0$ which is 0. Thus, they are nonnegative. □

We assume that the solutions Z_i^n of (2.91) are of the form

$$Z_i^n(\xi) = \xi^{\mu_i^n} X_i^n(\xi), \quad \text{for all } i = 1, 2, \ldots N \tag{2.92}$$

where

$$\mu_i^n = \frac{1}{2}\left(1 - q_{i,i}^n\right), \quad \text{for all } i = 1, 2, \ldots, N \tag{2.93}$$

It follows from Proposition 2.3 that $-1 < \mu_i^n \leq -\frac{1}{2}$ for all $i = 1, 2, \ldots, N$. Define

$$\nu_i^n = \sqrt{(\mu_i^n)^2 + r_{i,i}^n} \quad \text{for all } i = 1, 2, \ldots N, \tag{2.94}$$

and observe that ν_i^n is real and positive by Proposition 2.4. Then we calculate

$$\mathcal{H}_{i,i}^n \xi^{\mu_i^n} X_i^n(\xi) = \xi^{\mu_i^n} \left\{ \frac{d^2}{d\xi^2} + \frac{1}{\xi} \frac{d}{d\xi} - \frac{(\nu_i^n)^2}{\xi^2} \right\} X_i^n(\xi) \tag{2.95}$$

and also

$$\mathcal{H}_{i,j}^n \xi^{\mu_j^n} X_j^n(\xi) = \xi^{\mu_j^n} \left\{ q_{i,j}^n \frac{1}{\xi} \frac{d}{d\xi} + \left[\mu_j^n q_{i,j}^n - r_{i,j}^n \right] \frac{1}{\xi^2} \right\} X_j^n(\xi). \tag{2.96}$$

Consider now the equation

$$\left\{ \frac{d^2}{d\xi^2} + \frac{1}{\xi} \frac{d}{d\xi} + \left(\lambda^2 - \frac{(\nu_i^n)^2}{\xi^2} \right) \right\} X_i^n(\xi) = 0$$

and observe that it has two linearly independent solutions, namely, Bessel functions of the first kind $J_{\pm\nu_i^n}(\lambda\xi)$. The definition (2.94) of the order ν_i^n implies $\nu_i^n \geq | \mu_i^n |$, hence $\nu_i^n \geq \frac{1}{2}$ and $-\nu_i^n < -1$. The boundary conditions (2.85) satisfied by the $X_i^n(\xi)$ are of the form

$$X_i^n(1) = 0 \tag{2.97}$$

while the square integrability conditions (2.86) read as

$$\int_0^1 \xi^{2+2\mu_i^n} |X_i^n(\xi)|^2 \, d\xi < \infty \tag{2.98}$$

for every $i = 1, 2, \ldots, N$. Thus, the functions $X_i^n(\xi)$ must be square integrable over the interval $[0,1]$ with respect to the weight function $w(\xi) = \xi^{2+2\mu_i^n}$. On the other hand, $0 \leq 2 + 2\mu_i^n \leq 1$, therefore, we have

$$\int_0^1 \xi \, |X_i^n(\xi)|^2 \, d\xi \leq \int_0^1 \xi^{2+2\mu_i^n} |X_i^n(\xi)|^2 \, d\xi < \infty. \tag{2.99}$$

In other words, the $X_i^n(\xi)$ can be regarded as square integrable functions over $[0,1]$ under the weight $w(\xi) = \xi$. The set $\left\{ J_{\nu_i^n}(\lambda_{i,1}\xi), J_{\nu_i^n}(\lambda_{i,2}\xi), J_{\nu_i^n}(\lambda_{i,3}\xi), \ldots \right\}$ forms a basis for this space, provided that $\nu_i^n \geq -\frac{1}{2}$ and $\lambda_{i,p}$ are the positive zeros of $J_{\nu_i^n}$. This suggests expanding each of the functions $X_i^n(\xi)$ into a Fourier-Bessel expansion in terms of $J_{\nu_i^n}$, that is, we propose

$$X_i^n(\xi) = \sum_{p=1}^{\infty} x_{i,p}^n J_{\nu_i^n}(\lambda_{i,p}\xi) \tag{2.100}$$

where the $x_{i,p}^n$ are the Fourier coefficients. Moreover,

$$X_i^n(1) = \sum_{p=1}^{\infty} x_{i,p}^n J_{\nu_i^n}(\lambda_{i,p}) = 0$$

that is, the expansion (2.100) satisfies the boundary condition. It is obvious that

$$\mathcal{H}_{i,i}^n \xi^{\mu_i^n} X_i^n(\xi) = \xi^{\mu_i^n} \sum_{p=1}^\infty (-\lambda_{i,p}^2) x_{i,p}^n J_{\nu_i^n}(\lambda_{i,p}\xi) \qquad (2.101)$$

for every $i = 1, 2, \ldots, N$. The differential expression (2.96) on the other hand, upon substitution of the expansion (2.100) becomes

$$
\begin{aligned}
\mathcal{H}_{i,j}^n \xi^{\mu_j^n} X_j^n(\xi) &= \xi^{\mu_j^n} \left(q_{i,j}^n \mu_j^n - r_{i,j}^n \right) \frac{1}{\xi^2} \sum_{p=1}^\infty x_{j,p}^n J_{\nu_j^n}(\lambda_{j,p}\xi) \\
&+ \xi^{\mu_j^n} q_{i,j}^n \frac{1}{\xi} \sum_{p=1}^\infty x_{j,p}^n \frac{\mathrm{d}}{\mathrm{d}\xi} J_{\nu_j^n}(\lambda_{j,p}\xi) \\
&= \xi^{\mu_j} s_{i,j}^n \frac{1}{\xi^2} \sum_{p=1}^\infty x_{j,p}^n J_{\nu_j^n}(\lambda_{j,p}\xi) - \xi^{\mu_j^n} \lambda_{j,p} q_{i,j}^n \frac{1}{\xi} \sum_{p=1}^\infty x_{j,p}^n J_{\nu_j^n+1}(\lambda_{j,p}\xi)
\end{aligned}
$$
$$(2.102)$$

where the difference-differential relation

$$\frac{\mathrm{d}}{\mathrm{d}\xi} J_\nu(\lambda\xi) = \frac{\nu}{\xi} J_\nu(\lambda\xi) - \lambda J_{\nu+1}(\lambda\xi)$$

avoids the derivative $\dfrac{\mathrm{d}}{\mathrm{d}\xi} J_{\nu_j^n}(\lambda_{j,p}\xi)$ and the matrix $\mathbf{S}^n := \left[s_{i,j}^n \right]$ defined by

$$s_{i,j}^n = q_{i,j}^n (\mu_j^n + \nu_j^n) - r_{i,j}^n$$

shortens the expression. For computational purposes, we must truncate the expansion (2.100), so, we take $p = 1, 2, \ldots, P$. Now, we use (2.101) and (2.102) to rewrite the system (2.89) as

$$
\begin{aligned}
- \sum_{j=1, j\neq i}^N \left\{ \sum_{p=1}^P \xi^{\mu_j^n} \left[s_{i,j}^n \frac{1}{\xi^2} J_{\nu_j^n}(\lambda_{j,p}\xi) x_{j,p}^n - q_{i,j}^n \frac{1}{\xi} J_{\nu_j^n+1}(\lambda_{j,p}\xi) \right] x_{j,p}^n \right\} \\
- \sum_{p=1}^P \left[(-\lambda_{i,p}^2) \xi^{\mu_i^n} J_{\nu_i^n}(\lambda_{i,p}\xi) x_{i,p}^n \right] = -E \sum_{j=1}^N \sum_{p=1}^P \left[t_{i,j}^n \xi^{\mu_j^n} J_{\nu_j^n}(\lambda_{j,p}\xi) x_{j,p}^n \right]
\end{aligned}
$$
$$(2.103)$$

for $i = 1, 2, \ldots, N$ and fixed n. Last, we multiply the i-th equation in (2.103) by $\xi^{1-\mu_i^n} J_{\nu_i^n}(\lambda_{i,s})$ where $s = 1, 2, \ldots P$ and $i = 1, 2, \ldots, N$ and integrate over $[0, 1]$. The orthogonality relation of the Bessel functions,

$$\int_0^1 \xi J_{\nu_t^n}(\lambda_{t,p}\xi) J_{\nu_t^n}(\lambda_{t,s}\xi) \mathrm{d}\xi = \frac{\left[J_{\nu_t^n+1}(\lambda_{t,p}) \right]^2}{2} \delta_{p,s} \qquad (2.104)$$

implies that

$$
\sum_{j=1}^{N}\sum_{p=1}^{P}\left\{\frac{\lambda_{i,s}^{2}}{2}\left[J_{\nu_{i}^{n}+1}(\lambda_{i,s})\right]^{2}\delta_{p,s}\delta_{i,j}\right.
$$

$$
-\left[s_{i,j}^{n}\int_{0}^{1}\xi^{\mu_{j}^{n}-\mu_{i}^{n}-1}J_{\nu_{i}^{n}}(\lambda_{i,s}\xi)J_{\nu_{j}^{n}}(\lambda_{j,p}\xi)\mathrm{d}\xi\right.
$$

$$
\left.\left.-q_{i,j}^{n}\lambda_{j,k}\int_{0}^{1}\xi^{\mu_{j}^{n}-\mu_{i}^{n}}J_{\nu_{i}^{n}}(\lambda_{i,s}\xi)J_{\nu_{j}^{n}+1}(\lambda_{j,p}\xi)\mathrm{d}\xi\right](1-\delta_{i,j})\right\}x_{j,p}^{n} \tag{2.105}
$$

$$
=E\sum_{j=1}^{N}\sum_{p=1}^{P}\left[t_{i,j}^{n}\int_{0}^{1}\xi^{\mu_{j}^{n}-\mu_{i}^{n}+1}J_{\nu_{i}^{n}}(\lambda_{i,s}\xi)J_{\nu_{j}^{n}}(\lambda_{j,p}\xi)\mathrm{d}\xi\right]x_{j,p}^{n}
$$

for every $i=1,2,\ldots N$ and $s=1,2,\ldots P$. In fact, we have replaced every operator $\mathcal{H}_{i,j}^{n}$ by its matrix representation, say $\mathbf{H}_{i,j}^{n}:=\left[h_{i,j,p,s}^{n}\right]$, in the basis set $\{\xi^{\mu_{i}^{n}}J_{\nu_{i}^{n}}(\lambda_{i,p})\}_{p=1}^{P}$. By using the notation

$$
\mathcal{I}(\rho,\nu,\sigma,\alpha,\beta)=\int_{0}^{1}\xi^{\rho}J_{\nu}(\alpha\xi)J_{\sigma}(\beta\xi)\mathrm{d}\xi \tag{2.106}
$$

for the integrals involved in (2.105) it can be easily seen that

$$
h_{i,j,p,s}^{n}=\begin{cases}\dfrac{\lambda_{i,s}^{2}}{2}\left[J_{\nu_{i}^{n}+1}(\lambda_{i,s})\right]^{2}\delta_{p,s} & \text{if } i=j\\[2ex]
-s_{i,j}^{n}\mathcal{I}(\mu_{j}^{n}-\mu_{i}^{n}-1,\nu_{i}^{n},\nu_{j}^{n},\lambda_{i,s},\lambda_{j,p})\\[2ex]
+q_{i,j}^{n}\lambda_{j,k}\mathcal{I}(\mu_{j}^{n}-\mu_{i}^{n},\nu_{i}^{n},\nu_{j}^{n}+1,\lambda_{i,s},\lambda_{j,p}) & \text{if } i\neq j\end{cases} \tag{2.107}
$$

Consider now the right-hand-side of (2.105). If we define the matrices $\mathbf{W}_{i,j}^{n}:=\left[w_{i,j,p,s}^{n}\right]$ as

$$
w_{i,j,p,s}^{n}=\begin{cases}\dfrac{t_{i,i}^{n}}{2}\left[J_{\nu_{i}^{n}+1}(\lambda_{i,s})\right]^{2}\delta_{p,s} & \text{if } i=j\\[2ex]
t_{i,j}^{n}\mathcal{I}(\mu_{j}^{n}-\mu_{i}^{n}+1,\nu_{i}^{n},\nu_{j}^{n},\lambda_{i,s},\lambda_{j,p}) & \text{if } i\neq j\end{cases} \tag{2.108}
$$

and the vectors $\mathbf{x}_{i}^{n}$ as

$$
\mathbf{x}_{i}^{n}=\left[x_{i,1}^{n},x_{i,2}^{n},\ldots,(x_{i,P}^{n}\right]^{T}
$$

36

then (2.91) becomes

$$
\begin{bmatrix} \mathbf{H}_{1,1}^n & \cdots & \mathbf{H}_{1,N}^n \\ \mathbf{H}_{2,1}^n & \cdots & \mathbf{H}_{2,N}^n \\ \vdots & \ddots & \vdots \\ \mathbf{H}_{N,1}^n & \cdots & \mathbf{H}_{N,N}^n \end{bmatrix} \begin{bmatrix} \mathbf{x}_1^n \\ \mathbf{x}_2^n \\ \vdots \\ \mathbf{x}_N^n \end{bmatrix} = E \begin{bmatrix} \mathbf{W}_{1,1}^n & \cdots & \mathbf{W}_{1,N}^n \\ \mathbf{W}_{2,1}^n & \cdots & \mathbf{W}_{2,N}^n \\ \vdots & \ddots & \vdots \\ \mathbf{W}_{N,1}^n & \cdots & \mathbf{W}_{N,N}^n \end{bmatrix} \begin{bmatrix} \mathbf{x}_1^n \\ \mathbf{x}_2^n \\ \vdots \\ \mathbf{x}_N^n \end{bmatrix}. \tag{2.109}
$$

The transformations

$$
\begin{aligned}
t &= (i-1)P + s & t = 1,2,\ldots NP \\
r &= (j-1)P + p & r = 1,2,\ldots NP
\end{aligned} \tag{2.110}
$$

on the indices can be employed to write block matrices and the block vector in (2.109) in the usual matrix and vector forms. More precisely, we set

$$
\begin{aligned}
\widehat{h}_{t,r}^n &= h_{i,j,p,s}^n \\
\widehat{w}_{t,r}^n &= w_{i,j,p,s}^n \\
\widehat{x}_r^n &= x_{j,p}^n
\end{aligned} \tag{2.111}
$$

so that (2.109) becomes

$$
\widehat{\mathbf{H}}^n \widehat{\mathbf{x}}^n = E \widehat{\mathbf{W}}^n \widehat{\mathbf{x}}^n \tag{2.112}
$$

Hence, we have finally transformed the Schrödinger equation to a generalized eigenvalue problem. As a matter of fact, it is expected that the matrices involved in (2.112) are symmetric and moreover that, the matrix $\widehat{\mathbf{W}}^n$ is positive definite. However, the non-orthogonal transformation (2.3) destroys these properties. Thus, we need to compute of the whole matrices $\widehat{\mathbf{H}}^n$ and $\widehat{\mathbf{W}}^n$.

Unfortunately, the integrals (2.106) involved in the definitions of $\widehat{\mathbf{H}}^n$ and $\widehat{\mathbf{W}}^n$ cannot be evaluated analytically by means of recurrence relations of the Bessel functions. This is the second and more serious drawback of the method. Theoretically, these integrals have been proven to be proper and finite. On the other hand, their numerical computation is a very difficult task. The detailed discussion about this subject is given in Chapter 4.

CHAPTER 3

TWO EXAMPLES: PROLATE SPHEROID AND A PARAMETER-DEPENDING BILLIARD

3.1 Prolate Spheroidal Billiard: Solution by the Method of Chapter 2

As a first application of the method, we consider the three dimensional billiard obtained by rotating an ellipse

$$\frac{y^2}{a^2} + \frac{z^2}{b^2} = 1, \quad \text{with} \quad 0 < a \le b \tag{3.1}$$

in the yz-plane about the z-axis. The solid region formed in this way is called prolate spheroid and in Cartesian coordinates can be written as

$$\mathcal{D} = \left\{ (x, y, z) \mid \frac{x^2 + y^2}{a^2} + \frac{z^2}{b^2} \le 1 \right\} \tag{3.2}$$

where $b^2 > a^2$, while in spherical coordinates takes the form

$$\mathcal{D} = \left\{ (r, \theta, \phi) \mid 0 \le r \le \frac{a}{\sqrt{1 - \beta \cos^2 \theta}}, 0 \le \theta \le \pi, 0 \le \phi \le 2\pi \right\} \tag{3.3}$$

with $\beta = 1 - \dfrac{a^2}{b^2}$. Obviously, $0 \le \beta < 1$ and the particular case $\beta = 0$ corresponds to a ball with radius a. The shape function

$$f(\theta) = \frac{a}{\sqrt{1 - \beta \cos^2 \theta}}$$

can be expanded into a power series in powers of $\cos\theta$ using the Binomial theorem

$$\frac{a}{\sqrt{1-\beta\cos^2\theta}} = a + 2a\sum_{k=1}^{\infty}\frac{\beta^k}{4^k}\frac{\Gamma(2k)}{\Gamma(k)\Gamma(k-1)}\cos^{2k}\theta \qquad (3.4)$$

for consistency with the general form (2.2). Therefore, the function $F(\eta)$ becomes

$$F(\eta) = a + 2a\sum_{k=1}^{\infty}\frac{\beta^k}{4^k}\frac{\Gamma(2k)}{\Gamma(k)\Gamma(k-1)}\eta^{2k} \qquad (3.5)$$

consequently, the truncated shape function $G(\eta)$ is

$$G(\eta) = a + 2a\sum_{k=1}^{K}\frac{\beta^k}{4^k}\frac{\Gamma(2k)}{\Gamma(k)\Gamma(k-1)}\eta^{2k}. \qquad (3.6)$$

The symmetric structure of $\mathcal{D}$ with respect to the xy-plane, or equivalently with respect to $\eta = 0$ verifies the lack of odd powers of η in (3.6) where clearly $\alpha_{2k+1} = 0$ and $\alpha_{2k} = 2a\dfrac{\beta^k}{4^k}\dfrac{\Gamma(2k)}{\Gamma(k)\Gamma(k-1)}$ for all $k = 1, 2, \dots K$. Recall that, the definitions of the coefficient matrices $\mathbf{A}^n$, $\mathbf{B}^n$, $\mathbf{C}^n$ and $\mathbf{D}^n$ have been based on the coefficients $\gamma_{l,m,k}^{(n)}$ of the expansion

$$\eta^k P_m^n(\eta) = \sum_{l=n}^{\infty}\gamma_{l,m,k}^{(n)}P_l^n(\eta)$$

and the coefficients $g_{i,k}$ of the polynomials $\mathcal{G}_i$ where i=0,1,2,3. The shape function $G(\eta)$ describing the prolate spheroid contains only even powers of η, hence, the polynomials $\mathcal{G}_i$ have the same structure. The product $G'(\eta)G(\eta)$ on the other hand, includes only odd powers of η. The polynomial part of the associated Legendre function

$$P_m^n(\eta) = \left(1-\eta^2\right)^{\frac{n}{2}}\frac{\mathrm{d}^n P_m(\eta)}{\mathrm{d}\eta^n},$$

that is, $\dfrac{\mathrm{d}^n P_m(\eta)}{\mathrm{d}\eta^n}$, contains only even or only odd powers of η in accordance with its degree. Therefore, the expansions

$$\eta^{2k} P_m^n(\eta) = \sum_{l=n}^{\infty}\gamma_{l,m,2k}^{(n)}P_l^n(\eta)$$

involved in the definitions in the coefficient matrices of the prolate spheroid have nonvanishing coefficients $\gamma_{l,m,2k}^{(n)}$ whenever l and m are both even or odd. Similarly, the coefficients $\gamma_{l,m+1,2k-1}^{(n)}$ of the expansions

$$\eta^{2k-1} P_{m+1}^n(\eta) = \sum_{l=n}^{\infty}\gamma_{l,m+1,2k-1}^{(n)}P_l^n(\eta)$$

taking place in the definition of $\mathbf{B}^n$ are nonzero if l is even and $m + 1$ is odd or l is odd and $m + 1$ is even. Thus, all the matrices $\mathbf{A}^n$, $\mathbf{B}^n$, $\mathbf{C}^n$, and $\mathbf{D}^n$ possess a special structure, that is,

$$
\begin{bmatrix}
\text{x} & 0 & \text{x} & 0 & \text{x} & \cdots \\
0 & \text{x} & 0 & \text{x} & 0 & \cdots \\
\text{x} & 0 & \text{x} & 0 & \text{x} & \cdots \\
0 & \text{x} & 0 & \text{x} & 0 & \cdots \\
\text{x} & 0 & \text{x} & 0 & \text{x} & \cdots \\
\vdots & \vdots & \vdots & \vdots & \vdots & \ddots
\end{bmatrix}
\tag{3.7}
$$

where x denotes the nonzero entries. This suggests the separate treatment of the even and odd eigenfunctions in η. Recall that we have already taken only the even eigenfunctions in ϕ. In fact, we have split the expansion (2.15) as

$$
\Psi(\xi, \eta, \phi) = \sum_{m=0}^{\infty} \sum_{n=0}^{m} \Phi_m^n(\xi) P_m^n(\eta) \cos n\phi + \sum_{m=0}^{\infty} \sum_{n=1}^{m} \psi_m^n(\xi) P_m^n(\eta) \sin n\phi
$$

and have considered only the first part, say $\Psi(\xi, \eta, \phi)_e$. Now, we decompose $\Psi(\xi, \eta, \phi)_e$ as

$$
\Psi(\xi, \eta, \phi)_e = \sum_{m=0}^{\infty} \sum_{n=0}^{m} \Phi_{2m}^n(\xi) P_{2m}^n(\eta) \cos n\phi + \sum_{m=0}^{\infty} \sum_{n=0}^{m} \Phi_{2m+1}^n(\xi) P_{2m+1}^n(\eta) \cos n\phi \tag{3.8}
$$

where the first sum contains even eigenfunctions in η and the second one odd eigenfunctions in η. In numerical computations we deal with the two parts of (3.8) independently and obtain two different sets of eigenvalues. This procedure is not necessary from mathematical point of view, however, the statistical analysis must be performed on eigenvalue sets that are not correlated, therefore, each symmetry class needs individual investigation.

In what follows, we employ our method to calculate the spectrum of three particular prolate spheroids with $a = 1$, $b = 1.01$, $a = 1$, $b = 1.5$ and $a = 1$, $b = 2$ (see Figures 3.1, 3.2, 3.3).
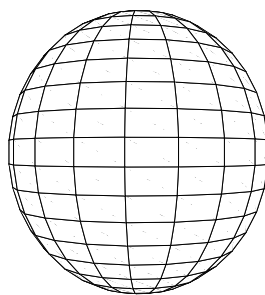
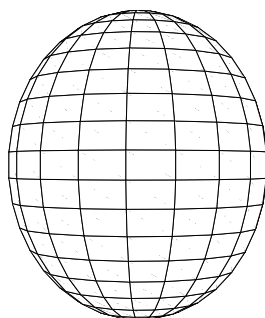Figure 3.1: Prolate spheroid $x^2 + y^2 + \dfrac{z^2}{(1.01)^2} \leq 1$

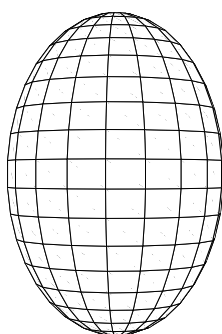Figure 3.2: Prolate spheroid $x^2 + y^2 + \dfrac{z^2}{(1.5)^2} \leq 1$

Figure 3.3: Prolate spheroid $x^2 + y^2 + \dfrac{z^2}{2^2} \leq 1$

The corresponding values of the parameter β are computed as $\beta = 0.17$, $\beta = 0.5556$, $\beta = 0.75$ respectively. Numerical results and detailed discussion of the algorithms and computer softwares are presented in Chapter 4. Precision of the method has been checked by comparing the results with those obtained by using an alternative method introduced in the next section.

3.2 Prolate Spheroidal Billiard: Solution by the Method of Moszkowski

In this section we give an elegant and powerful method developed by Moszkowski [35] and used by Ayant and Arvieu [2, 3] for solving the Schrödinger equation of a particle enclosed in a prolate spheroidal box. The method is very efficient, therefore, can be relied upon for comparison purposes. However, it works only for prolate spheroids.

Let $\mathcal{D}$ be the prolate spheroid defined in (3.2). The Schrödinger equation in Cartesian coordinates for a particle moving freely in $\mathcal{D}$ is

$$-\Delta\Psi(x, y, z) = -\left\{\frac{\partial^2}{\partial x^2} + \frac{\partial^2}{\partial y^2} + \frac{\partial^2}{\partial z^2}\right\}\Psi(x, y, z) = E\Psi(x, y, z) \qquad (3.9)$$

where the wavefunction $\Psi(x, y, z)$ vanishes on $\partial\mathcal{D}$ and satisfies the square integrability condition

$$\int\int_{\mathcal{D}}\int \mid \Psi \mid^2 dV < \infty \qquad (3.10)$$

as usual. The coordinate transformation

$$x' = \frac{R}{a}x, \;\; y' = \frac{R}{a}y, \;\; z' = \frac{R}{b}z \qquad (3.11)$$

where

$$\frac{3}{R^2} = \frac{2}{a^2} + \frac{1}{b^2} \qquad (3.12)$$

transforms the prolate spheroid into a ball of radius R. Denote the Laplace operator in terms of the coordinates x', y', and z' by Δ' and observe that

$$\Delta = \Delta' + c\left(\Delta' - 3\frac{\partial^2}{\partial z'^2}\right) \qquad (3.13)$$

where $c = \dfrac{b^2 - a^2}{a^2 + 2b^2}$. Rewrite (3.13) as $\Delta = \mathcal{H}_0 + \mathcal{H}_1$, where $\mathcal{H}_0 = \Delta'$ can be regarded as an exactly solvable Hamiltonian operator, and

$$\mathcal{H}_1 = c\left(\Delta' - 3\frac{\partial^2}{\partial z'^2}\right) \tag{3.14}$$

as a perturbation term. Since the region has been transformed into a ball, it is more appropriate to use spherical coordinates $x' = r\sin\theta\cos\phi$, $y' = r\sin\theta\sin\phi$ and $z' = r\cos\theta$. Letting also $\eta = \cos\theta$ for convenience, we can transform the operator $\mathcal{H}_1$ into

$$\mathcal{H}_1 = c\left\{\Delta'' - 3\left[\eta^2\frac{\partial^2}{\partial r^2} + \frac{1-\eta^2}{r}\frac{\partial}{\partial r} + 2\frac{\eta(1-\eta^2)}{r}\frac{\partial^2}{\partial r\partial\eta}\right.\right.$$
$$\left.\left. + \frac{(1-\eta^2)^2}{r^2}\frac{\partial^2}{\partial\eta^2} - 3\eta\frac{1-\eta^2}{r^2}\frac{\partial}{\partial\eta}\right]\right\} \tag{3.15}$$

where Δ'' denotes the Laplace operator in coordinates (r, η, ϕ). The eigenvalues of the unperturbed Hamiltonian $\mathcal{H}_0$ are known to be $-\lambda_{m,p}^2$, $m = n, n+1, \ldots$, $p = 1, 2, \ldots$, where $\lambda_{m,p}$ is the p-th positive zero of the equation

$$J_{m+\frac{1}{2}}(\lambda R) = 0 \tag{3.16}$$

and correspond to the normalized eigenfunctions

$$\Psi(r, \eta, \phi)_{n,m,p} = \mathcal{N}_{m,p}^n j_m(\lambda_{m,p}r)Y_m^n(\eta, \phi) \tag{3.17}$$

where the $Y_m^n(\eta, \phi)$ are the Spherical harmonics, defined by (2.14). Here the j_m denote the spherical Bessel functions [1]

$$j_m(\xi) = \left(\frac{\pi}{2\xi}\right)^{\frac{1}{2}} J_{m+\frac{1}{2}}(\xi).$$

and

$$\mathcal{N}_{m,p}^n = \left\{\frac{1}{\sqrt{2\pi}}\sqrt{\frac{(m+n)!}{(2m+1)(m-n)!}}J_{m+\frac{3}{2}}(\lambda_{m,p})\right\}^{-1}$$

the normalization constant. Then the wavefunction can be expanded in terms of the eigenfunctions of the unperturbed Hamiltonian

$$\Psi(r, \eta, \phi) = \sum_{m=0}^{\infty}\left\{\sum_{n=0}^{m}\sum_{p=1}^{\infty} a_{m,p}^n \mathcal{N}_{m,p}^n P_m^n(\eta)\frac{1}{\sqrt{r}}J_{m+\frac{1}{2}}(\lambda_{m,p}r)\cos n\phi\right.$$
$$\left. + \sum_{n=1}^{m}\sum_{p=1}^{\infty} b_{m,p}^n \mathcal{N}_{m,p}^n P_m^n(\eta)\frac{1}{\sqrt{r}}J_{m+\frac{1}{2}}(\lambda_{m,p}r)\sin n\phi\right\} \tag{3.18}$$

where the $a_{m,p}^n$ and $b_{m,p}^n$ denote the Fourier coefficients. The two symmetries of the region, namely, the axial symmetry and the symmetry with respect to xy-plane allow decomposition of (3.18) into 4 parts as

$$
\begin{aligned}
\Psi(r,\eta,\phi) = \ & \sum_{m=0}^{\infty}\sum_{n=0}^{m}\sum_{p=1}^{\infty} a_{2m,p}^n \mathcal{N}_{2m,p}^n P_{2m}^n(\eta)\frac{1}{\sqrt{r}}J_{2m+\frac{1}{2}}(\lambda_{2m,p}r)\cos n\phi \\
+ \ & \sum_{m=0}^{\infty}\sum_{n=0}^{m}\sum_{k=1}^{\infty} a_{2m+1,p}^n \mathcal{N}_{2m+1,p}^n P_{2m+1}^n(\eta)\frac{1}{\sqrt{r}}J_{2m+\frac{3}{2}}(\lambda_{2m+1,p}r)\cos n\phi \\
+ \ & \sum_{m=0}^{\infty}\sum_{n=1}^{m}\sum_{p=1}^{\infty} b_{2m,p}^n \mathcal{N}_{2m,p}^n P_{2m}^n(\eta)\frac{1}{\sqrt{r}}J_{2m+\frac{1}{2}}(\lambda_{2m,p}r)\sin n\phi \\
+ \ & \sum_{m=0}^{\infty}\sum_{n=1}^{m}\sum_{p=1}^{\infty} b_{2m+1,p}^n \mathcal{N}_{2m+1,p}^n P_{2m+1}^n(\eta)\frac{1}{\sqrt{r}}J_{2m+\frac{3}{2}}(\lambda_{2m+1,p}r)\sin n\phi
\end{aligned}
$$

$$(3.19)$$

where each part can be treated separately. By employing the relations [1]

$$
\begin{aligned}
\eta P_m^n(\eta) &= \frac{1}{(2m+1)}\left[(m+1)P_{m+1}^n(\eta)+(m-n+1)P_{m-1}^n(\eta)\right] \\
(1-\eta^2)\frac{\mathrm{d}}{\mathrm{d}\eta}P_m^n(\eta) &= \frac{1}{(2m+1)}\left[(m+1)(m+n)P_{m-1}^n(\eta)-m(m-n+1)P_{m+1}^n(\eta)\right] \\
\frac{1}{\xi}J_\nu(\xi) &= \frac{1}{2\nu}\left[J_{\nu-1}(\xi)+J_{\nu+1}(\xi)\right] \\
\frac{\mathrm{d}}{\mathrm{d}\xi}J_\nu(\xi) &= \frac{1}{2}\left[J_{\nu-1}(\xi)-J_{\nu+1}(\xi)\right]
\end{aligned}
$$

$$(3.20)$$

between the associated Legendre functions and the Bessel functions, the expression

$$
\mathcal{H}_1 P_m^n(\eta)\frac{1}{\sqrt{r}}J_{m+\frac{1}{2}}(\lambda_{m,k}r)\cos n\phi
$$

$$
= c\left\{-\lambda_{m,p}^2 P_m^n(\eta)\frac{1}{\sqrt{r}}J_{m+\frac{1}{2}}(\lambda_{m,p}r)-3\lambda_{m,p}^2\times\right.
$$

$$
\left[\frac{(m-n+1)(m-n+2)}{(2m+1)(2m+3)}P_{m+2}^n(\eta)\frac{1}{\sqrt{r}}J_{m+\frac{5}{2}}(\lambda_{m,p}r)\right.
$$

$$(3.21)$$

$$
-\frac{2m^2-2n^2+2m-1}{(2m-1)(2m+3)}P_m^n(\eta)\frac{1}{\sqrt{r}}J_{m+\frac{1}{2}}(\lambda_{m,p}r)
$$

$$
\left.\left.+\frac{(m+n)(m+n-1)}{(2m+1)(2m-1)}P_{m-2}^n(\eta)\frac{1}{\sqrt{r}}J_{m-\frac{3}{2}}(\lambda_{m,p}r)\right]\right\}\cos n\phi
$$

can be derived after a long computation and will be used to appraise the matrix

elements of the operator $\mathcal{H}_1$. We now substitute the first part of the expansion (3.18) in the equation

$$- \left[\mathcal{H}_0 + \mathcal{H}_1 \right] \Psi(r, \eta, \phi) = E \Psi(r, \eta, \phi)$$

and use (3.21) which result in

$$\sum_{m=0}^{\infty} \sum_{n=0}^{m} \sum_{p=1}^{\infty} a_{2m,p}^n \left\{ (1+c) \lambda_{2m,p}^2 \mathcal{N}_{2m,p}^n P_{2m}^n(\eta) \frac{1}{\sqrt{r}} J_{2m+\frac{1}{2}}(\lambda_{2m,p} r) \right.$$

$$+ 3c\lambda_{2m,p}^2 \times$$

$$\left[\frac{(2m-n+1)(2m-n+2)}{(4m+1)(4m+3)} \mathcal{N}_{2m,p}^n P_{2m+2}^n(\eta) \frac{1}{\sqrt{r}} J_{2m+\frac{5}{2}}(\lambda_{2m,p} r) \right.$$

$$\qquad\qquad (3.22)$$

$$- \frac{8m^2 - 2n^2 + 4m - 1}{(4m-1)(4m+3)} \mathcal{N}_{2m,p}^n P_{2m}^n(\eta) \frac{1}{\sqrt{r}} J_{2m+\frac{1}{2}}(\lambda_{2m,p} r)$$

$$+ \left. \left. \frac{(2m+n)(2m+n-1)}{(4m+1)(4m-1)} \mathcal{N}_{2m,p}^n P_{2m-2}^n(\eta) \frac{1}{\sqrt{r}} J_{2m-\frac{3}{2}}(\lambda_{2m,p} r) \right] \right\} \cos n\phi$$

$$= E \sum_{m=0}^{\infty} \sum_{n=0}^{m} \sum_{p=1}^{\infty} a_{2m,p}^n \mathcal{N}_{2m,p}^n P_{2m}^n(\eta) \frac{1}{\sqrt{r}} J_{2m+\frac{1}{2}}(\lambda_{2m,p} r) \cos n\phi.$$

Recalling the truncation order notations adopted in Chapter 2, that is M and P, we truncate the infinite series in (3.22) so that, $m = 0, 1, \ldots, M$, $n = 0, 1, \ldots m$ and $p = 1, 2, \ldots, P$. The double sum $\sum_{m=0}^{M} \sum_{n=0}^{m}$ can be reordered as $\sum_{n=0}^{M} \sum_{m=n}^{M}$ as it has been done in Section 2.2, which permits the removal of $\sum_{n=0}^{M}$ implied by the linear

independence of $\cos n\phi$. Then (3.22) yields $M + 1$ equations of the form

$$\sum_{m=n}^{M} \sum_{p=1}^{P} a_{2m,p}^n \left\{ (1 + c)\, \lambda_{2m,p}^2 \mathcal{N}_{2m,p}^n P_{2m}^n(\eta) \frac{1}{\sqrt{r}} J_{2m+\frac{1}{2}}(\lambda_{2m,p} r) \right.$$

$$+ 3c\lambda_{2m,p}^2 \times$$

$$\left[\frac{(2m - n + 1)(2m - n + 2)}{(4m + 1)(4m + 3)} \mathcal{N}_{2m,p}^n P_{2m+2}^n(\eta) \frac{1}{\sqrt{r}} J_{2m+\frac{5}{2}}(\lambda_{2m,p} r) \right.$$

$$\hspace{4cm} (3.23)$$

$$- \frac{8m^2 - 2n^2 + 4m - 1}{(4m - 1)(4m + 3)} \mathcal{N}_{2m,p}^n P_{2m}^n(\eta) \frac{1}{\sqrt{r}} J_{2m+\frac{1}{2}}(\lambda_{2m,p} r)$$

$$\left. \left. + \frac{(2m + n)(2m + n - 1)}{(4m + 1)(4m - 1)} \mathcal{N}_{2m,p}^n P_{2m-2}^n(\eta) \frac{1}{\sqrt{r}} J_{2m-\frac{3}{2}}(\lambda_{2m,p} r) \right] \right\}$$

$$= E \sum_{m=n}^{M} \sum_{p=1}^{P} a_{2m,p}^n \mathcal{N}_{2m,p}^n P_{2m}^n(\eta) \frac{1}{\sqrt{r}} J_{2m+\frac{1}{2}}(\lambda_{2m,p} r)$$

corresponding to each $n = 0, 1, \ldots M$. Now, we multiply (3.23) by

$$\mathcal{N}_{2l,s}^n P_{2l}^n(\eta) \frac{1}{\sqrt{r}} J_{2l+\frac{1}{2}}(\lambda_{2l,s} r), \qquad l = n, n+1, \ldots, M \qquad s = 1, 2, \ldots, P$$

and integrate over the region $[-1, 1] \times [0, R]$ with respect to the weight function $w(r) = r^2$ which gives

$$\sum_{m=n}^{M} \sum_{p=1}^{P} [h_{l,m,s,p} - E] \, a_{2m,p}^n = 0 \hspace{4cm} (3.24)$$

for each $l = n, n+1, \ldots M$ and $s = 1, 2, \ldots P$ where n is assumed to be fixed. Recall also that $n = 0, 1, \ldots M$, that is, (3.24) will be solved $M + 1$ times. Making use of the identities (3.20) and the integral [59]

$$\int_0^R r J_\nu(\alpha r) J_\nu(\beta r) \mathrm{d}r = \frac{R}{\alpha^2 - \beta^2} \left[\alpha J_{\nu+1}(\alpha R) J_\nu(\beta R) - \beta J_\nu(\alpha R) J_{\nu+1}(\beta R) \right]$$

we evaluate $h_{l,m,s,p}$ as

$$
h_{l,m,s,p} = \begin{cases}
\lambda_{2l,s}^2 \left(1 + 2c \dfrac{3n^2 - 2l(2l+1)}{(4l-1)(4l+3)} \right) \delta_{s,p} & \text{if } l = m \\[3em]
2c \dfrac{\lambda_{2l,s} \lambda_{2l+2,p}}{\lambda_{2l,s}^2 - \lambda_{2l+2,p}^2} \sqrt{\dfrac{\left[(2l+1)^2 - n^2 \right]\left[(2l+2)^2 - n^2 \right]}{(4l+1)(4l+5)}} & \text{if } l = m-1 \\[3em]
-2c \dfrac{\lambda_{2l,s} \lambda_{2l-2,p}}{\lambda_{2l-2,p}^2 - \lambda_{2l,s}^2} \sqrt{\dfrac{\left[(2l-1)^2 - n^2 \right]\left[4l^2 - n^2 \right]}{(4l+1)(4l-3)}} & \text{if } l = m+1
\end{cases}
\tag{3.25}
$$

which may be regarded as entries of a block matrix, say $\mathbf{H} := [\mathbf{H}_{l,m}]$, where (l,m) label the blocks and (s,p) the entries of each block. Equation (3.24) describes then an algebraic eigenvalue problem for the eigenvalues of the block matrix $\mathbf{H}$. A similar eigenvalue problem is obtained if the second part of the expansion (3.18) is used. A careful inspection of the matrix $\mathbf{H}$ shows that it has a symmetric block tridiagonal structure, hence, the matrix form of (3.24) becomes

$$
\begin{bmatrix}
\widehat{\mathbf{H}}_n & \mathbf{U}_n & \mathbf{0} & \cdots & \mathbf{0} \\
\mathbf{U}_n^T & \widehat{\mathbf{H}}_{n+1} & \mathbf{U}_{n+1} & & \vdots \\
\mathbf{0} & \mathbf{U}_{n+1}^T & \widehat{\mathbf{H}}_{n+2} & \ddots & \mathbf{0} \\
\vdots & & \ddots & \ddots & \mathbf{U}_{M-1} \\
\mathbf{0} & \cdots & \mathbf{0} & \mathbf{U}_{M-1}^T & \widehat{\mathbf{H}}_M
\end{bmatrix}
\begin{bmatrix}
a_n \\ a_{n+1} \\ \vdots \\ a_{M-1} \\ a_M
\end{bmatrix}
= E
\begin{bmatrix}
a_n \\ a_{n+1} \\ \vdots \\ a_{M-1} \\ a_M
\end{bmatrix}
\tag{3.26}
$$

where we have set

$$
\begin{aligned}
\widehat{\mathbf{H}}_m &:= \mathbf{H}_{m,m} \\
\mathbf{U}_m &:= \mathbf{H}_{m,m+1}
\end{aligned}
$$

for $m = n, n+1, \ldots, M$. The method exposed in this section seems to be very efficient and numerically powerfull, which is obvious from the fact that the matrix elements can be evaluated analytically and very rapidly. Moreover, the block tridiagonal and symmetric structure of the matrix reduces considerably the computer time required for this evaluation. On the other hand, the perturbation is regular, since the coefficient c of the perturbation term $\mathcal{H}_1$ is smaller than 1 for all possible values of $b > a > 0$, which guaranties the convergence.

3.3   A Billiard Family Depending on a Parameter: Classical and Quantum Mechanics

As a second application, we consider a family of billiards, defined by the shape function

$$f(\theta) = 1 + \delta \cos^2 \theta, \text{where } 0 \leq \delta < 1. \tag{3.27}$$

More precisely, the region $\mathcal{D}$ is,

$$\mathcal{D} = \left\{ (r, \theta, \phi) \,\middle|\, 0 \leq r \leq 1 + \delta \cos^2 \theta, 0 \leq \theta \leq \pi, 0 \leq \phi \leq 2\pi \right\}. \tag{3.28}$$

Despite its simple form, this function generates various shapes becoming nonconvex for $\frac{1}{2} < \delta < 1$ and clearly becomes the unit ball for the special choice $\delta = 0$. To our knowledge, this billiard has not been studied earlier, neither classically nor as a quantum system, hence, we are not certain whether or not it may be important from a physical point of view. However, it seems to provide a good testing ground for our method.

Hereafter, the billiard (3.28) shall be refereed to as δ-billiard. In fact, it is beyond the scope of this study to investigate classical behavior of billiard systems, yet, one may wonder if the δ-billiards exhibit classical or regular motion. Therefore, we studied the classical motion in the two dimensional billiard

$$\mathcal{B} = \left\{ (r, \theta) | 0 \leq r \leq 1 + \delta \cos^2 \theta, 0 \leq \theta \leq 2\pi \right\} \tag{3.29}$$

generating $\mathcal{D}$ for simplicity. We use the method described by Berry [9], the details of which are given below.

Consider a particle moving in a closed region in the plane. At impact with the boundary, it is reflected according to the rule "angle of incidence equals angle of reflection" and between impacts it moves in straight line trajectories. Therefore an orbit (or trajectory) is completely determined by giving the positions and directions of the particle immediately after each impact. The position round the boundary can be specified in different ways according to the parametrization of the curve - arc length (s) or polar angle(ϕ) or direction of the counterclockwise directed tangent (ψ) measured from the origin. Direction can be described by the angle (α) between the orbit and the counterclockwise directed tangent or equivalently by the tangential
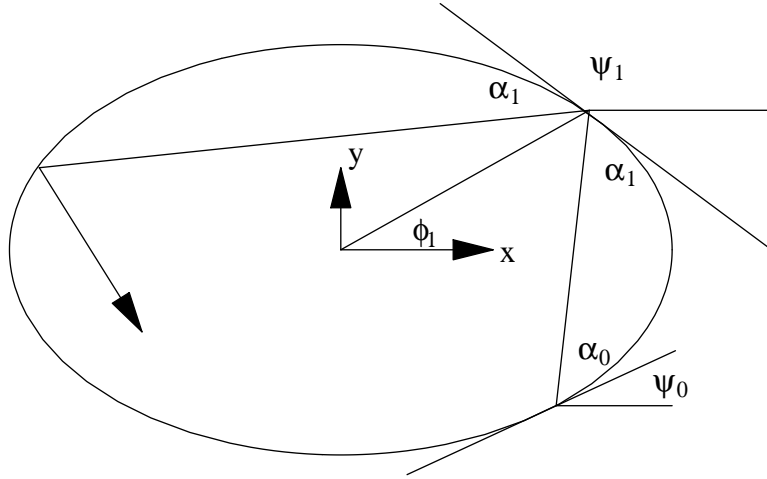
Figure 3.4: Classical Motion in Two-Dimensional Billiard

momentum $p = \cos \alpha$ (see Figure 3.4). In terms of the arc length and the tangential momentum the discrete dynamics of the system is a two dimensional mapping M of the form

$$\begin{pmatrix} s_{n+1} \\ p_{n+1} \end{pmatrix} = M \begin{pmatrix} s_n \\ p_n \end{pmatrix} \tag{3.30}$$

and is nonlinear in general. The phase space of the system is then restricted to the rectangle $-1 \leq p \leq 1$, $0 \leq s \leq L$, where L is the length of the boundary curve. One can show that in terms of s and p the mapping M is area preserving, i.e., it satisfies

$$\frac{\partial(s_{n+1}, p_{n+1})}{\partial(s_n, p_n)} = \det \begin{pmatrix} \frac{\partial s_{n+1}}{\partial s_n} & \frac{\partial s_{n+1}}{\partial p_n} \\ \frac{\partial p_{n+1}}{\partial s_n} & \frac{\partial p_{n+1}}{\partial p_n} \end{pmatrix} = 1.$$

Started with the initial position-direction pair (s_0, p_0), an orbit in the phase space can be represented in three different ways: N points can be encountered repeatedly, which corresponds to periodic orbit case; the orbit can be given by a smooth curve, called invariant curve, which shows the existence of a constant of motion, and the motion is regular; the orbit can be specified by an area in the phase space, that is, the motion is not restricted by any conserved quantity and is said to be chaotic.

We now apply the method of Berry to the two dimensional δ-billiard (3.29). Figures 3.5, 3.6, and 3.7 show the form of the billiard for $\delta = 0.1$, 0.5, 0.9 respectively.
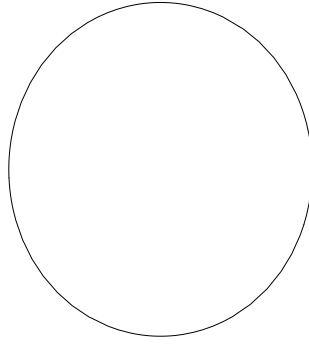
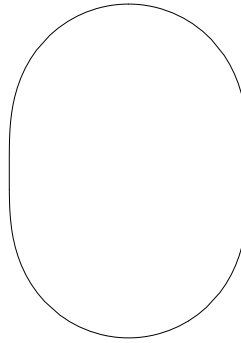Figure 3.5: Two-Dimensional δ-billiard with $\delta = 0.1$

Figure 3.6: Two-Dimensional δ-billiard with $\delta = 0.5$
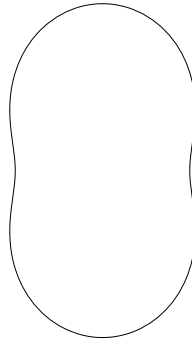

Figure 3.7: Two-Dimensional δ-billiard with $\delta = 0.9$

The billiard mapping M can be constructed by means of the following relations between the arc length s of the curve measured from the origin, the turning angle ψ (angle between the forward tangent and the positive x-axis), the polar angle ϕ and the angle α between forward tangent and the orbit. Observe that as a function of the polar angle ϕ, the boundary curve can be written as $r = 1 + \delta \sin^2 \phi$, so that then the arc length s can be computed from

$$s = \int_0^\phi \left[(r'(t))^2 + r^2(t) \right]^{1/2} \mathrm{d}t.$$

On the other hand, the relation between the turning angle and the arc length is known to be

$$\psi = \frac{\pi}{2} + \int_0^\phi \kappa(t) \left[(r'(t))^2 + r^2(t) \right]^{1/2} \mathrm{d}t$$

where $\kappa(t)$ is the local curvature. It can be seen from Figure 3.4 that the slope of the trajectory between two bounces is $\dfrac{y(\phi_1) - y(\phi_0)}{x(\phi_1) - x(\phi_0)}$ and is also expressible as $\tan(\psi_0 + \alpha_0)$. Since

$$\begin{aligned}
x(\phi) &= r(\phi) \cos \phi = (1 + \delta \sin^2 \phi) \cos \phi \\
y(\phi) &= r(\phi) \sin \phi = (1 + \delta \sin^2 \phi) \sin \phi
\end{aligned}$$

we obtain

$$\frac{r(\phi_1) \sin \phi_1 - r(\phi_0) \sin \phi_0}{r(\phi_1) \cos \phi_1 - r(\phi_0) \cos \phi_0} = \frac{\sin(\psi_0 + \alpha_0)}{\cos(\psi_0 + \alpha_0)}.$$

This relation can be simplified as

$$r(\phi_1) \sin(\phi_1 - \psi_0 - \alpha_0) = r(\phi_0) \sin(\phi_0 - \psi_0 - \alpha_0)$$

Figure 3.4 shows that the slope of the orbit through two consecutive bounces can be also given by $\tan(\psi_1 - \alpha_1)$. Hence, we have

$$\tan(\psi_0 + \alpha_0) = \tan(\psi_1 - \alpha_1).$$

We express the curvature

$$\kappa(\phi) = \frac{|2(r'(\phi))^2 + r^2(\phi) - r(\phi)r''(\phi)|}{\left((r'(\phi))^2 + r^2(\phi) \right)^{3/2}}$$

of the boundary curve as a function of the polar angle and employ these relations to construct the following algorithm for computing successive bounces.

Algorithm

Given the initial position by the polar angle ϕ_0 and the angle α_0, compute ψ_0, s_0 and p_0 from the equations

$$\psi_0 = \frac{\pi}{2} + \int_0^{\phi_0} \frac{2\delta^2 \sin^2(2t) + (1 + \delta \sin^2 t)^2 - 4\delta^2 \cos^2(2t)}{\delta^2 \sin^2(2t) + (1 + \delta \sin^2 t)^2} dt$$

$$s_0 = \int_0^{\phi_0} \left[\delta^2 \sin^2(2t) + (1 + \delta \sin^2 t)^2\right]^{1/2} dt$$

$$p_0 = \cos(\alpha_0),$$

using a suitable quadrature for computation of ψ_0 and s_0 . From $n = 0$ to $n = N$ repeat the following steps:

1. Solve the equation

$$(1 + \delta \sin^2 \phi_{n+1}) \sin(\phi_{n+1} - \alpha_n - \psi_n) = (1 + \delta \sin^2 \phi_n) \sin(\phi_n - \alpha_n - \psi_n)$$

   for ϕ_{n+1}. Obviously, the equation has two solutions in $[0, 2\pi]$, one of which is ϕ_n.

2. Compute the turning angle ψ_{n+1} from the following expression

$$\psi_{n+1} = \frac{\pi}{2} + \int_0^{\phi_{n+1}} \frac{2\delta^2 \sin(2t) + (1 + \delta \sin^2 t)^2 - 4\delta^2 \cos^2(2t)}{\delta^2 \sin^2(2t) + (1 + \delta \sin^2 t)^2} dt$$

3. Evaluate α_{n+1} from

$$\alpha_{n+1} = \psi_{n+1} - \alpha_n - \psi_n$$

4. Calculate

$$s_{n+1} = \int_0^{\phi_{n+1}} \left[\delta^2 \sin^2(2t) + (1 + \delta \sin^2 t)^2\right]^{1/2} dt$$

$$p_{n+1} = \cos(\alpha_{n+1})$$

This algorithm is well suited for rapid computer calculations. We computed 800 successive bounces of an orbit starting with $\phi_0 = 0.8$, $\alpha_0 = 0.6$ for the billiards given in Figures 3.5, 3.6, 3.7. For approximate evaluation of the integrals we have used the IMSL Library routine called QDAGS. From Figures 3.8, 3.9 and 3.10 we see how the orbits so obtained show themselves in the phase space (s, p) for the corresponding billiards. It is obvious that for $\delta = 0.1$ the motion is regular, since the orbit forms a

curve in the phase space, for $\delta = 0.5$ and $\delta = 0.9$ the orbit is represented by an area which indicates the presence of a chaotic motion.

Next, consider the three-dimensional quantum δ-billiards (3.28) for the same values of the parameter δ, i.e., $\delta = 0.1, \ 0.5, \ 0.9$ (see Figures 3.11,3.12,3.13). The shape function in terms of the transformed variable η, becomes simply

$$F(\eta) = 1 + \delta\eta^2 \tag{3.31}$$

so that the truncated shape function $G(\eta)$ is exactly $F(\eta)$. The derivatives of $F(\eta)$ can be easily computed and the entries of the coefficient matrices read as,

$$\widehat{a}_{i,j}^n \ = \ \gamma_{i+n-1,j+n-1,0}^{(n)} + 2\delta(1+2\delta)\gamma_{i+n-1,j+n-1,2}^{(n)} - 3\delta\gamma_{i+n-1,j+n-1,4}^{(n)}$$

$$\begin{aligned}\widehat{b}_{i,j}^n \ = \ & 2(1-\delta)\gamma_{i+n-1,j+n-1,0}^{(n)} + 2\delta(5-3\delta)\gamma_{i+n-1,j+n-1,2}^{(n)} \\ & -4(j+n-1)(j+n)\delta\left[\gamma_{i+n-1,j+n-1,2}^{(n)} + \delta\gamma_{i+n-1,j+n-1,4}^{(n)}\right] \\ & +4j\delta\left[\gamma_{i+n-1,j+n,1}^{(n)} + \delta\gamma_{i+n-1,j+n,3}^{(n)}\right]\end{aligned}$$

$$\widehat{c}_{i,j}^n \ = \ (j+n-1)(j+n)\left[\gamma_{i+n-1,j+n-1,0}^{(n)} + 2\delta\gamma_{i+n-1,j+n-1,2}^{(n)} + \delta^2\gamma_{i+n-1,j+n-1,4}^{(n)}\right]$$

$$\begin{aligned}\widehat{d}_{i,j}^n \ = \ & \gamma_{i+n-1,j+n-1,0}^{(n)} + 4\delta\gamma_{i+n-1,j+n-1,2}^{(n)} + 6\delta^2\gamma_{i+n-1,j+n-1,4}^{(n)} \\ & +4\delta^3\gamma_{i+n-1,j+n-1,6}^{(n} + \delta^4\gamma_{i+n-1,j+n-1,8}^{(n)}.\end{aligned}$$

$$\tag{3.32}$$

The three dimensional δ-billiard is also symmetric with respect to the xy-plane, equivalently, with respect to $\eta = 0$, therefore, eigenvalues corresponding to even and odd eigenfunctions in η must be calculated separately. We have obtained 6 particular spectra, namely, eigenvalues related to the even and odd eigenfunctions in η, for δ-billiards with $\delta = 0.1, \ 0.5, \ $ and 0.9. We have also plotted the Nearest Neighbor Spacing Histograms for these eigenvalue sets and observed good agreement with the theoretical models. The results and a detailed discussion can be found in Chapter 4.
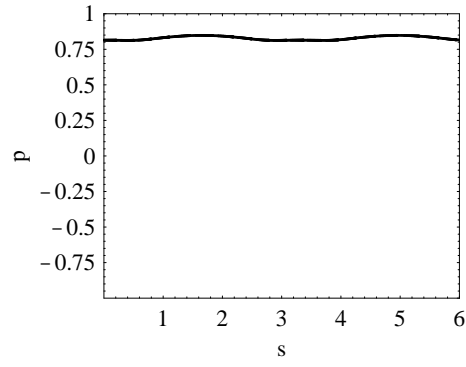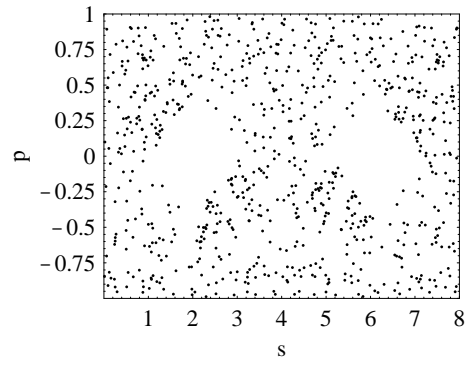
Figure 3.8: Phase space of δ-billiard with δ = 0.1
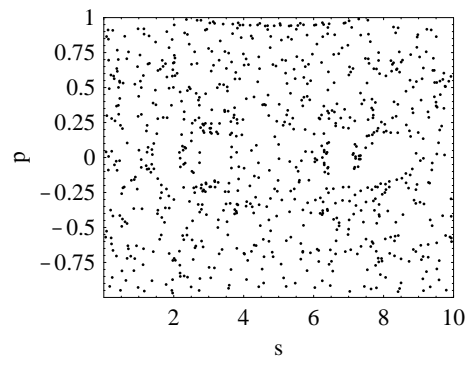

Figure 3.9: Phase space of δ-billiard with δ = 0.5

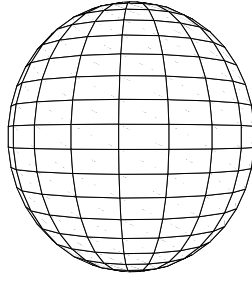Figure 3.10: Phase space of δ-billiard with δ = 0.9

54

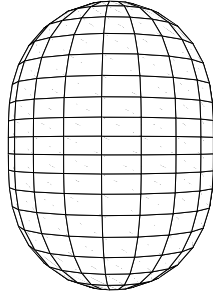Figure 3.11: Three-Dimensional δ-billiard with $\delta = 0.1$

Figure 3.12: Three-Dimensional δ-billiard with $\delta = 0.5$
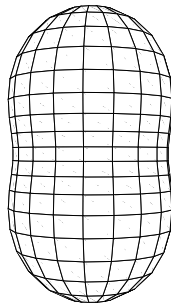

Figure 3.13: Three-Dimensional δ-billiard with $\delta = 0.9$

CHAPTER 4

NUMERICAL RESULTS AND DISCUSSION

In this chapter we present the results and discuss in detail the numerical methods, algorithms and computer softwares necessary to perform the numerical implementations.

4.1 Numerical Results for the Prolate Spheroidal Billiard

The results related to the first example introduced in Chapter 3, namely, the prolate spheroid are shown in this section. They include six different sets of eigenvalues. More precisely, we consider three particular sets of values for the parameters a and b. Each set provides two classes of spectra which have been computed using both our method and that of Moszkowski. They can be listed as:

- 1. Eigenvalues corresponding to eigenfunctions even in η and even in ϕ for a prolate spheroid with $a = 1$, $b = 1.01$ (Table 4.1).

- 2. Eigenvalues corresponding to eigenfunctions odd in η and even in ϕ for a prolate spheroid with $a = 1$, $b = 1.01$ (Table 4.2).

- 3. Eigenvalues corresponding to eigenfunctions even in η and even in ϕ for a prolate spheroid with $a = 1$, $b = 1.5$ (Table 4.3).

- 4. Eigenvalues corresponding to eigenfunctions odd in η and even in ϕ for a prolate spheroid with $a = 1$, $b = 1.5$ (Table 4.4).

- 5. Eigenvalues corresponding to eigenfunctions even in η and even in ϕ for a prolate spheroid with $a = 1$, $b = 2$ (Table 4.5).

- 6. Eigenvalues corresponding to eigenfunctions odd in η and even in ϕ for a prolate spheroid with $a = 1$, $b = 2$ (Table 4.6).

We have employed two different types of software, namely, Fortran and Mathematica [61]. The method of Moszkowski needs the zeros of the spherical Bessel functions which have been computed using the Mathematica package `BesselZeros` and stored in a data file. This data is required to evaluate the entries of the symmetric matrix $\mathbf{H}$ given in (3.26). A Fortran program performs this evaluation within a desired precision and then calls two EISPACK routines to find the eigenvalues of the matrix. The first routine, called `TRED2` reduces $\mathbf{H}$ to a tridiagonal form, and the second one, called `TQL2` computes the eigenvalues of the resulting matrix. We have observed that the method is very efficient in the sense of computing time and numerical performance.

The numerical implementation of our method is much more complicated. In order to follow up the procedure and reduce the size of the memory, we executed each step of the method in an individual computer program. First, a Fortran program evaluates and stores the coefficients $\gamma_{i,j,k}^{(n)}$. A second Fortran program computes and stores the coefficient matrices $\widehat{\mathbf{A}}^n$, $\widehat{\mathbf{B}}^n$, $\widehat{\mathbf{C}}^n$ and $\widehat{\mathbf{D}}^n$. Then this data is used in a Mathematica program which performs the Cholesky decomposition of $\widehat{\mathbf{A}}^n$ and consequently gives the matrices $\mathbf{Q}^n$, $\mathbf{R}^n$ and $\mathbf{T}^n$, the numbers μ_i^n, the orders ν_i^n of the Bessel functions and their zeros $\lambda_{i,s}$. Another Fortran program evaluates the integrals $I(\rho, \mu, a, \sigma, b)$ and the matrices $\widehat{\mathbf{H}}$ and $\widehat{\mathbf{W}}$. The last Fortran program calls the EISPACK routine `QZIT`, based on the QZ-factorization method for computation of the eigenvalues of the generalized eigenvalue problem

$$\widehat{\mathbf{H}}\mathbf{x} = E\widehat{\mathbf{W}}\mathbf{x}. \tag{4.1}$$

Truncation orders of the shape function have been taken as $K = 8$, $K = 16$ and $K = 20$ for the cases $a = 1$, $b = 1.01$, $a = 1$, $b = 1.5$ and $a = 1$, $b = 2$

respectively. This choice has been done after checking the precision of the eigenvalues obtained by taking two consecutive values of K. To be specific, we have observed that the significant digits in the computed eigenvalues do not increase by taking $K = 9$ in the first case, $K = 17$ in the second, and $K = 21$ in the last case. Thus, for each particular prolate spheroid, we obtained the eigenvalues corresponding eigenfunctions even and odd in η. Hereafter they shall be refereed to as "even" and "odd" eigenvalues for brevity. Truncation order M has been taken as 16 for each case and both the methods, while the truncation order P varies in accordance with M. Thus, we have solved the problem (4.1) 16 times. More specifically, we have taken $n = 0$ and $P = 20$; $n = 1$ and $P = 19$, ..., $n = 16$ and $P = 4$. On the other hand, we have determined a minimum precision requirement, which has been achieved for all eigenvalues in the following ranges:

- $a = 1$, $b = 1.01$ even eigenvalues in the range $0 - 375$; odd eigenvalues in the range $0 - 375$

- $a = 1$, $b = 1.5$ even eigenvalues in the range $0 - 220$; odd eigenvalues in the range $0 - 220$

- $a = 1$, $b = 2$ even eigenvalues in the range $0 - 155$; odd eigenvalues in the range $0 - 155$.

Thus, we have observed that it actually suffices to take $n = 12$, since for larger values of n the resulting eigenvalues are out of the given ranges. The convergence rates have been routinely checked one more time, by comparing the results obtained for two consecutive values of the truncation order M. The tables clearly show that the accuracy is 7 digits in the case $a = 1$, $b = 1.01$, 4 digits in the case $a = 1$, $b = 1.5$ and 3 digits for $a = 1$, $b = 2$. The poor convergence in the last case is a consequence of the "large" value of $\beta = 0.75$. In this last example, the significance of the choice of the shape function clearly shows itself. In fact, the truncation order $K = 20$ implies $|F(\eta) - G(\eta)| \approx 10^{-4}$, i.e., this is a "bad" approximation. On the other hand, increase of K yields other problems, like large memory requirements. Furthermore, recalling that the shape function $F(\eta)$ has been defined as

$$F(\eta) = 1 + \sum_{k=1}^{\infty} \alpha_k \eta^k$$

it is also worth mentioning here that it is necessary to have $\sum_{k=1}^{\infty} \alpha_k \eta^k < 1$ in order that the perturbation is regular. For this reason, we have not treated prolate spheroids with larger values of β. However, in the study of billiard systems the shape of the billiard is of importance but not its volume, therefore, this additional condition on the shape function does not restrict the variety of the billiards too much.

The most "expensive" part of the algorithm is the approximate calculation of the integrals

$$\mathbf{I}(\rho, \nu, \sigma, \alpha, \beta) = \int_0^1 \xi^\rho J_\nu(\alpha\xi) J_\sigma(\beta\xi) \mathrm{d}\xi$$

and in fact, it takes nearly the whole computing time. We have used the formula [31]

$$\int_0^1 \xi^\rho J_\nu(\alpha\xi) J_\sigma(\beta\xi) \mathrm{d}\xi = \frac{\alpha^\nu \beta^\sigma}{2^{\nu+\sigma} \Gamma(\nu+1)\Gamma(\sigma+1)} \times \sum_{i=0}^{\infty} \frac{(-1)^i (\alpha/2)^{2i} {}_2F_1(-i, -\nu+i; \sigma+1; \frac{\beta^2}{\alpha^2})}{i!(\rho+\nu+\sigma+2i+1)(\nu+1)_i} \tag{4.2}$$

where ${}_2F_1$ denotes the Hypergeometric function and $(\nu+1)_i$ the Pochammer's symbol. The series has been proven to be convergent for $\beta/\alpha < 1$. However, for large values of α and β the convergence is very slow, so that, the formula (4.2) is meaningless. Moreover, the convergence rate of the series cannot be improved by means of some known methods. Therefore, for large α and β, a suitable quadrature seems to be more appropriate. One can then take advantage of some standard routines available elsewhere to evaluate the Bessel functions for small variables and asymptotic expansions for large variables [59]. For the eigenvalue ranges considered in this work, relatively small values of α and β have been needed, so, we have applied the formula (4.2), yet, even in this case we have performed a suitable scaling on the terms of the series to get better results.

Next, we give the tabulated eigenvalues. In all the tables $E^{(1)}$ denotes eigenvalues obtained using our method, and $E^{(2)}$ denotes eigenvalues obtained using the method of Moszkowski.

Table 4.1: First 60 even eigenvalues for a prolate spheroidal billiard with $a = 1$ and $b = 1.01$

n	$E_n^{(1)}$	$E_n^{(2)}$	n	$E_n^{(1)}$	$E_n^{(2)}$
1	9.8047447	9.8047447	31	161.96988	161.96986
2	32.867762	32.867761	32	161.99303	161.99301
3	32.936688	32.936688	33	162.06243	162.06241
4	33.123826	33.123826	34	162.17791	162.17790
5	39.225609	39.225609	35	162.33921	162.33920
6	66.278007	66.278005	36	162.54596	162.54595
7	66.313557	66.313555	37	162.79772	162.79771
8	66.419504	66.419503	38	163.09393	163.09393
9	66.593947	66.593946	39	163.43399	163.43399
10	66.834143	66.834142	40	199.82184	199.82182
11	81.834023	81.834012	41	199.87228	199.87226
12	82.026250	82.026243	42	200.02307	200.02305
13	82.489096	82.489092	43	200.27261	200.27260
14	88.281146	88.281146	44	200.61845	200.61844
15	109.41235	109.41233	45	201.05744	201.05743
16	109.43946	109.43945	46	201.58596	201.58596
17	109.52067	109.52066	47	223.75105	223.75111
18	109.65554	109.65553	48	223.77192	223.77178
19	109.84339	109.84338	49	223.83435	223.83429
20	110.0833	110.08330	50	223.88109	223.88109
21	110.37419	110.37419	51	223.93827	223.93822
22	135.61419	135.61418	52	224.01140	224.01138
23	135.68947	135.68947	53	224.08359	224.08354
24	135.91179	135.91179	54	224.27011	224.27010
25	136.27261	136.27261	55	224.39027	224.39024
26	136.76108	136.76108	56	224.49759	224.49756
27	150.19793	150.19786	57	224.76577	224.76575
28	150.59847	150.59844	58	224.99324	224.99323
29	151.43987	151.43985	59	225.07432	225.07431
30	156.99778	156.99778	60	225.42288	225.42287

Table 4.2: First 60 odd eigenvalues for a prolate spheroidal billiard with $a = 1$ and $b = 1.01$

n	$E_n^{(1)}$	$E_n^{(2)}$	n	$E_n^{(1)}$	$E_n^{(2)}$
1	19.951901	19.951901	31	167.36979	167.36979
2	20.111077	20.111077	32	185.65408	185.68407
3	48.332619	48.332619	33	185.88459	185.88458
4	48.377655	48.377654	34	186.42431	186.42431
5	48.510056	48.510055	35	187.23407	187.23406
6	48.724101	48.724101	36	191.71746	191.71744
7	58.979987	58.979987	37	191.73931	191.73929
8	59.448188	59.448188	38	191.80483	191.80480
9	86.651620	86.651617	39	191.91388	191.91387
10	86.682014	86.682012	40	192.06632	192.06630
11	86.772914	86.772912	41	192.50021	192.50020
12	86.923498	86.923496	42	192.78097	192.78096
13	87.132493	87.132492	43	193.10370	193.10370
14	107.39960	107.39960	44	193.46793	193.46793
15	107.50594	107.50594	45	195.61456	195.61456
16	107.80834	107.80834	46	197.13426	197.13426
17	108.28084	108.28084	47	235.73757	235.73756
18	117.52558	117.52557	48	235.78175	235.78174
19	118.45063	118.45063	49	235.91401	235.91399
20	134.52736	134.52736	50	236.13346	236.13345
21	134.55220	134.55220	51	236.43874	236.43873
22	134.62663	134.62662	52	237.29913	237.29913
23	134.75039	134.75038	53	237.84961	237.84961
24	134.92308	134.92307	54	258.05433	258.05429
25	135.41288	135.41288	55	258.07430	258.07430
26	135.72851	135.72851	56	258.13419	258.13413
27	166.43532	166.43531	57	258.23390	258.23390
28	166.49511	166.49510	58	258.37340	258.37335
29	166.67328	166.67327	59	258.77103	258.77099
30	166.96647	166.96647	60	259.02881	259.02875

Table 4.3: First 60 even eigenvalues for a prolate spheroidal billiard with $a = 1$ and $b = 1.5$

n	$E_n^{(1)}$	$E_n^{(2)}$	n	$E_n^{(1)}$	$E_n^{(2)}$
1	7.9953	7.9953	31	119.90	119.90
2	20.394	20.393	32	120.49	120.48
3	24.986	24.986	33	127.70	127.70
4	30.410	30.410	34	128.87	128.87
5	34.893	34.893	35	130.44	130.44
6	39.909	39.905	36	130.73	130.73
7	44.098	44.097	37	138.02	138.01
8	49.663	49.662	38	138.16	138.12
9	55.982	55.980	39	140.07	140.07
10	56.121	56.121	40	141.88	141.87
11	63.279	63.279	41	143.84	143.84
12	66.357	66.350	42	144.42	144.40
13	66.514	66.512	43	147.84	147.84
14	69.742	69.740	44	148.01	148.01
15	75.053	75.050	45	148.45	148.40
16	77.319	77.317	46	150.47	150.45
17	81.570	81.570	47	154.10	154.09
18	81.579	81.577	48	157.83	157.81
19	84.133	84.115	49	158.28	158.28
20	89.011	89.010	50	163.54	163.48
21	95.037	95.031	51	165.31	165.31
22	97.188	97.187	52	166.25	166.23
23	99.257	99.243	53	167.01	167.01
24	101.81	101.78	54	172.96	172.94
25	106.01	106.01	55	175.57	175.54
26	106.38	106.38	56	180.56	180.56
27	106.66	106.65	57	182.31	182.30
28	111.65	111.64	58	182.82	182.76
29	113.01	113.01	59	184.05	184.03
30	118.28	118.28	60	184.32	184.27

Table 4.4: First 60 odd eigenvalues for a prolate spheroidal billiard with $a = 1$ and $b = 1.5$

n	$E_n^{(1)}$	$E_n^{(2)}$	n	$E_n^{(1)}$	$E_n^{(2)}$
1	13.316	13.316	31	121.33	121.33
2	17.839	13.839	32	123.31	123.31
3	29.260	29.260	33	124.78	124.76
4	33.727	33.727	34	129.16	129.15
5	39.283	39.282	35	130.97	130.95
6	44.595	44.595	36	130.99	130.98
7	45.584	45.584	37	135.41	135.41
8	52.290	52.287	38	138.43	138.41
9	54.704	54.704	39	140.72	140.70
10	56.106	56.103	40	145.69	145.68
11	61.581	61.580	41	146.84	146.83
12	68.110	68.109	42	148.13	148.13
13	69.125	69.123	43	150.81	150.79
14	75.438	75.438	44	156.09	156.08
15	79.937	79.934	45	159.77	159.73
16	82.032	82.022	46	161.42	161.42
17	83.436	83.436	47	161.46	161.42
18	84.989	84.980	48	162.12	162.10
19	90.084	90.080	49	162.29	162.28
20	91.072	91.070	50	165.57	165.53
21	95.806	95.803	51	166.07	166.05
22	96.546	96.540	52	166.81	166.80
23	101.02	101.02	53	169.45	169.42
24	102.68	102.68	54	171.46	171.41
25	104.02	104.02	55	174.38	174.36
26	111.29	111.29	56	176.69	176.69
27	111.86	111.86	57	178.72	178.68
28	112.32	112.32	58	179.20	179.20
29	117.97	117.96	59	186.67	186.63
30	120.18	120.16	60	187.11	187.07

Table 4.5: First 60 even eigenvalues for a prolate spheroidal billiard with $a = 1$ and $b = 2$

n	$E_n^{(1)}$	$E_n^{(2)}$	n	$E_n^{(1)}$	$E_n^{(2)}$
1	7.284	7.284	31	100.3	100.3
2	15.20	15.20	32	101.2	101.1
3	21.76	21.76	33	102.8	102.8
4	27.14	27.13	34	103.7	103.6
5	29.25	29.24	35	104.0	104.0
6	33.57	33.57	36	111.6	111.5
7	34.18	34.18	37	113.2	113.0
8	42.43	42.42	38	113.5	113.5
9	43.34	43.30	39	114.2	114.1
10	47.75	47.72	40	117.6	117.4
11	50.42	50.41	41	119.0	119.0
12	51.62	51.62	42	120.5	120.5
13	59.11	59.10	43	123.2	123.0
14	61.28	61.27	44	124.6	124.4
15	61.69	61.69	45	126.0	126.0
16	63.85	68.80	46	126.8	126.8
17	65.56	65.51	47	128.4	128.4
18	68.95	68.94	48	129.4	129.2
19	70.23	70.59	49	131.9	131.9
20	75.45	75.45	50	136.1	136.0
21	79.49	79.45	51	138.9	138.9
22	79.61	79.60	52	141.0	141.0
23	79.76	79.76	53	141.3	141.3
24	80.24	80.22	54	142.4	142.3
25	87.31	87.19	55	143.4	143.1
26	88.63	88.49	56	145.4	145.4
27	89.75	89.72	57	146.1	146.0
28	91.47	91.47	58	146.3	146.2
29	94.89	94.79	59	150.8	150.8
30	95.53	95.51	60	152.5	152.2

Table 4.6: First 60 odd eigenvalues for a prolate spheroidal billiard with $a = 1$ and $b = 2$

n	$E_n^{(1)}$	$E_n^{(2)}$	n	$E_n^{(1)}$	$E_n^{(2)}$
1	10.76	10.76	31	101.5	101.5
2	16.90	16.90	32	102.1	102.1
3	20.64	20.64	33	102.6	102.6
4	27.51	27.51	34	106.9	106.9
5	34.69	34.68	35	108.5	108.5
6	35.41	35.41	36	109.0	109.0
7	40.21	40.21	37	111.9	111.9
8	41.82	41.81	38	113.1	113.1
9	44.21	44.21	39	115.0	115.0
10	50.31	50.31	40	115.6	115.6
11	53.04	53.00	41	117.3	117.3
12	53.09	53.09	42	123.4	123.4
13	56.15	56.14	43	125.8	125.8
14	59.86	59.86	44	127.7	127.7
15	60.02	60.00	45	127.8	127.8
16	68.83	68.81	46	128.8	128.8
17	70.32	70.32	47	132.2	132.2
18	70.33	70.33	48	132.9	132.9
19	75.68	75.68	49	133.7	133.7
20	75.87	75.87	50	137.9	137.9
21	78.91	78.91	51	139.0	139.0
22	81.65	81.65	52	139.4	139.4
23	82.26	82.26	53	139.8	139.8
24	85.07	85.07	54	140.7	140.7
25	89.53	89.53	55	144.2	144.2
26	90.03	90.03	56	147.4	147.4
27	91.09	91.09	57	149.6	149.6
28	91.11	91.11	58	153.0	153.0
29	99.65	99.65	59	153.9	153.9
30	100.6	100.6	60	154.3	154.3

4.2 Numerical Results for the δ-billiard

In this section we exhibit the results obtained for the second example considered in section 3.2, which we named δ-billiard. We have treated numerically three particular cases of the parameter δ, i.e., $\delta = 0.1$, 0.5 and 0.9. Because of the symmetric structure of the region with respect to the η variable, the results have been grouped in six sets as follows:

- 1. Eigenvalues corresponding to eigenfunctions even in η and even in ϕ for a δ-billiard with δ=0.1 (Table 4.7).

- 2. Eigenvalues corresponding to eigenfunctions odd in η and even in ϕ for a δ-billiard with δ=0.1 (Table 4.8).

- 3. Eigenvalues corresponding to eigenfunctions even in η and even in ϕ for a δ-billiard with δ=0.5 (Table 4.9).

- 4. Eigenvalues corresponding to eigenfunctions odd in η and even in ϕ for a δ-billiard with δ=0.5 (Table 4.10).

- 5. Eigenvalues corresponding to eigenfunctions even in η and even in ϕ for a δ-billiard with δ=0.9 (Table 4.11).

- 6. Eigenvalues corresponding to eigenfunctions odd in η and even in ϕ for a δ-billiard with δ=0.9 (Table 4.12).

We have constructed the same algorithm as for the prolate spheroid and have assigned a separate computer program for each step of the procedure. Truncation order M has been taken as 16 again and P varied with M. Specifying a precision for the computed eigenvalues, we have obtained all the eigenvalues in the following ranges:

- For $\delta = 0.1$ even eigenvalues in the range $0 - 300$; odd eigenvalues in the range $0 - 290$

- For $\delta = 0.5$ even eigenvalues in the range $0 - 235$; odd eigenvalues in the range $0 - 215$

- For $\delta = 0.9$ even eigenvalues in the range $0 - 180$; odd eigenvalues in the range $0 - 160$.

This yields between 75-106 eigenvalues for each case. The convergence rate has been checked simply by comparing the results for two consecutive values of the truncation order M. The accuracy has been observed to be 7 digits for $\delta = 0.1$, 6 digits for $\delta = 0.5$ and 5 digits for $\delta = 0.9$. It is not surprising that the accuracy for large values of δ is better than the accuracy for large β values in the prolate spheroid case, since the δ-billiard is represented by an exact shape function.

Table 4.7: First 60 even eigenvalues for δ-billiard with delta=0.1

n	E_n	n	E_n	n	E_n
1	9.2648693	21	109.04901	41	182.13966
2	29.679455	22	122.70606	42	183.85682
3	30.569025	23	123.94873	43	186.52479
4	32.301069	24	126.56978	44	190.03627
5	37.480382	25	130.22474	45	194.31993
6	60.259803	26	134.71446	46	199.30631
7	60.650335	27	135.60845	47	201.48657
8	61.734874	28	141.57409	48	204.00534
9	63.450691	29	147.61835	49	204.17384
10	65.753952	30	147.83988	50	204.73425
11	73.636906	31	148.44418	51	204.78135
12	76.572412	32	148.52729	52	205.76271
13	80.654640	33	149.60912	53	207.13801
14	85.266749	34	151.15737	54	208.91226
15	99.650129	35	152.79380	55	209.61725
16	99.918484	36	153.15113	56	211.08938
17	100.71749	37	155.59581	57	213.67917
18	102.03540	38	158.49972	58	215.69867
19	103.86453	39	161.87156	59	216.68956
20	106.20266	40	181.52288	60	216.73828

Table 4.8: First 60 odd eigenvalues for δ-billiard with delta=0.1

n	E_n	n	E_n	n	E_n
1	17.559769	21	122.57297	41	177.32378
2	19.424857	22	122.81398	42	178.08131
3	43.844223	23	123.53441	43	179.95377
4	44.394358	24	124.73127	44	182.25145
5	45.748407	25	126.40166	45	182.62976
6	47.770606	26	128.54752	46	184.20558
7	53.670901	27	131.17296	47	184.98372
8	57.692134	28	134.28392	48	188.15912
9	78.871013	29	150.97369	49	191.78903
10	79.182967	30	151.80400	50	192.96604
11	80.095465	31	153.90056	51	214.33942
12	81.579386	32	157.00606	52	214.84022
13	83.616893	33	160.98186	53	216.29328
14	86.194402	34	165.71539	54	218.65050
15	96.821516	35	166.80616	55	221.74827
16	98.767459	36	171.39408	56	225.62496
17	102.08042	37	174.76614	57	230.20703
18	106.34513	38	174.97499	58	235.30151
19	108.32473	39	175.59104	59	235.45127
20	115.49426	40	176.62946	60	235.49092

Table 4.9: First 60 even eigenvalues for δ-billiard with delta=0.5

n	E_n	n	E_n	n	E_n
1	7.63575	21	87.5637	41	138.057
2	19.9003	22	90.5275	42	138.766
3	22.8837	23	96.5736	43	139.999
4	29.1090	24	99.1163	44	140.435
5	32.6498	25	101.907	45	140.625
6	40.4220	26	102.310	46	140.900
7	42.3942	27	102.901	47	142.910
8	46.0214	28	104.310	48	146.518
9	51.0549	29	106.808	49	149.079
10	51.7918	30	109.750	50	154.247
11	59.8284	31	112.445	51	154.383
12	61.0811	32	115.087	52	155.271
13	67.7435	33	118.767	53	162.552
14	69.0006	34	119.767	54	164.716
15	71.4522	35	121.279	55	164.945
16	74.3095	36	124.331	56	168.682
17	76.0218	37	126.662	57	168.841
18	76.7052	38	127.649	58	169.138
19	80.2864	39	131.369	59	171.490
20	82.0830	40	134.833	60	174.826

Table 4.10: First 60 odd eigenvalues for δ-billiard with delta=0.5

n	E_n	n	E_n	n	E_n
1	12.2859	21	87.3057	41	137.826
2	16.9854	22	90.8215	42	141.256
3	29.1935	23	96.4084	43	144.165
4	31.6739	24	98.3090	44	145.778
5	36.0811	25	99.1083	45	148.008
6	39.4753	26	103.695	46	149.735
7	43.8364	27	104.767	47	152.223
8	51.8458	28	105.833	48	153.921
9	53.3723	29	112.973	49	155.976
10	54.8707	30	113.474	50	156.854
11	58.0045	31	115.462	51	160.070
12	62.8447	32	120.557	52	162.148
13	64.1069	33	120.560	53	162.642
14	69.9554	34	122.691	54	164.464
15	72.5582	35	122.844	55	166.382
16	80.7841	36	126.835	56	167.847
17	82.8514	37	127.398	57	168.823
18	83.2611	38	130.077	58	170.516
19	84.7115	39	131.256	59	173.116
20	85.7076	40	136.363	60	174.069

Table 4.11: First 60 even eigenvalues for δ-billiard with delta=0.9

n	E_n	n	E_n	n	E_n
1	6.5913	21	67.529	41	108.42
2	15.127	22	74.879	42	109.75
3	17.743	23	75.745	43	112.39
4	25.933	24	76.614	44	114.58
5	27.720	25	77.800	45	115.56
6	29.957	26	80.657	46	116.44
7	32.317	27	80.675	47	117.26
8	36.664	28	82.889	48	117.89
9	39.812	29	86.044	49	118.21
10	42.251	30	88.581	50	119.42
11	46.868	31	89.105	51	122.22
12	50.195	32	91.380	52	125.48
13	52.051	33	93.106	53	129.76
14	55.007	34	93.535	54	130.53
15	55.208	35	96.381	55	131.48
16	58.677	36	101.18	56	132.12
17	60.098	37	101.20	57	138.53
18	64.850	38	105.54	58	138.96
19	65.592	39	106.52	59	139.12
20	66.999	40	107.47	60	139.91

Table 4.12: First 60 odd eigenvalues for δ-billiard with delta=0.9

n	E_n	n	E_n	n	E_n
1	9.0270	21	70.377	41	109.47
2	14.913	22	70.743	42	113.83
3	21.387	23	73.273	43	115.17
4	24.697	24	77.175	44	115.94
5	28.845	25	79.103	45	116.21
6	30.137	26	86.373	46	117.71
7	39.380	27	87.371	47	119.04
8	39.402	28	87.410	48	119.33
9	41.381	29	88.484	49	121.54
10	44.859	30	90.092	50	122.34
11	45.154	31	90.765	51	123.98
12	47.107	32	91.159	52	124.49
13	50.952	33	93.410	53	129.64
14	57.899	34	95.753	54	130.65
15	58.223	35	95.954	55	130.81
16	62.238	36	100.41	56	131.87
17	63.698	37	101.54	57	136.95
18	65.805	38	103.65	58	136.99
19	67.192	39	107.24	59	139.86
20	67.325	40	108.51	60	140.37

4.3 Statistical analysis of the spectra

Statistical analysis performed in this study includes only plotting the nearest neighbor spacing histogram for a specific eigenvalue class and comparing it with the theoretical models given in Section 1.2. However, since all the theoretical models have mean unity, one must "unfold" the original spectra first as described in [11]. In other words, the sequence $\{E_n\}_{n=1}^{N}$ of eigenvalues must be transformed to a new sequence having mean spacing unity. The usual procedure is to use the transformation

$$x_n = N(E_n), \quad n = 1, 2, \ldots, N, \tag{4.3}$$

where $N(E)$ is the so called spectral staircase or counting function and counts the number of eigenvalues$\leq E$. This function is defined as

$$N(E) = \int_0^E \rho(E') \mathrm{d}E' \tag{4.4}$$

where $\rho(E)$ is the eigenvalue density function. It has been shown by Balian and Bloch [5] that for three-dimensional regions enclosed by a smooth surface, $\rho(E)$ has an asymptotic expansion of the form

$$\rho(E) = \frac{V\sqrt{E}}{4\pi^2} \pm \frac{S}{16\pi} + \frac{1}{12\pi^2\sqrt{E}} \int\!\!\int_S \frac{1}{2}\left(\frac{1}{R_1} + \frac{1}{R_2}\right) \mathrm{d}S + \cdots \tag{4.5}$$

where V and S are the volume and the surface area of the billiard respectively while R_1 and R_2 are the two principal radii of curvature at each point of the boundary. The - and + signs correspond to Dirchlet and Neumann type boundary conditions respectively. For a billiard defined by the truncated shape function

$$G(\eta) = 1 + \sum_{k=1}^{K} \alpha_k \eta_k$$

the volume V can be obtained evaluating the integral

$$V = \frac{2\pi}{3} \int_{-1}^{1} [G(\eta)]^3 \, \mathrm{d}\eta \tag{4.6}$$

and the surface area S is computed from

$$S = 2\pi \int_{-1}^{1} G(\eta)\sqrt{[G(\eta)]^2 + [G'(\eta)]^2} \mathrm{d}\eta. \tag{4.7}$$

The two principal radii of curvature can be obtained using the first and second fundamental forms of the boundary surface, (see [55] for details), so that, the integral term in (4.5) becomes

$$-\pi \left\{ G(-1) + G(1) + \int_{-1}^{1} G(\eta)\mathrm{d}\eta \right\}$$
$$+\pi \int_{-1}^{1} \frac{(1-\eta^2)\left\{G''(\eta)G(\eta) - [G'(\eta)]^2\right\} - \eta G'(\eta)G(\eta)}{[G(\eta)]^2 + [G'(\eta)]^2}\mathrm{d}\eta. \qquad (4.8)$$

It must be pointed out that the eigenvalue sets obtained for each case represent actually 1/4-th of the total number of eigenvalues in the corresponding interval. This is due to the fact that we have separated the eigenfunctions according to their symmetries. This separation is necessary for the statistical analysis, since the degeneracies implied by the symmetries must be avoided.

In what follows, we transformed the eigenvalue sequence $\{E_n\}_{n=1}^{N}$ to the sequence $\{x_n\}_{n=1}^{N}$ by means of the transformation

$$x_n = N(E_n) = \frac{1}{4}\left\{\frac{VE_n^{3/2}}{6\pi^2} - \frac{SE_n}{16\pi} + \frac{KE_n^{1/2}}{6\pi^2}\right\}. \qquad (4.9)$$

The values of V, S and K have been evaluated numerically using Mathematica. Then we have calculated the spacing $s_n = x_{n+1} - x_n$ and have observed that the mean $\bar{s}$ of the sequence (s_n) is $\bar{s} \approx 1$ in each case. Figures 4.1-4.5 show the distribution of the sequence (s_n) for each eigenvalue set computed for the δ-billiard, that is, the so-called Nearest Neighbor Spacing (NNS) Histograms. In each Figure, the graph of the Poisson distribution

$$p(s) = \mathrm{e}^{-s}$$

is plotted. In the first two figures the NNS histograms of even and odd eigenvalues of the δ-billiard with δ=0.1 are given. The graph of the probability distribution function of the Gaussian Orthogonal Ensemble,

$$p(s) = \frac{\pi}{2}s\mathrm{e}^{-\frac{\pi}{4}s^2}$$

is also plotted for comparison. The resemblance between the Poisson distribution function and the histograms is remarkable for both cases. Recall that the two dimensional cross-sectional billiard with $\delta = 0.1$ exhibited regular motion. In the Figures

4.3 and 4.4 the NNS histograms of even and odd eigenvalues of the δ-billiard with δ=0.5 are given. The Brody distribution

$$p(s) = (\nu + 1)a_\nu s^\nu \exp(-a_\nu s^{\nu+1}),\tag{4.10}$$

where

$$a_\nu = \left[\Gamma\left(\frac{\nu + 2}{\nu + 1}\right)\right]^{\nu+1}.\tag{4.11}$$

and $\nu = 0.5$ is also plotted and obviously, the agreement between the histogram and the Brody model is quite good. NNS histograms for the even and odd eigenvalues of the δ-billiard with $\delta = 0.9$ are given in Figures 4.5 and 4.6 respectively. The graph of Brody model with $\nu = 0.9$ is also given for comparison. The similarity of the last two histograms and the Brody distribution is also noticeable.

Despite the relatively small number of eigenvalues included in the histograms, we have observed good agreement with the theoretical models. Thus, we expect that increasing the number of the eigenvalues we will get much better statistical results. However, the main purpose of this work is the development of the method rather than the statistical investigation, therefore, we do not further extend our statistical analysis.
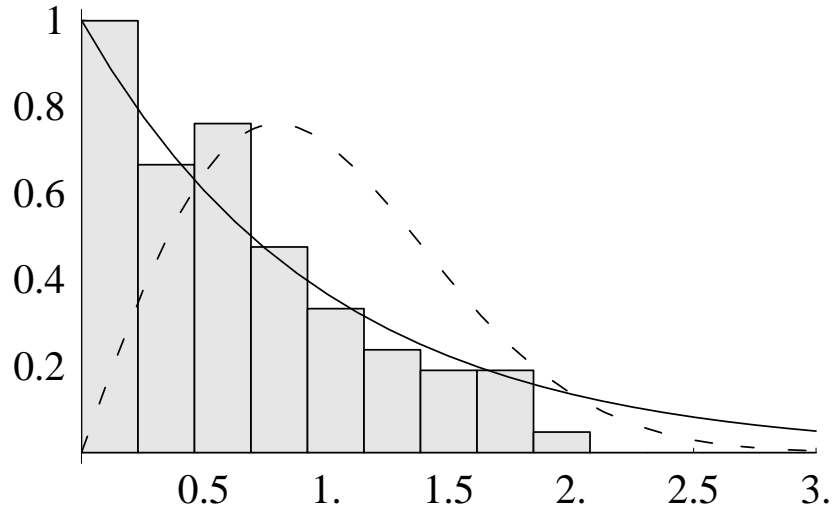
Figure 4.1: Nearest-Neighbor Spacing Histogram for even eigenvalues of the billiard with δ=0.1. Solid line-Poisson distribution. Dashed line-GOE distribution
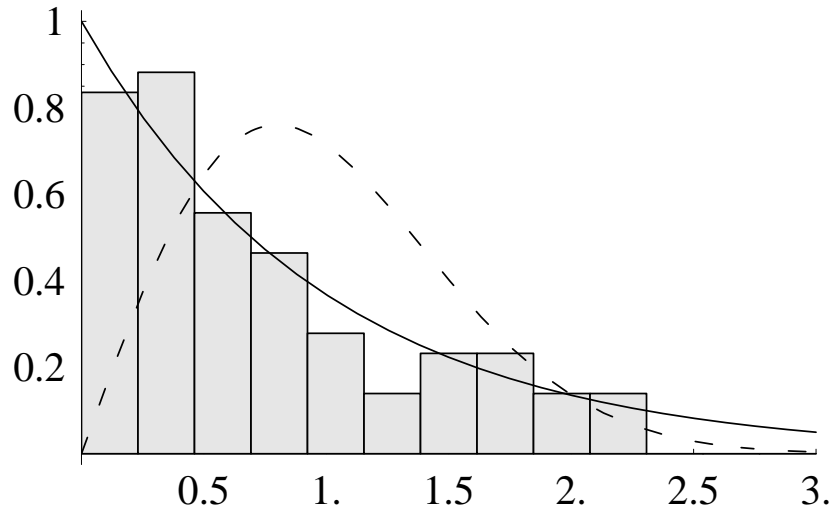

Figure 4.2: Nearest-Neighbor Spacing Histogram for odd eigenvalues of the billiard with δ=0.1. Solid line-Poisson distribution. Dashed line-GOE distribution
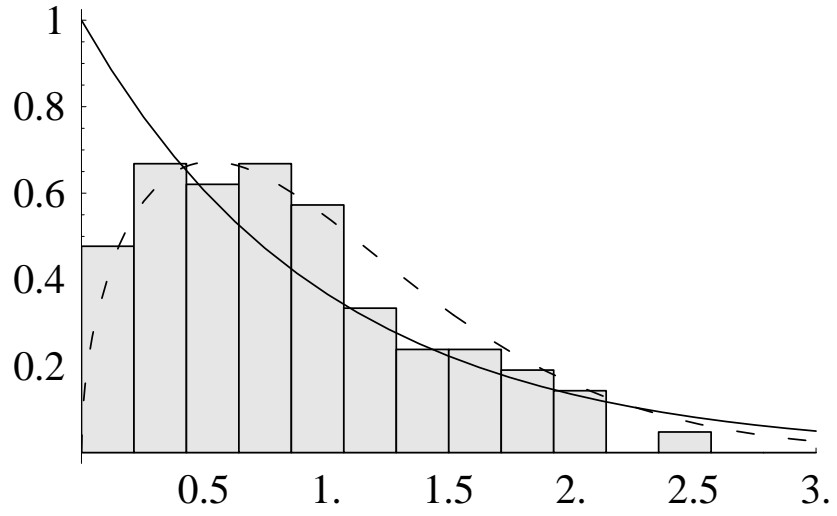
Figure 4.3: Nearest-Neighbor Spacing Histogram for even eigenvalues of the billiard with δ=0.5. Solid line-Poisson distribution. Dashed line- Brody distribution with $\nu = 0.5$
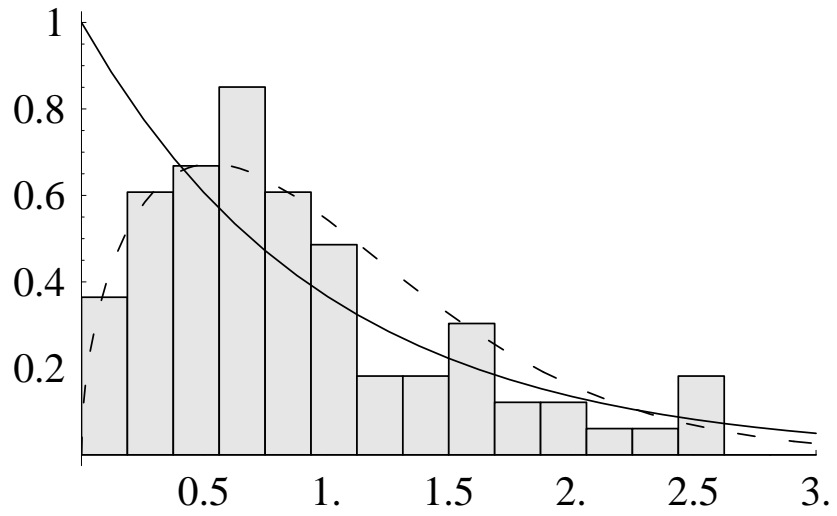

Figure 4.4: Nearest-Neighbor Spacing Histogram for odd eigenvalues of the billiard with δ=0.5. Solid line-Poisson distribution. Dashed line- Brody distribution with $\nu = 0.5$

Figure 4.5: Nearest-Neighbor Spacing Histogram for even eigenvalues of the billiard with δ=0.9. Solid line-Poisson distribution. Dashed line- Brody distribution with $\nu = 0.9$

Figure 4.6: Nearest-Neighbor Spacing Histogram for odd eigenvalues of the billiard with δ=0.9. Solid line-Poisson distribution. Dashed line- Brody distribution with $\nu = 0.9$
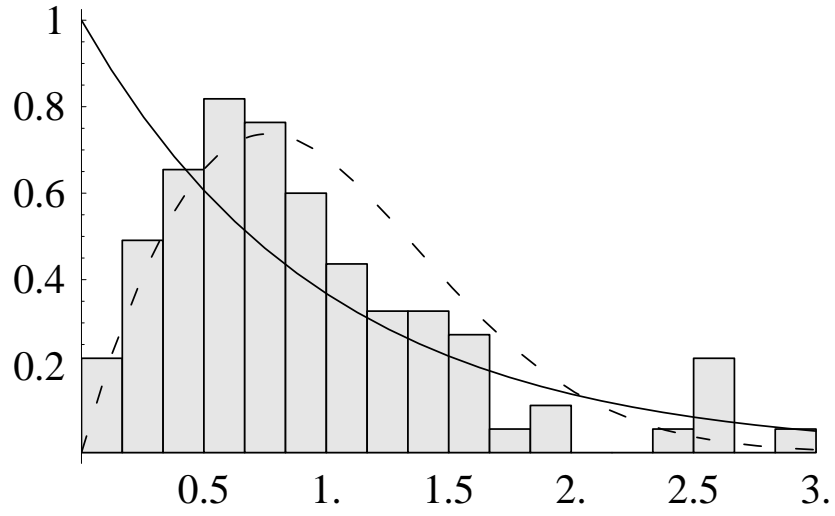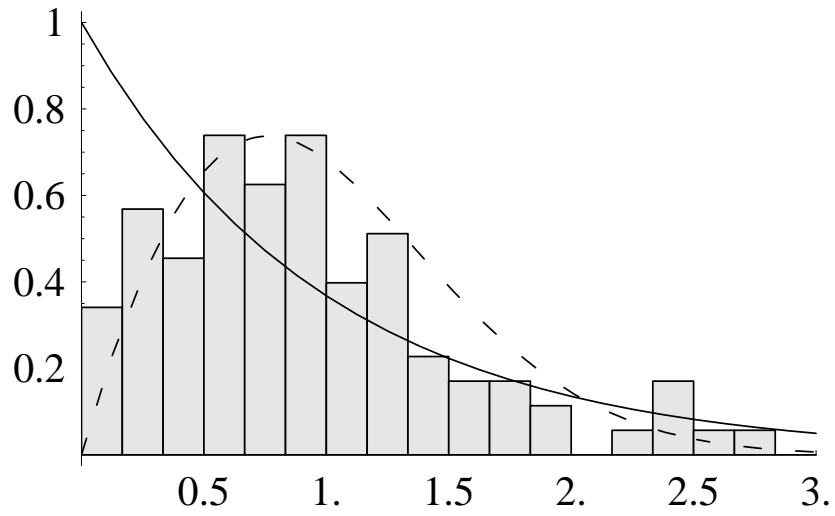
CHAPTER 5

CONCLUSION

In this thesis we have presented a numerical method for computation of the eigenvalues of the Schrödinger equation for a particle moving freely in a closed axisymmetric three-dimensional region. In the theory of partial differential equations, this is an eigenvalue problem for the eigenvalues and eigenfunctions of the self-adjoint Laplace operator subject to some additional conditions. The method employs an unusual non-orthogonal coordinate transformation leading to an expansion in terms of Bessel functions with real orders. Therefore, it seems to be interesting from mathematical point of view. In fact, the expansions in Bessel functions with real orders is not as common a tool as the expansions in terms of Bessel functions with integral or half-an-odd integral orders.

The method is also interesting from classical and quantum mechanical points of view, more precisely, in the study of quantum chaos, since it deals with quite general three-dimensional billiard systems. Unlike the boundary element or collocation methods resulting in a nonlinear problem, our method ends up with a generalized matrix eigenvalue problem, which is more appropriate in quantum mechanics. A similar matrix eigenvalue problem is obtained if the problem is treated with the constraint operator method [33] for example, however, this method represents the wavefunction of a chaotic billiard in terms of the eigenfunctions of a regular billiard. The expansion basis of our method is closely related to the shape of the billiard, which seems more natural.

The method has one very serious drawback. It requires computation of integrals of products of Bessel functions of real orders, which is a very difficult numerical task.

In this study, computation of such integrals has been done by using a method which is not numerically efficient, for, it is very "expensive" in the sense of computing time. Therefore, this problem needs to be reconsidered. Moreover, for each new parameter the integrals must be computed again. For this reason, the use of an expansion basis of spherical Bessel functions may seem to be more appropriate. Then, it would be sufficient to compute the integrals needed to evaluate the matrix elements once, and use them for each new parameter. Although not reported here, we have tried such a basis during the period of preparing the thesis. However, we have observed that the accuracy of the eigenvalues computed in this way is less than the accuracy obtained using the basis presented here. It must be pointed out that, despite its drawbacks, the accuracy of our method is quite good compared with the results reported in the literature.

The second numerical example considered in this thesis is a billiard family depending on a parameter. This billiard has not been investigated before. However, related statistical results, seem to be very interesting and we expect that they may attract the attention of people studying chaos in classical and quantum systems.

References

[1] M. Abramowitz and I. A. Stegun. *Handbook of Mathematical Functions*. Dover, New York, 1970.

[2] Y. Ayant and R. Arvieu. Semiclassical study of particle motion in two-dimensional and three-dimensional elliptical boxes:i. *J. Phys. A. Math. Gen.*, 20:397–409, 1987.

[3] Y. Ayant and R. Arvieu. Semiclassical study of particle motion in two-dimensional and three-dimensional elliptical boxes:ii. *J. Phys. A. Math. Gen.*, 20:1115–1136, 1987.

[4] A. Bäcker and F. Steiner. Spectral statistics in the quantized cardioid billiard. *Phys. Rev. E*, 52:2463–2472, 1995.

[5] R. Balian and C. Block. Distribution of eigenfrequences for the wave function in a finite domain i three-dimensional problem with smooth boundary surface. *Annals of Physics*, 60:401–447, 1970.

[6] P. K. Banerjee. *The Boundary Element Method in Engineering*. McGraw-Hill, New York, 1994.

[7] H. Bateman. *Higher Transcendental Functions I*. Robert E. Krieger Publishing Company Malabar, Florida, 1953.

[8] M. V. Berry. Quantizing a classically ergodic system: Sinai's billiard and the kkr method. *Ann. Phys.*, 131:163–216, 1981.

[9] M. V. Berry. Regularity and chaos in classical mechanics, illustrated by three deformations of a circular billiard. *Eur. J. Phys.*, 2:91–102, 1981.

[10] M. V. Berry and M. Tabor. Level clustering in regular spectrum. *Proc. R. Soc. Lond. A*, 356:375–395, 1977.

[11] O. Bohigas. Random matrix theories and chaotic dynamics. In M. J. Giannoni, A. Voros, and J. Zinn-Justin, editors, *Chaos and Quantum Physics, Proceedings of the Les Houches Summer School 1989: Session LII*, pages 87–199. North-Holland, Amsterdam, 1991.

[12] O. Bohigas, M. J. Giannoni, and C. Schmit. Characterization of chaotic quantum spectra and universality of level fluctuation laws. *Phys. Rev. Lett.*, 52:1–4, 1984.

[13] O. Bohigas, M. J. Giannoni, and C. Schmit. Spectral properties of the laplacian and random matrix theory. *J. Physique. Lett.*, 45:L1015–L1022, 1984.

[14] G. Cassati and T. Prosen. The quantum mechanics of chaotic billiards. *Physica D*, 131:293–310, 1999.

[15] R. Courant and D. Hilbert. *Methods of Mathematical Physics*. New York, Interscience Publisher, 1962.

[16] R. Dutt, R. Gangopadhyaya, and U. P. Sukhatme. Noncentral potentials and spherical harmonics using supersymmetry and shape invariance. *Am. J. Phys.*, 65:400–403, 1997.

[17] B. Grèmaud and S. R. Jain. Spacing distribution for rhombus billiards. *J. Phys. A: Math. Gen.*, 31:L637–L643, 1998.

[18] F. Haake. *Quantum Signatures of Chaos 2nd. ed.* Springer-Verlag, Berlin, 2000.

[19] E. J. Heller. Bound-state eigenfunctions of classically chaotic hamiltonian systems: scars of periodic orbits. *Phys. Rev. Lett.*, 53:1515–1518, 1984.

[20] E. J. Heller. Wavepacket dynamics and quantum chaology. In M. J. Giannoni, A. Voros, and J. Zinn-Justin, editors, *Chaos and Quantum Physics, Proceedings of the Les Houches Summer School 1989: Session LII*, pages 547–664. North-Holland, Amsterdam, 1991.

[21] E. J. Heller, P. W. O'Connor, and J. Gehlen. The eigenfunctions of classically chaotic systems. *Physica Scripta*, 40:354–359, 1989.

[22] Y. Hlushchuk and L. Sirko et all. Experimental investigation of a regime of wigner ergodicity in microwave rough billiard. *Phys. Rev. E*, 64:art. no. 046208, 2001.

[23] F. M. Izrailev. Quantum localization and statistics of quasienergy spectrum in a classically chaotic system. *Phys. Lett. A*, 134:13–18, 1988.

[24] R. D. Riddell Jr. Numerical solution of the helmholtz equation for two-dimensional polygonal regions. *J. Comput.Phys.*, 31:42–59, 1979.

[25] D. L. Kaufmann, I. Kosztin, and K. Schulten. Expansion method for stationary states of quantum billiards. *American Journal of Physics*, 67:133–141, 1999.

[26] B. Li and M. Robnik. Spectral properties of high-lying chaotic eigenstates. *J. Phys. A: Math. Gen.*, 27:5509–5523, 1994.

[27] R. L. Liboff. The polygon quantum billiard problem. *J. Math. Phys.*, 35:596–607, 1994.

[28] R. L. Liboff. Conical quantum billiard. *Lett. Math. Phys.*, 42:389–391, 1997.

[29] R. L. Liboff. Conical quantum billiard revisited. *Quarterly of Applied Mathematics*, 59:343–351, 2001.

[30] V. Lopac, I. Mrkonjìc, and D. Radìc. Classical and quantum chaos in the generalized parabolic lemon-shaped billiard. *Phys. Rev. E*, 59:303–311, 1999.

[31] Y. D. Luke. *Integrals of Bessel Functions*. McGraw-Hill, New York, 1962.

[32] R. Markarian, S. O. Kampshort, and S. P. Carvalho. Chaotic properties of the elliptical stadium. *Commun. Math. Phys.*, 174:661–679, 1996.

[33] D. A. McGrew and W. Bauer. Constraint operator solution to quantum billiard problem. *Phys. Rev. E*, 54:5809–5818, 1996.

[34] M. L. Mehta. *Random Matrices 2.nd enlarged ed.* Acad. Press, New York, 1991.

[35] Steven A. Moszkowski. Particle states in spheroidal nuclei. *Phys Rev.*, 99:803–809, 1955.

[36] T. Papenbrock. Numerical study of a three-dimensional generalized stadium billiard. *Phys. Rev. E*, 61:4626–4628, 2000.

[37] I. C. Percival. Regular and irregular spectra. *J. Phys. B: Atom. Molec. Phys.*, 6:L229–L232, 1973.

[38] N. Pomphrey. Numerical identification of regular and irregular spectra. *J. Phys. B: Atom. Molec. Phys.*, 7:1909–1915, 1974.

[39] H. Primak and U. Smilansky. Quantization of the three-dimensional sinai billiard. *Phys. Rev. Lett.*, 74:4831–4834, 1995.

[40] H. Primak and U. Smilansky. The quantum three-dimensional sinai billiard- a semiclassical analysis. *Phys. Rep.*, 327:1–107, 2000.

[41] T. Prosen and M. Robnik. Energy level statistics in the transition region between integrability and chaos. *J. Phys. A: Math. Gen.*, 26:2371–2387, 1993.

[42] P. J. Richens and M. V. Berry. Pseudointegrable systems in classical and quantum mechanics. *Physica 2D*, 2:495–512, 1981.

[43] M. Robnik. Classical dynamics of a family of billiards with analytic boundaries. *J. Phys. A: Math. Gen.*, 16:3971–3986, 1983.

[44] M. Robnik. Quantising a generic family of billiards with analytic boundaries. *J. Phys. A: Math. Gen.*, 17:1049–1074, 19834.

[45] M. Sieber and F. Steiner. Classical and quantum mechanics of a strongly chaotic billiard system. *Physica D*, 44:248–266, 1990.

[46] M. Sieber and F. Steiner. Quantum chaos in the hyperbola billiard. *Physics Letters A*, 148:415–420, 1990.

[47] L. Sirko and P. M. Koch. Practical tests with irregular and regular finite spectra of a proposed statistical measure for quantum chaos. *Phys. Rev. E*, 54:R21–R24, 1996.

[48] H. J. Stöckmann. *Quantum Chaos: An Introduction.* Cambridge Univ. Press, 1999.

[49] W. A. Strauss. *Partial Differential Equations An Introduction.* John Wiley, 1992.

[50] J. Flores et al. T. A. Brody, P. A. Mello. Doorway states and nuclear spectrum statistics. *Lett. Nuovo Cimento,* 7:707–712, 1973.

[51] H. Taşeli and M. Demiralp. A new approach to the classical stokes flow problem: Part i metodology and first-order analytical results. *J. Comput. Appl. Math.,* 78:213–232, 1997.

[52] H. Taşeli and R. Eid. A new approach to the classical stokes flow problem: Part ii series solutions and higher-order applications. *J. Comput. Appl. Math.,* 78:233–254, 1997.

[53] H. Taşeli and A. Zafer. Bessel basis with applications: N-dimensional isotropic polynomial oscillators. *Int. J. Quantum Chem.,* 63:935–947, 1996.

[54] H. Taşeli, İnci M. Erhan, and Ö. Uğur. An eigenfunction expansion for the schrödinger equation with arbitrary non-central potentials. *J. Math. Chem.,* 32:323–338, 2002.

[55] C. Tezer. Lecture notes on differential geometry. web page: www.math.metu.edu.tr \~rauf\.

[56] A. N. Tikhonov and A. A. Samarskii. *Equations in Mathematical Physics, 2.nd Translated Edition.* Pergamon Press, 1963.

[57] E. Vergini and M. Saraceno. Calculation by scaling of highly excited states of billiards. *Phys. Rev. E,* 52:2204–2207, 1995.

[58] D. S. Watkins. *Fundamentals of Matrix Computations.* New York, Wiley, 1991.

[59] G. N. Watson. *A Treatise on the Theory of Bessel Functions.* Cambridge Univ. Press, 1944.

[60] Maciej Wojtkowski. Principles for the design of billiards with non-vanishing lyapunov exponents. *Comm. Math. Phys.,* 105:391–414, 1986.

[61] S. Wolfram. *The Mathematica Book, 3rd ed.* Wolfram Media, 1996.

[62] Karol Życzkowski. Classical and quantum billiards: Integrable, nonintegrable and pseudo-integrable. *Acta Phys. Polonica B.*, 23:245–270, 1992.

VITA

İnci (Müftüoğlu) Erhan was born in Rousse-Bulgaria, on 9 April, 1971. She completed her primary, secondary and high school education in Rousse.

She started her undergraduate studies at the Department of Mathematics, Marmara University in 1990 and took her B.S. degree in 1994. In the same year, she became research assistant at the Department of Mathematics, Marmara University, and started her graduate studies. İnci Erhan received her M.Sc. degree in Mathematics in 1996, with a thesis entitled "A Basis Operator Expansion Method for Quantum Mechanical Systems with Yukawa Potential". She started her Ph.D studies in 1997 at the Middle East Technical University. In 2000 İnci Erhan received a grant from TÜBİTAK, The Scientific and Technical Research Council of Turkey and joined the study group of Christine Böckmann in Potsdam University, Germany for a period of 9 months.